EGG-SEMI-5201
July 1980

ANALYSIS OF SEMISCALE MOD-3 SMALL BREAK TESTS S-07-10 AND S-07-10D

D. J. Shimeck

U.S. Department of Energy
Idaho Operations Office • Idaho National Engineering Laboratory

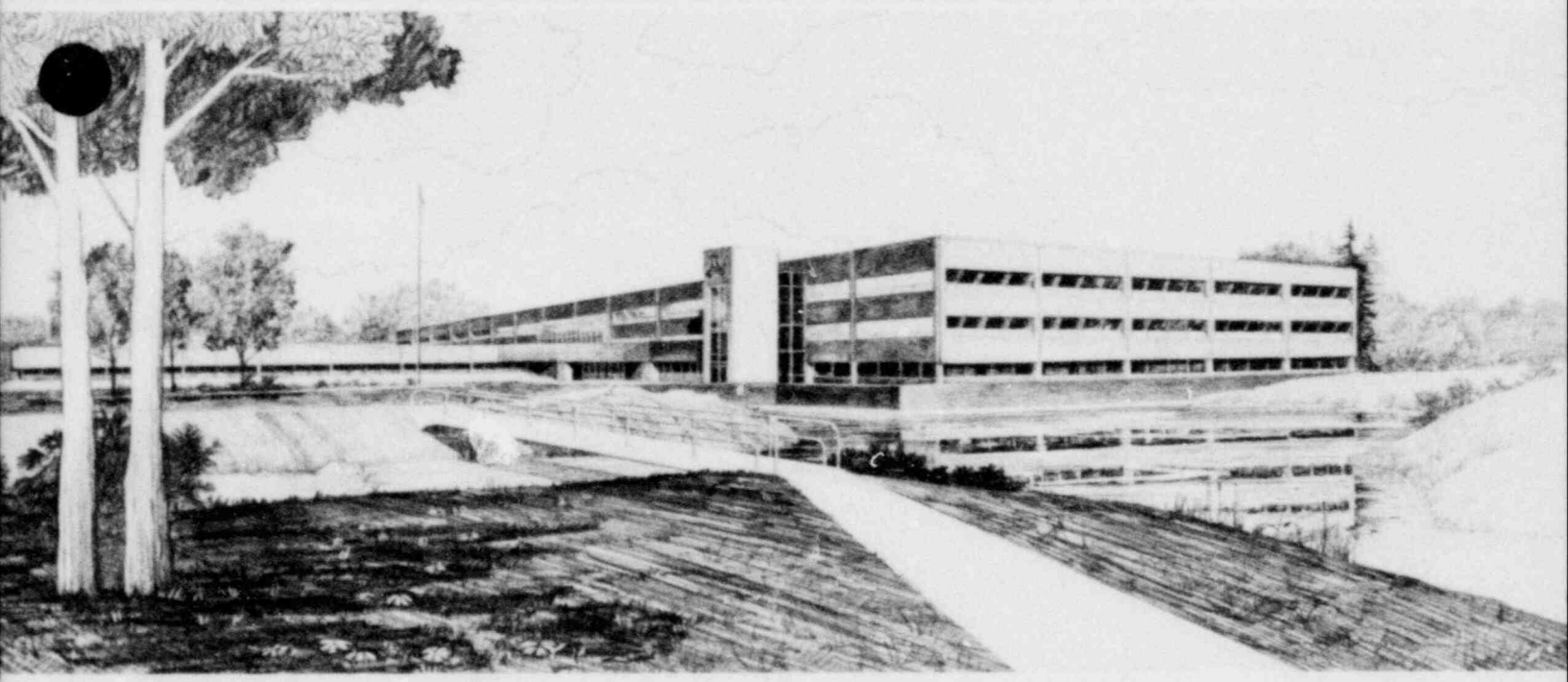

This is an informal report intended for use as a preliminary or working document

Prepared for the
U.S. Nuclear Regulatory Commission
under DOE Contract No. DE-AC07-761D01570
FIN No. A6038

EG&G Idaho

EG&G Idaho, Inc.

FORM EG&G-398
(Rev. 05-79)

INTERIM REPORT

Accession No. _____

Report No. EGG-SEMI-5201

Contract Program or Project Title:

Semiscale Program

Subject of this Document:

Analysis of Semiscale Mod-3 Small Break
Tests S-07-10 and S-07-10D

Type of Document:

Analysis Report

Author(s):

D. J. Shimeck

Date of Document:

July 1980

Responsible NRC Individual and NRC Office or Division:

W. C. Lyon
Reactor Safety Research

This document was prepared primarily for preliminary or internal use. It has not received full review and approval. Since there may be substantive changes, this document should not be considered final.

EG&G Idaho, Inc.
Idaho Falls, Idaho 83401

Prepared for the
U.S. Nuclear Regulatory Commission
Washington, D.C.
Under DOE Contract No. DE-AC07-76ID01570
NRC FIN No. A6038

INTERIM REPORT

ANALYSIS

OF

SEMISCALE MOD-3 SMALL BREAK

TESTS S-07-10 AND S-07-10D

by

D. J. Shimeck

Approved: _____

G. W. Johnsen, Manager
Semiscale Experiment Specification and
Analysis Branch

Approved: _____

L. P. Leach, Manager
Semiscale Program

The information contained in this summary report is preliminary and incomplete. Selected pertinent data are presented in order to draw preliminary conclusions and to expedite the reporting of research results.

ACKNOWLEDGEMENTS

Special thanks are due to J. R. Hewitt and J. E. Blakeley for assistance in performing calculations and plotting results, and to M. G. Heaton and E. Jenkins for creating special plots.

CONTENTS

FIGURES

FIGURES (Contd)

FIGURES (Contd)

TABLES

ABSTRACT

Results are presented from Semiscale Mod-3 Tests S-07-10 and S-07-10D. These tests were 10%, communicative, cold leg break loss-of-coolant tests in which no emergency core coolant (ECC) was injected until elevated core heater rod temperatures were obtained. These tests were performed to assist the United States Nuclear Regulatory Commission (NRC) in evaluation of computer models used by U.S. nuclear power plant vendors to assure the safety of commerical reactors. As such, Test S-07-10D is designated as USNRC standard problem SBE. The special emphasis of this standard problem is on the system behavior leading to and accompanying dryout and heatup of a core during a small break transient. For Test S-07-10 the steam generator secondaries were isolated at 17 s into the transient, while for Test S-07-10D the broken loop steam generator was allowed to blowdown throughout the transient, as the standard problem calculations were performed in this manner. Dryout of the core occurred beginning at 210 and 230 s in Tests S-07-10 and S-07-10D, respectively. The predominant influence of steam generator blowdown was to extend the time of complete core dryout from 370 s, as observed in Test S-07-10, to 440 s in Test S-07-10D. Peak core temperatures of 1060 and 1145 K occurred in Test S-07-10 and Test S-07-10D, respectively, prior to ECC injection. Also, as a result of steam generator heat transfer in Test S-07-10D, a significant amount of liquid remained in the broken loop pump suction throughout the blowdown. When ECC injection was initiated this liquid was forced into the vessel and assisted rapid filling and quenching of the core.

SUMMARY

This report presents the results of an analysis of data from Semiscale Mod-3 small break Tests S-07-10 and S-07-10D. The primary objective of these tests was to assist the United States Nuclear Regulatory Commission (NRC) licensing staff in evaluating the acceptablity of small break licensing models used by pressurized water reactor (PWR) vendors. To accomplish this, Test S-07-10 was designated a United States standard problem. Each of the PWR vendors provided calculations of expected performance of S-07-10 to the NRC prior to release of the data. Semiscale Tests S-07-10 and S-07-10D simulated a 10% cold leg break in which no emergency core coolant (ECC) was injected until elevated core heater rod temperatures were obtained. Additionally, in Test S-07-10D the broken loop steam generator secondary side was allowed to blow down to investigate the effect of secondary side conditions on primary behavior. The break size for these tests was 0.223 cm^2 which is volumetrically scaled to represent a 10% pipe break in a pressurized water reactor. Initial conditions were also equivalent to, or scaled from, PWR operating conditions.

Following rupture of the pressure boundary, continuous depressurization of the system took place and the system voided from the upper elevations downward. Heat transfer to the broken loop steam generator in Test S-07-10D apparently caused the pressure to drop slightly below that for Test S-07-10 for the first 150 s. Asymmetric behavior of the broken loop in Test S-07-10D, resulting from steam generator heat transfer, resulted in a higher liquid inventory in the broken loop pump suction throughout the blowdown. This led to somewhat lower quality fluid conditions upstream of the break, and eventually caused the pressure to decrease more slowly than observed for Test S-07-10. After 150 s, the system pressure in Test S-07-10D was higher than that of S-07-10. After the initial 50 to 100 s in the tests, the primary and secondary behaviors appeared to be decoupled. The broken loop secondary became a heat source to the primary after 110 s in Test S-07-10 and 190 s in Test S-07-10D.

With continuous loss of mass through the break and no ECC injection the loops were voided at about 200 s and the vessel liquid level then began to boil off. Core uncovery was first observed at 210 s in Test S-07-10 and 230 s in Test S-07-10D. The core progressively dried out from the top down. The predominant effect of the steam generator blowdown in Test S-07-10D was to extend the time for complete voiding of the vessel from 370 to 440 s. In both tests the core high power zones were at elevated temperatures (1145 K peak for Test S-07-10, 1060 K for Test S-07-10D) and increasing rapidly prior to ECC injection.

ECC injection was manually initiated at 438 and 460 s in Tests S-07-10 and S-07-10D, respectively. Due to nearly complete loop voiding ECC liquid quickly penetrated to the core in about 7 s and reflood commenced. The core progressively quenched from the bottom up with a good deal of precursory cooling observed. In Test S-07-10D, liquid from the broken loop pump suction was pushed into the vessel. In conjunction with a somewhat larger injected accumulator mass, this assisted in a more rapid reflood and quench of core than was observed in Test S-07-10. The core was completely quenched by 562 s in Test S-07-10 and 525 s in Test S-07-10D.

1. INTRODUCTION

Testing performed in the Semiscale Mod-3 system is part of the overall reator safety researcn effort directed towards assessing and improving the analytical capability of computer codes to accurately predict the behavior of a pressurized water reactor (PWR) during a postulated loss-of-coolant accident (LOCA). For this purpose the Mod-3 system nas been designed as a small-scale model of the primary system of a four loop PWR nuclear generating plant. The system incorporates the major components of a PWR including steam generators, vessel, pumps, pressurizer, and loop piping. One intact loop is scaled to simulate the three intact loops in a PWR, while a broken loop simulates the single loop in which a break is postulated to occur in a PWR. Geometric similarity nas been maintained between a PWR and Mod-3, most notably in the design of a 25 rod, full-length (3.66 m), electrically heated core, full length upper head and upper plenum, component layout, and relative elevations of various components. The scaling philosophy followed in the design of the Mod-3 system (modified volume scaling) preserves most of the important first order effects thougnt important for small break LOCA transients.[1]

This document presents a preliminary analysis of data obtained from Semiscale small (10%) break, delayed emergency core coolant (ECC), blowdown-reflood Tests S-07-10 and S-07-10D. At the request of the Nuclear Regulatory Commission, Test S-07-10 was conducted on January 19, 1979 as an extension of Test Series 7. This was the first series of tests conducted in the Mod-3 system to establish baseline data on system performance. Data from Test S-07-10 was to be used for evaluation of standard problem calculations,[a] and was therefore not released until January 1980 following submittal of predictions by the standard problem participants.

---

a. United States Standard Problem Small Break Experiment (SBE).

Test conditions supplied to participants for Test S-07-10[2] reported that the broken loop steam generator steam valve had failed to close, a conclusion that was drawn from faulty instrumentation. Analysis following release of the data concluded that the valve had indeed closed at approximately the correct time of 17 s, thus precluding meaningful comparisons between calculations and data. Test S-07-10D attempted to duplicate the reported operating conditions used in these calculations in order to provide a useful comparison. Additionally, data from Test S-07-10D provides a check on the repeatability of results from a 10% break test and, in conjunction with data from Test S-07-10 will be useful in quantifying the sensitivity of primary system behavior to secondary conditions.

The primary objective of Test S-07-10 was to examine the system behavior leading to, and accompanying, the attainment of elevated rod temperatures in the simulated core. To this end, no broken loop emergency core coolant injection was used and ECC injection in the intact loop was delayed until being manually initiated late in the transient. With no ECC liquid addition, the continuous loss of mass through the break and core heat addition eventually resulted in complete voiding of the core by 370 s accompanied by high temperature excursions of the rods progressing from the top to the bottom of the core. Rod cladding temperatures were allowed to climb to a peak value of 1145 K at 438 s at which time ECC injection was manually initiated. Water reached the core several seconds later resulting in a slight repressurization due to steam generation. The core was observed to progressively quench from the bottom up and was completely quenched by 562 s. The system stablized and the test was terminated at 748 s.

The objectives of Test S-07-10D were twofold. The first again being an examination of system behavior with delayed ECC injection. The second, associated objective, was to examine the influence of steam generator secondary side conditions on primary behavior. To accomplish this the broken loop steam generator was allowed to blow down through the steam discharge valve throughout the transient.

Following rupture of the pressure boundary, continuous system depressurization occurred with core power decay, pump coastdown and steam generator feedwater valve closures initiated at 7.7 s. This was 1 s after a 12.41 MPa pressurizer pressure trip as specified,[3] and compares favorably with the 7.2 s time from Test S-07-10. The intact loop steam generator valve closed at about 21 s while the broken loop steam valve remained at its initial position throughout the test. Core heater rod thermocouples registered near saturation temperature until 230 s. The core then dried out from the top down. In-core gamma densitometer measurements indicated the core was completely voided by 440 s. The rods were allowed to heat up to a peak temperature of 1060 K. Accumulator and high pressure injection system (HPIS) injection were initiated at 460 s and a system pressure of 1600 kPa. The core progressively quenched from the bottom up beginning approximately 7 s after initiation of ECC injection and was completely quenched by 525 s.

Some asymmetrical loop behavior was observed in Test S-07-10D as would be expected from the preferential condensation potential in the broken loop. Most differences observed appear to be the result of a significant quantity of liquid collecting in the broken loop pump suction during blowdown. Overall impact of the early heat removal and vapor condensation appears to have been small. The major effect seems to have been delaying the initiation of various phenomena, such as a 25 s delay in intact loop pump suction seal blowout at 90 s, a 20 s delay in initial core uncovery at 230 s, and a 100 s longer period of time required to completely void the core. Heater rod cladding temperatures in the upper core region were still excessive and climbing rapidly prior to emergency core coolant injection. The liquid in the broken loop pump suction was forced into the vessel at the initiation of ECC injection. This assisted in a more rapid reflood of the core than observed in Test S-07-10.

The following sections present a summary of results from Tests S-07-10 and S-07-10D. The actual test conditions, test procedures, and system hardware are described initially, followed by a comparison of data from the two tests.

2. SYSTEM CONFIGURATION AND TEST CONDUCT

2.1 System Configuration

An isometric of the Semiscale Mod-3 system, as configured for Tests S-07-10 and S-07-10D, is shown in Figure 1 with major components identified. The break was located in the broken loop cold leg between the pump and the vessel and was communicative in nature. The break orifice is shown in detail in Figure 2. The break size was 0.223 $cm,^2$ which is volumetrically scaled to represent 10% of the area of a cold leg pipe in a PWR. In order to be representative of an orifice-like break in a PWR pipe the orifice was designed as sharp edged with a length-to-diameter ratio of 0.27.

Figures 3 and 4 are plan views of the Mod-3 core for Tests S-07-10 and S-07-10D, respectively, showing the location of unpowered rods, its orientation with respect to the remainder of the system, and the distribution of internal cladding thermocouples monitored during each test. Internally heated electric rods are used to simulate the nuclear rods in a PWR. The rods are geometrically similar to nuclear rods with a heated length of 3.66 m and an outside diameter of 1.072 cm. The axial power profile for the rods is illustrated in Figure 5 showing the step cosine shape with a 1.55 peak to average power factor. The relative locations of in-core instrumentation (gamma densitometers and core inlet drag screen) and grid spacers are indicated in Figure 6.

The 5 x 5 rod core was in a somewhat different configuration for Test S-07-10D than for Test S-07-10. For Test S-07-10 the 9 center rods operated at an initial, maximum linear heat generation rate (MLHGR) of 46.7 kW/m and 14 peripheral rods were operated at an MLHGR of 28.7 kW/m with rods A1 and E5 unpowered. For Test S-07-10D the 9 center rods still operated at approximately the same MLHGR. However, heater rods A1, A3, and A4 were unpowered for this test. The 13 remaining peripheral rods had an initial MLHGR of 30.71 kW/m thus providing the same total core power as for Test S-07-10 of

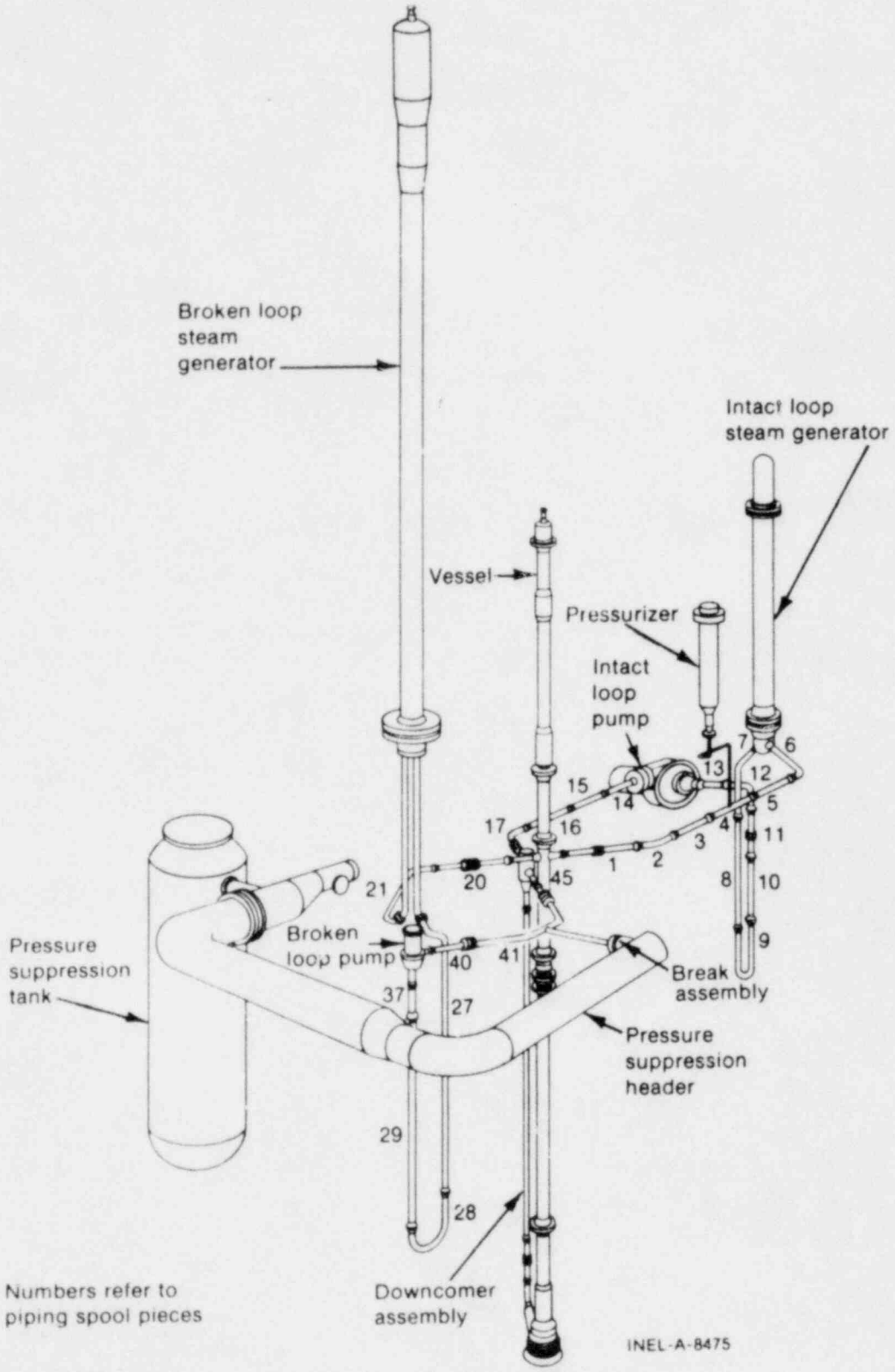

Figure 1. Semiscale Mod-3 system cold leg communicative small break configuration isometric.

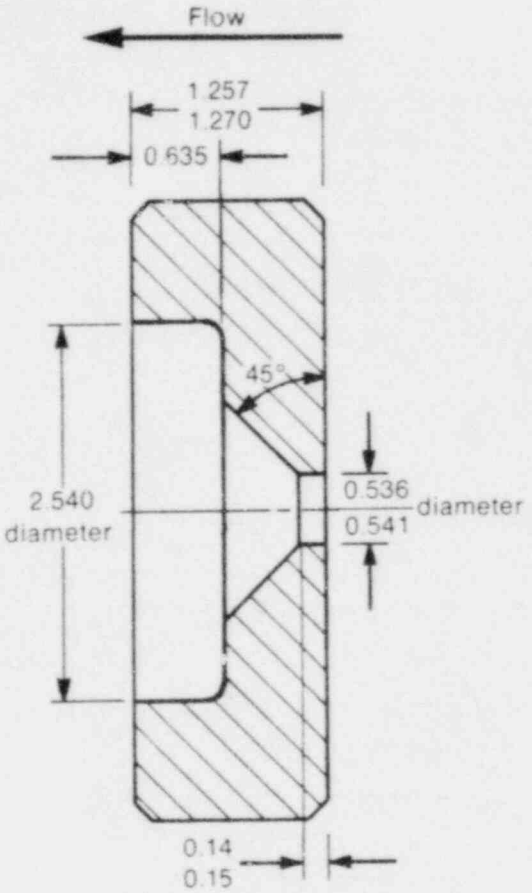

Figure 2. Semiscale 10% break orifice, flow area = 0.223 cm^2.

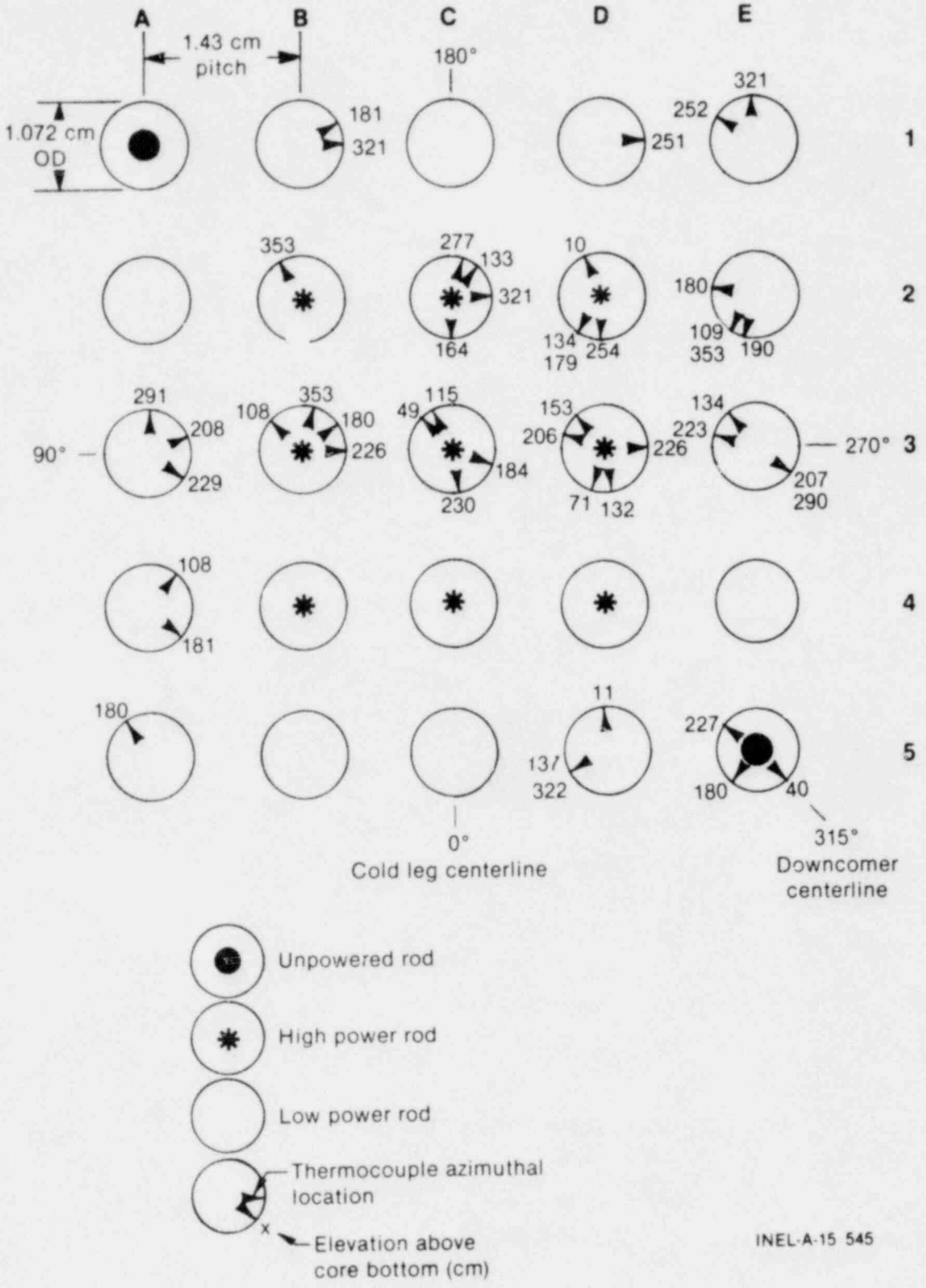

Figure 3. Plan view of core for Test S-07-10.

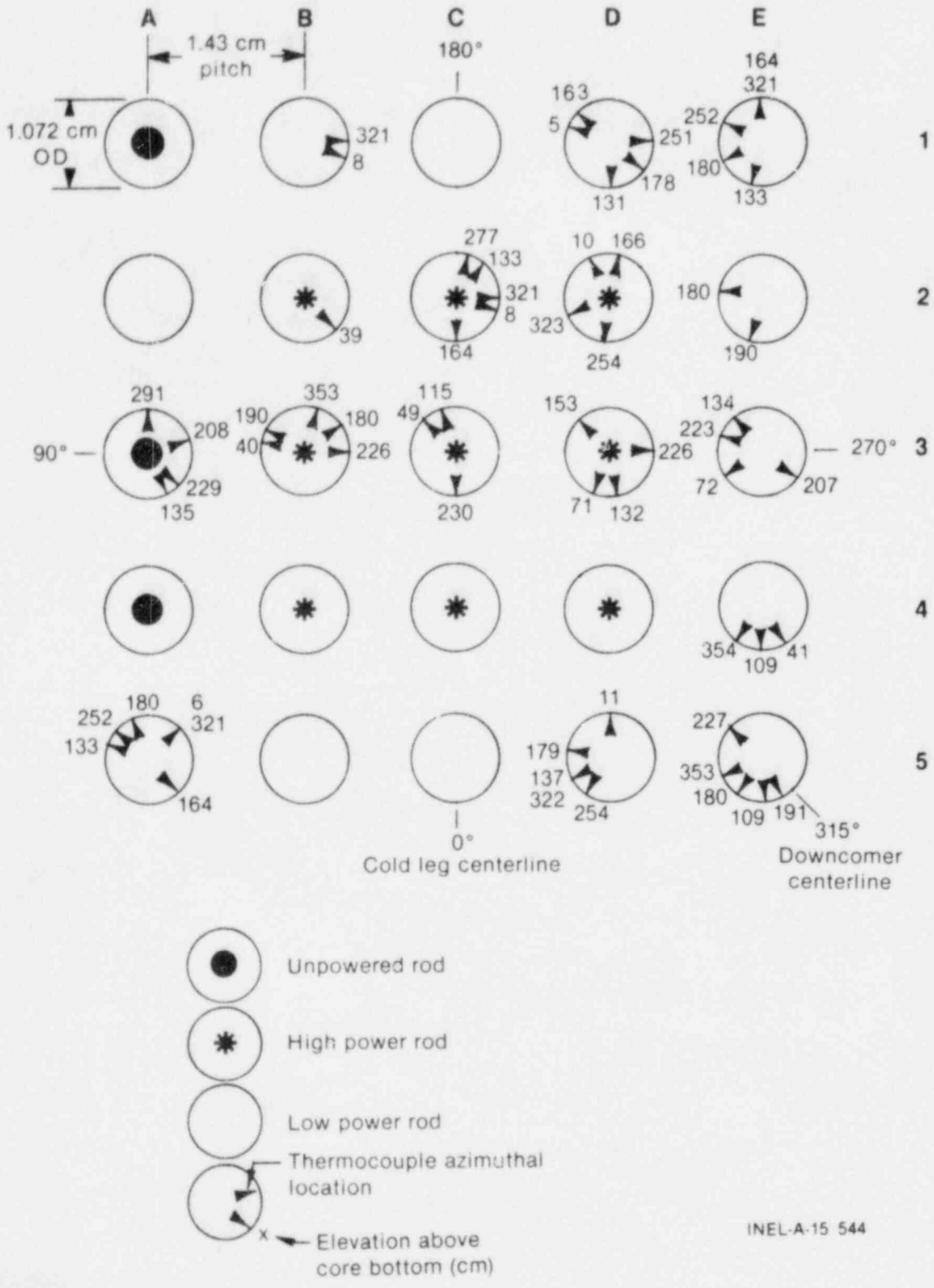

Figure 4. Plan view of core for Test S-07-10D.

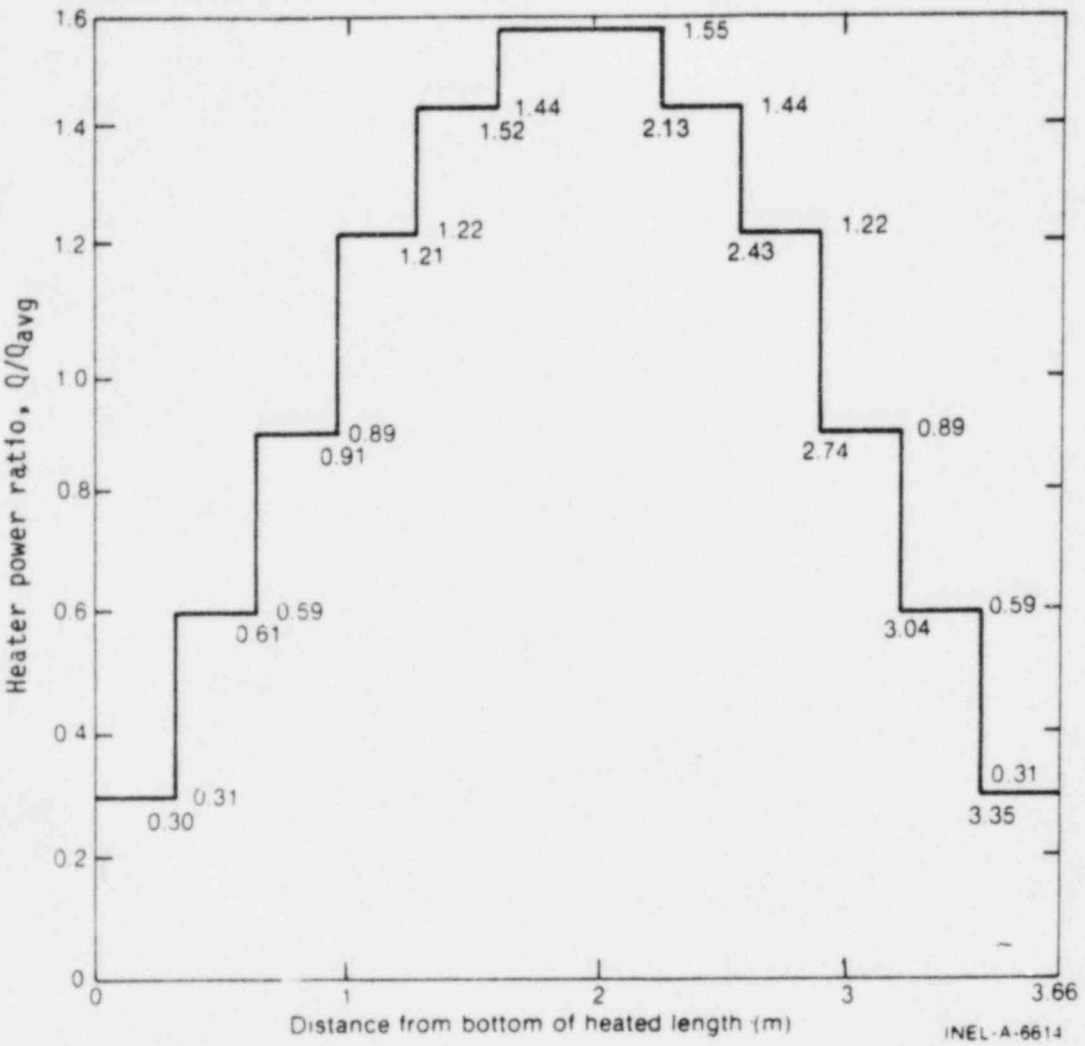

Figure 5. Semiscale Mod-3 heater rod axial power distribution.

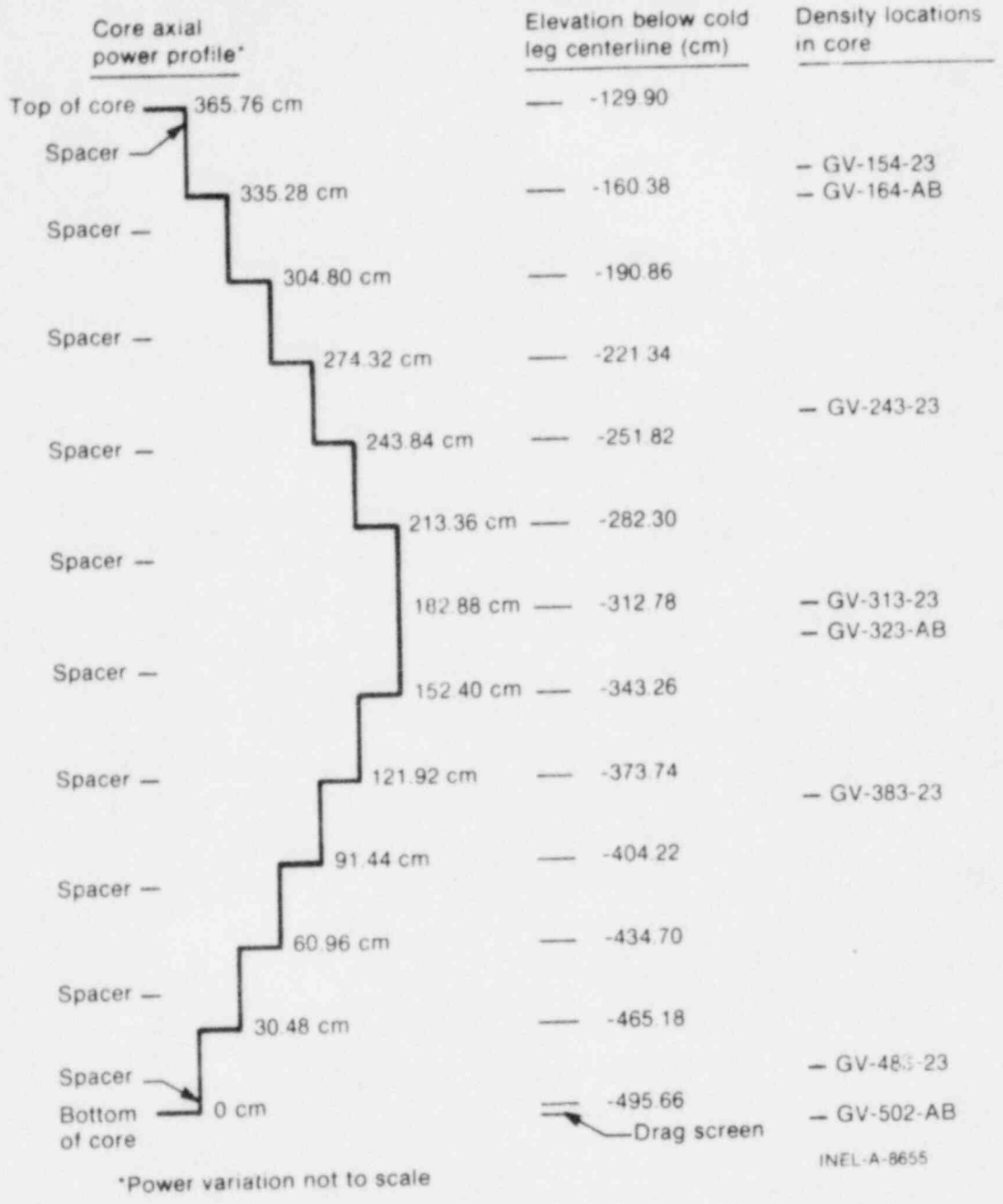

Figure 6. Axial power profile in relation to vessel instrumentation.

1.94 ± 0.01 MW. This difference in powered rod configuration is not expected to impact overall test performance but must, of course, be taken into consideration when comparing certain localized in-core phenomena.

Approximately 250 measurements consisting of various pressures, temperatures and other fluid conditions were taken during Test S-07-10. Additionally, a direct measurement of break flow was obtained with instrumentation located downstream of the break orifice in spool piece 41 (Figure 1).

Figure 7 is a simplified view of the small break spoolpiece showing the location of the break plane and downstream instrumentation. A more detailed description of Mod-3 system hardware and instrumentation may be found in the System Design Description.[4]

2.2 Test Procedures and Conditions

Prior to the initiation of the test, the Semiscale system was filled with demineralized water and vented to ensure a liquid full system. Water in the steam generator feedwater tanks was heated to the desired temperature and the required levels were established in the steam generator secondary sides. Accumulator water level was established and the accumulator was pressurized with nitrogen gas to the desired pressure. Instrumentation was calibrated and zeroed as necessary and a system hydrostatic test was preformed.[a] After the necessary protective trip controls and peripheral hardware controls (pumps, valves, etc.) had been set, the system was brought up to initial conditions and allowed to equilibrate. When initial

---

a. While an actual measurement of leakage was not made for Test S-07-10, it is estimated that it was less than 0.03 kg/s. This value is rather negligible relative to break flow for a 10% break (see Section 3.3).

Leakage was measured prior to Test S-07-10D and was found to be 0.007 kg/s at 8.27 MPa system pressure and 0.03 kg/s at 15.5 MPa system pressure.

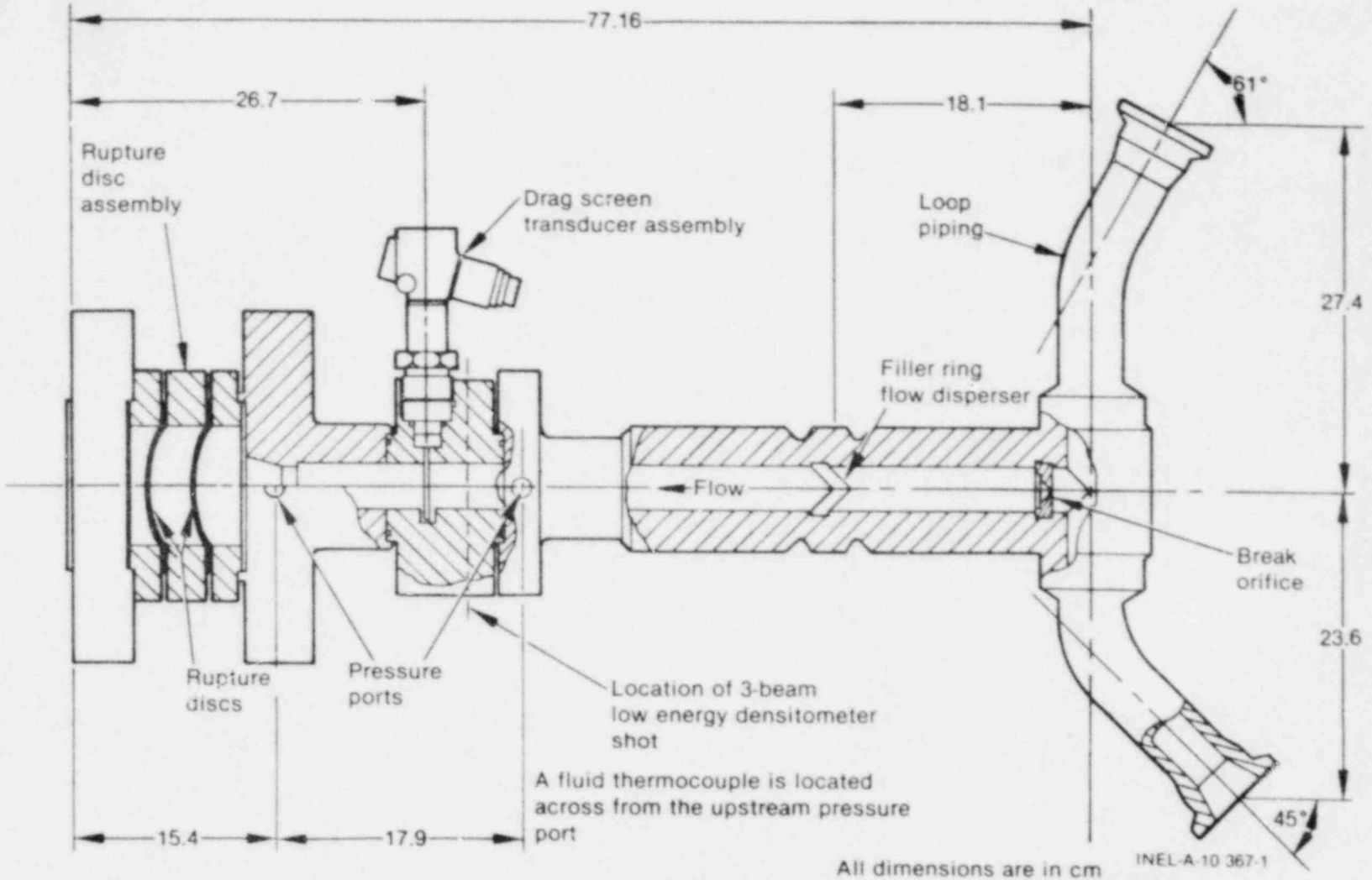

Figure 7. Communicative break assembly for Semiscale Mod-3 broken loop cold leg.

conditions were within specified tolerances, the test was initiated by rupturing discs downstream of the break orifice to break the system pressure boundary. Transient core power control and the intact and broken loop pump speed controllers were initiated by a pressure trip 1 s after the pressurizer pressure reached 12.41 MPa. The pressure suppression system (PSS) tank pressure was held initially at 1034 kPa, then ramped down to 241 kPa from 50 to 100 s in Test S-07-10 and from 50 to 150 s in Test S-07-10D, then held there for the remainder of the test. This was done so as to keep the downstream drag screen measurement within range while not affecting the choked flow through the break orifice. Both steam generator feedwater valves were sequenced to close 1 s after the pressurizer pressure reached 12.41 MPa. The steam valves were sequenced to close 11 s later. For Test S-07-10D, the broken loop steam generator steam discharge valve was left open in its initial position for the entire test. The secondary steam flow paths from the steam generator are shown schematically in Figure 8. A discussion of how the core electric power curve was determined, and how other various component controls were selected, may be found in Reference 5.

For these tests, all of the ECC systems (only intact loop cold leg ECC injection was used) were inactive until it had been determined that sufficiently elevated core temperatures had been obtained as evidenced by on-line core temperature monitors. The ECC systems were then enabled and their operation was automatic with regard to pressure. Prior to enabling of the accumulator, by opening a block valve, the nitrogen in the accumulator tank was bled off, as necessary, to maintain approximately 1380 kPa differential pressure above the system.

The specified and actual test conditions for Tests S-07-10 and S-07-10D are compared in Table 1. In general, the initial conditions and test parameters were judged as satisfactory to meet the test objectives. The core power curves, pump speed curves and PSS tank pressure curves are shown in Figures 9, 10, and 11, respectively. Table 2 compares the timing of specified operations to the actual time of their execution. Noteworthy variations from the desired conditions are noted in the following areas.

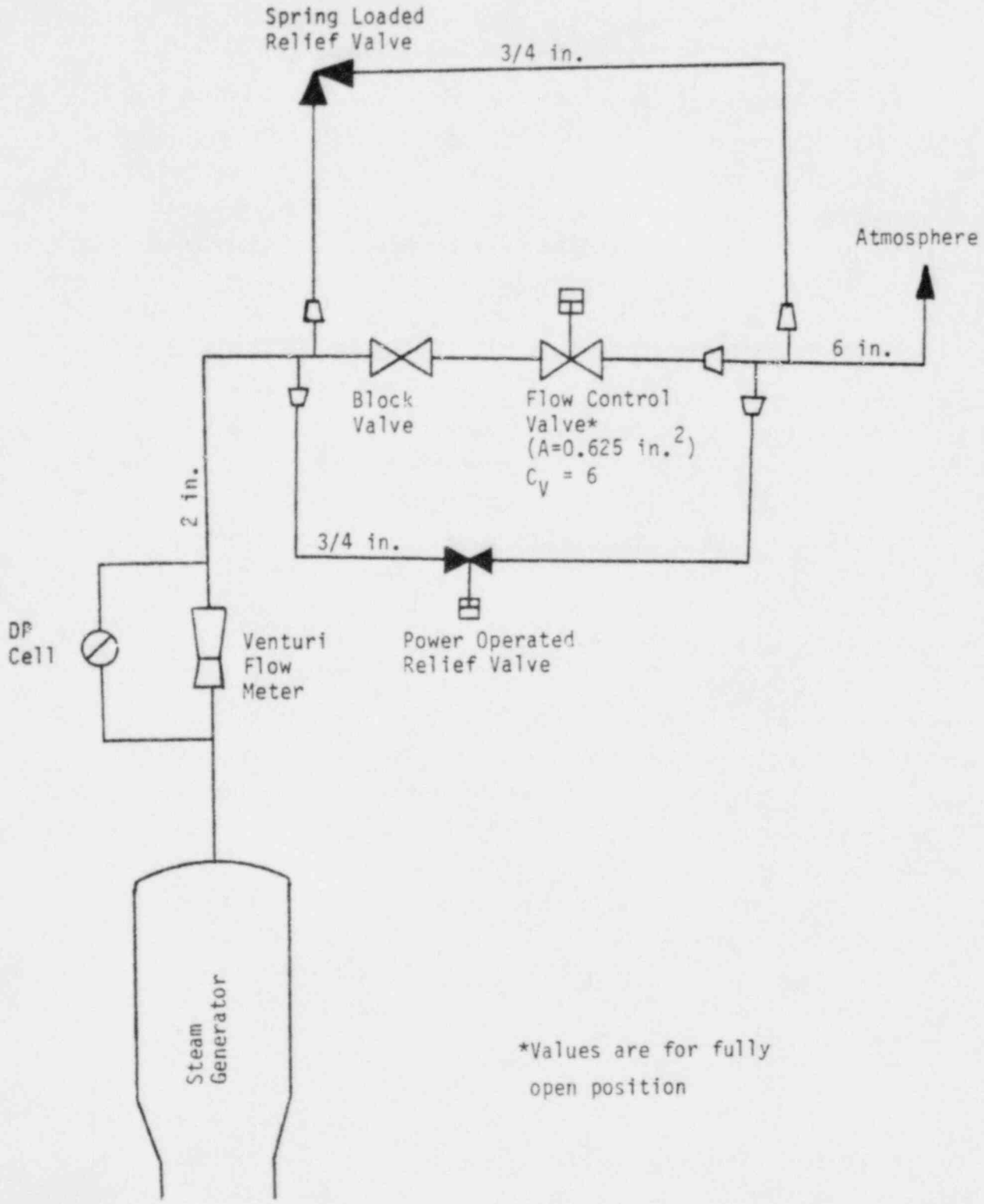

Figure 8. Broken loop steam generator outlet flow paths.

TABLE 1. INITIAL CONDITIONS AND ECC REQUIREMENTS FOR TESTS S-07-10 and S-07-10D

Configuration	S-07-10 Specified	S-07-10 Actual	S-07-10D[a]
Break size	0.223 cm^2 (10%)	✓	✓
Break type	Communicative	✓	✓
Break location	Cold leg	✓	✓
Break orientation	Side of pipe	✓	✓
Pressurizer location	Intact loop	✓	✓
Initial Conditions			
Nominal system pressure	15.5 MPa	15.7 MPa	15.74 MPa
Hot leg fluid temperature	594 K	591 K	592 K
Cold leg fluid temperature	557 K	556 K	556 K
Core ΔT	37 K	35 K	35 K
Core inlet flow	9.77 kg/s	9.72 kg/s	9.7 kg/s
Total core power	2 MW	1.94 MW	1.927 MW
High power rods	1.010 MW	0.992 MW	0.985 MW
Low power rods	0.990 MW	0.948 MW	0.984 MW
Core radial power peaking	29%	26.7%	24.95%
Power decay curve	See Figure 7		
Pressurizer liquid mass[b]	10.4 kg	10.4 kg	10.4 kg
Pressurizer line resistance[b]	5798 s^2/m^3-cm^2	✓	✓
Steam generator secondary[b]			
Initial water level			
Intact Loop	295 ± 5 cm	295 ± 5 cm	295 ± 5 cm
Broken Loop	998 ± 5 cm	998 ± 5 cm	998 ± 5 cm

TABLE 1. (Continued)

Configuration	S-07-10 Specified	S-07-10 Actual	S-07-10D[a]
ECC Parameters[c]			
Intact loop accumulator			
Location	Cold leg	✓	✓
System pressure at actuation	---	1450 kPa	1600 kPa
Tank pressure at actuation	---	2740 kPa	3100 kPa
Liquid volume[b]	0.045 m^3	0.045 m^3	0.045 m^3
Gas volume[b]	0.025 m^3	0.025 m^3	0.025 m^3
Line resistance[b]	10675 s^2/m^3-cm^2	✓	✓
Temperature	300 K	300 K	300 K
Intact Loop HPIS			
Location	Cold leg	✓	✓
Actuation pressure	---	1450 kPa	1600 kPa
Injection rate (average)	0.062 kg/s	0.062 kg/s	0.075 kg/s
Temperature	300 K	300 K	300 K
Intact Loop LPIS			
Location	Cold leg	✓	✓
Actuation pressure[d]	---	1730 kPa	2100 kPa
Injection rate (average)	0.16 kg/s	0.135 kg/s	0.11 kg/s
Temperature	300 K	300 K	300 K
PSS Tank Pressure	See Figure 9		

a. Values for Test S-07-10D were specified to be equal to those for Test S-07-10.

b. These values are established through the use of process instrumentation.

c. Note that only intact loop ECC systems were used.

d. The LPIS was enabled approximately 100 s after the HPIS and accumulator.

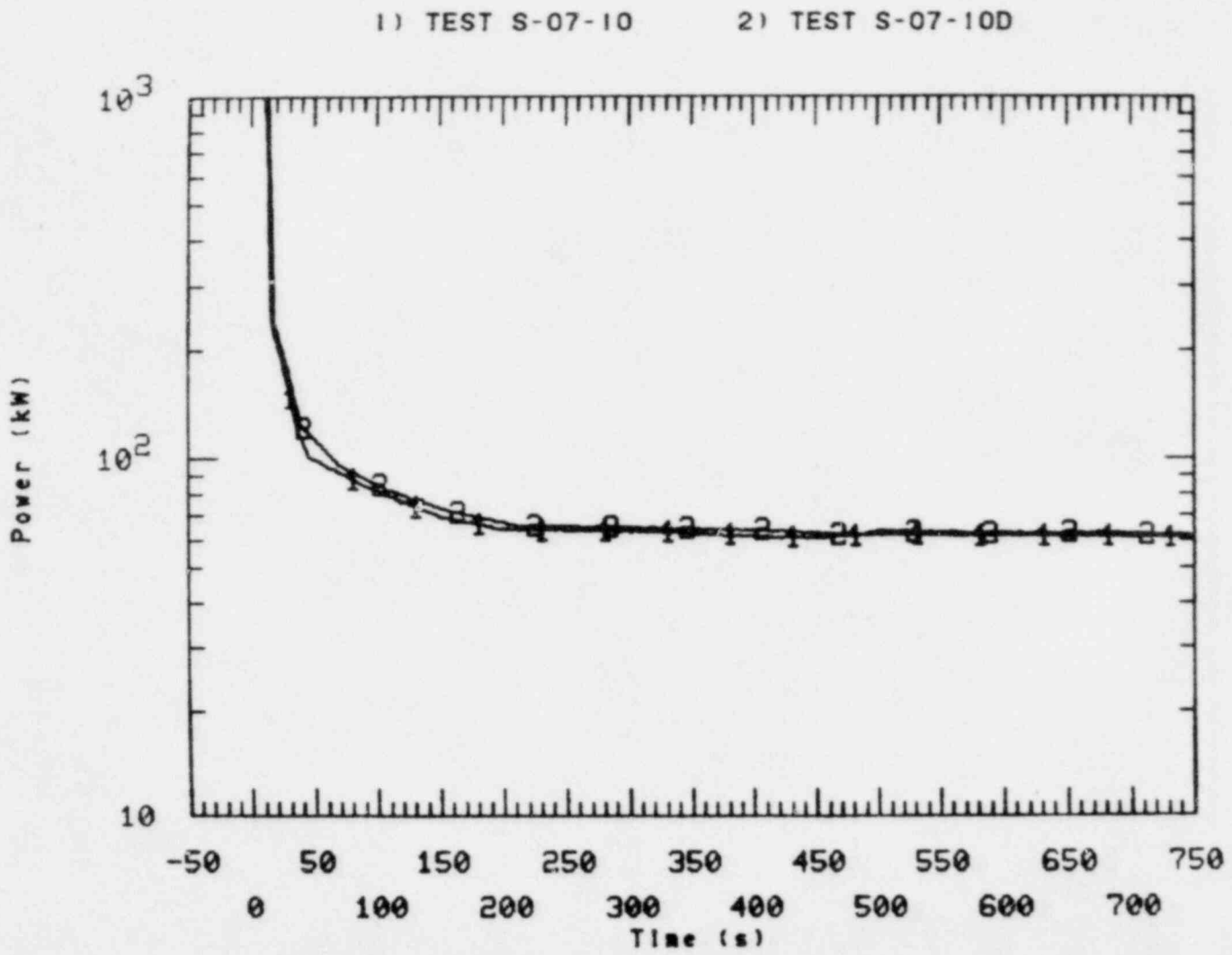

Figure 9. Comparison of core power curves from Tests S-07-10 and S-07-10D.

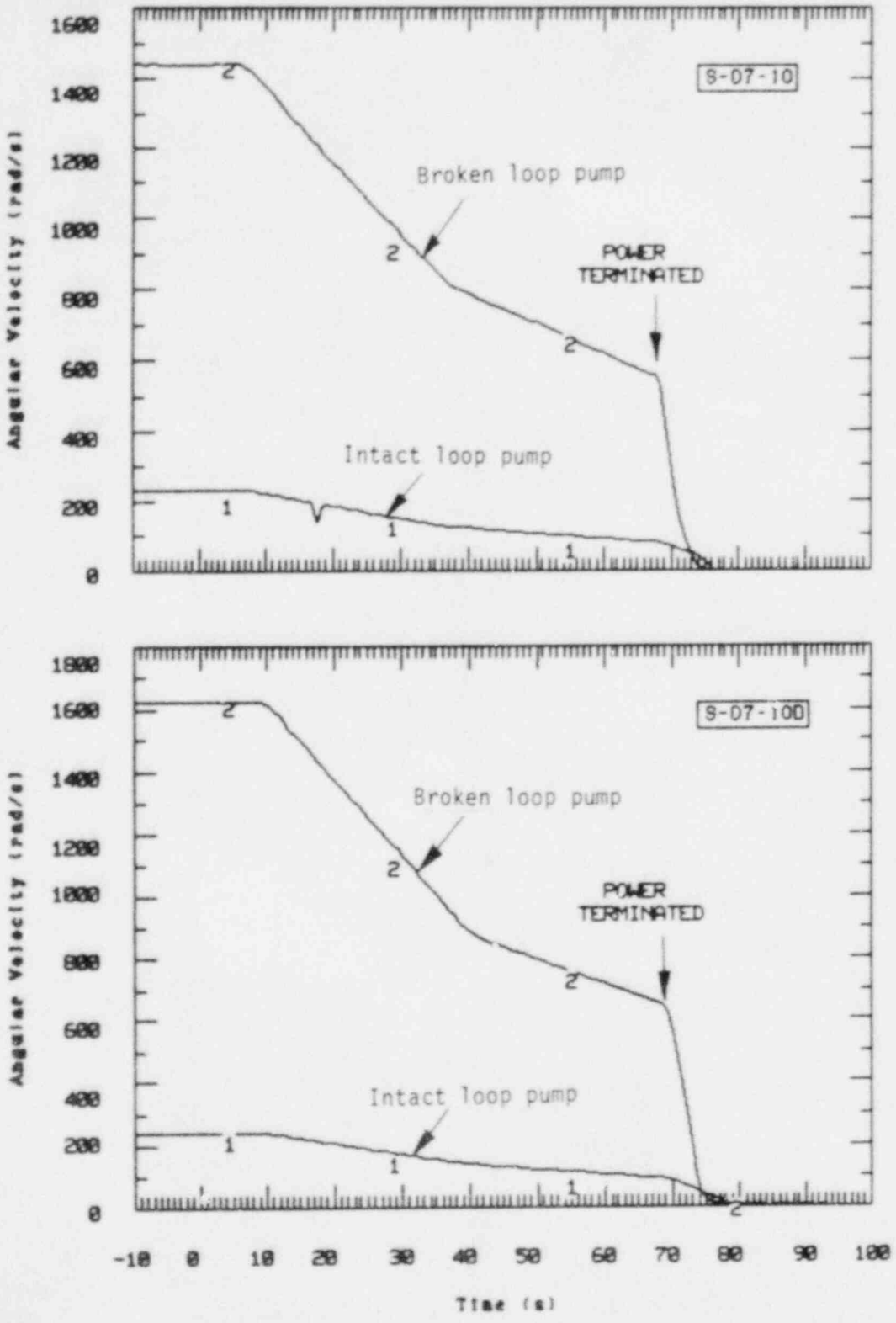

Figure 10. Pump speed curves from Tests S-07-10 and S-07-100.

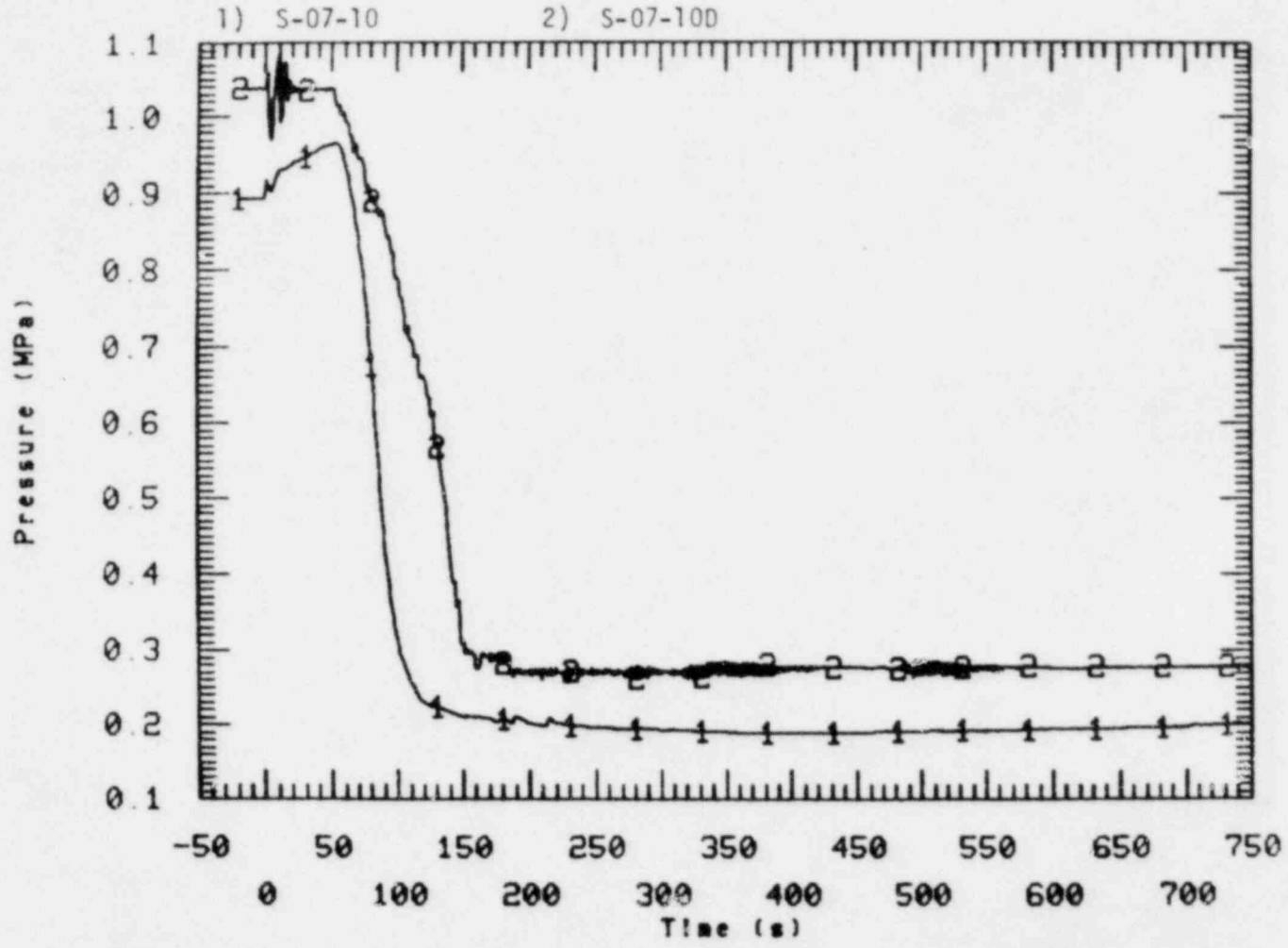

Figure 11. Pressure suppression system tank pressures.

TABLE 2. SEQUENCE OF OPERATIONAL PROCEDURES FOR TESTS S-07-10 AND S-07-10D

Event	Specified Time(s)	Actual Time(s) S-07-10	Actual Time(s) S-07-10D
Rupture	0.0	0.0	0.0
Core power decay initiated Intact and broken loop pumps begin coastdown Intact and broken loop steam generator feedwater valves begin to close	1 s after pressurizer pressure reads 12.41 MPa	7.2	7.7
Intact loop steam generator steam valve begins to close	12 s after pressurizer pressure reaches 12.41 MPa	17	21
Broken loop steam generator steam valve begins to close	12 s after pressurizer pressure reaches 12.41 MPa	17[a]	N/A
Initiate PSS tank pressure reduction	50	50	50
Enable accumulator and HPIS injection	When on-line monitors indicate high core temperatures	438	460
Enable LPIS injection		540	560
Terminate test		748	748

a. Time for broken loop valve closure is approximate.

Test S-07-10:

1. An incorrect pump speed coastdown curve was followed. At the time of pump power trip pump speeds were approximately 70% greater than specified. The rapid degradation of pump head, which reduced the effect of pump speed, and the fact that accurate determination of the actual coastdown was made, led to the conclusion that this variance did not have an unacceptable influence on test results or usefulness.

2. Several instrumentation failures occurred. Most were deemed minor and had no impact on overall test analysis. One failure was the differential pressure measurement on the broken loop steam generator steam discharge line which should have indicated when the steam valve closed. Definitive determination of actual valve closure time is not possible, but post data release analysis indicates that it probably closed at approximately the same time as the corresponding intact loop valve.

3. The LPIS pump provided flow against a back pressure of 1730 kPa versus the specified value of 1035 kPa. This has little bearing on test results since the LPIS was enabled 100 s after the accumulator and HPIS which began refilling the vessel, and nearly all the core had been quenched prior to LPIS injection.

Test S-07-10D:

1. The broken loop high pressure injection system pump was used to provide leakage makeup which was to be terminated at test initiation. However, the makeup flow was left on until 150 s into the transient and was injecting ambient temperature water at a flow rate of 0.0373 kg/s upstream of

the break into spool piece 40. Calculations show the combined mass injection and the associated vapor condensation potential, which comes from heating of the fluid to saturation temperature, amount to, at most, 0.063 kg/s, which is on the order of 10% of the average break flow during this period. No prominent differences in system behavior attributable to make up flow were observed. Additionally, the Storz lens videotape of the break during the test (see Appendix A) shows no apparent change in upstream-of-break conditions associated with termination of makeup flow. A violently turbulent flow was observed on the upstream side of the break orifice from about 100 to 250 s. While the makeup flow may have complicated the ability to derive redundant break flow measurements from upstream flow differencing techniques, based on a preliminary data review, it was concluded that the downstream flow measurement worked quite well. Since a break flow measurement was obtained and little impact on system behavior was observed, it was concluded that the test would satisfy its objectives.

3. TEST RESULTS

The following sections present a preliminary evaluation of the results obtained during Tests S-07-10 and S-07-10D.

3.1 Thermal-Hydraulic Response of the Mod-3 System for Tests S-07-10 and S-07-10D

As presented in the following analysis, the test conditions and procedures followed for Tests S-07-10 and S-07-10D resulted in the complete voiding of the Mod-3 core and accompanying elevated rod cladding temperatures. Table 3 presents a sequence of events derived from test data outlining the important operations and thermal-hydraulic phenomena which occurred. The overall conduct and results can be briefly summarized as follows: For Test S-07-10, no broken loop emergency core coolant (ECC) injection was used and the intact loop ECC was delayed. Following rupture in the broken loop cold leg a continuous depressurization took place and voiding of the loops from the upper elevations down was observed out to about 150 s. The break uncovered between 65 and 85 s. The vessel and downcomer liquid then boiled off, progressively drying out the rods from the top down. By 370 s, the densitometers, ΔP cells, and the Storz lens[a] in the lower downcomer indicated that the vessel was completely voided. As steam flow decreased, several upper core thermocouples indicated temperature turnover and/or rewet between 395 and 415 s, indicative of a small amount of liquid fallback. Rod temperatures were allowed to climb to 1050 K at 438 s, at which time ECC injection was manually initiated. Water reached the core several seconds later resulting in a slight repressurization due to steam generation. The core was observed to progressively quench from the bottom up and was completely quenched by 562 s. The system stablized and the test was terminated at 748 s.

---

a. See Appendix A for further examples of use of the Storz lens in Tests S-07-10 and S-07-10D.

TABLE 3. SEQUENCE OF EVENTS FOR TESTS S-07-10 AND S-07-10D

Event	Time(s) S-07-10	S-07-10D
Blowdown initiated	t = 0	0
Pressurizer pressure = 12.41 MPa	t = 6.2	6.9
Begin core power decay	t = 7.2	7.7
Intact loop and broken loop pump coastdown initiated		
Intact loop steam generator feedwater valve begins to close (4 s to close)		
Broken loop steam generator feedwater valve begins to close (1.5 s to close)		
Upper plenum fluid saturates	t = 8.5	8.0
Intact loop steam generator steam valve begins to close (3 s to close)	t = 17	21
Broken loop steam generator steam valve closed	t = 17[a]	N/A
Pressurizer empties	t = 20	20
Entire system saturated, system pressure = 7.1 MPa	t = 22	27
Upper plenum liquid level reaches intact loop hot leg	t = 45	42
Pressure suppression system pressure reduction begins	t = 56	52
Intact loop pump suction blows out	t = 60	85
Liquid from cold legs drains to vessel and pump suctions resulting in two-phase mixture at break	t = 65 to 85	65 to 90
Power to pumps terminated	t = 68	69
Pumps stop	t = 77	79

a. Actual time unknown.

TABLE 3. (Continued)

Event	Time(s) S-07-10	S-07-10D
Top of support tubes uncovered in upper head	t = 95	80
Pressure suppression system tank pressure reduction finished.	t = 120	160
Broken loop pump suction swept out	t = 140	N/A
First dryouts indicated in upper regions of the core	t = 211	268 - 300
Dryout of core peak power zone from top down	t = 226 to 245	268 - 300
Core completely voided	t = 370	435
Fallback turns over and/or rewets thermocouples progressively from upper to mid core	t = 395 to 415	N/A
Accumulator injection begins	t = 438	460
HPIS injection begins		
ECC water reaches bottom of core	t = 445	467
Accumulator flow falls to zero as accumulator "floats" on the system	t = 460	482
System repressurized due to steam generation	t = 475	490
Core peak power zone quenched	t = 472 to 485	488 to 498
LPIS injection initiated	t = 540	560
Entire core quenched	t = 562	525
Test terminated	t = 748	748

For Test S-07-10D no broken loop ECC injection was used and the intact loop ECC was delayed. Following rupture in the broken loop cold leg a continuous depressurization took place and voiding of the loops from the upper elevations downward was observed out to about 150 s. Conditions upstream of the break become two-phase between 65 to 90 s. Heat transfer to the broken loop steam generator resulted in condensation and preferential flow to that loop which acted to keep liquid in the broken loop pump suction for the entire test. The vessel and downcomer liquid boiled off, progressively drying out the rods from the top down. By 440 s, the vessel was completely voided. Rod temperatures were allowed to climb to an average of 920 K at 460 s before ECC injection was initiated. Water reached the core several seconds later causing a slight system repressurization. The core was observed to progressively quench from the bottom up and was completely quenched by 5[illegible] s.

In the following paragraphs a more detailed analysis is presented of factors which influenced system behavior. Data from Test S-07-10 has been released. The following plots and additional data from that test may be found in Reference 6.

3.2 Pressure Response

The upper plenum pressures for Tests S-07-10 and S-07-10D are compared in Figure 12. Immediately following rupture the system fluid was subcooled and depressurization was relatively rapid. A brief plateau occurred in Test S-07-10 at 2.5 s when system pressure reached the upper plenum saturation pressure of 12.0 MPa. Figure 13 compares the upper plenum, hot leg, and cold leg temperatures to the saturation temperature for each test. Structural heat transfer caused the hot leg fluid temperature to remain several degrees above saturation temperature for a period, as was evidenced by several metal temperature measurements in the system. Rapid depressurization continued until the entire system became saturated. At that point, the resultant flashing of fluid caused a decrease in the rate of depressurization seen in Figure 12. The knee in the pressure curve was rather sharp for Test S-07-10 while being more gradual in

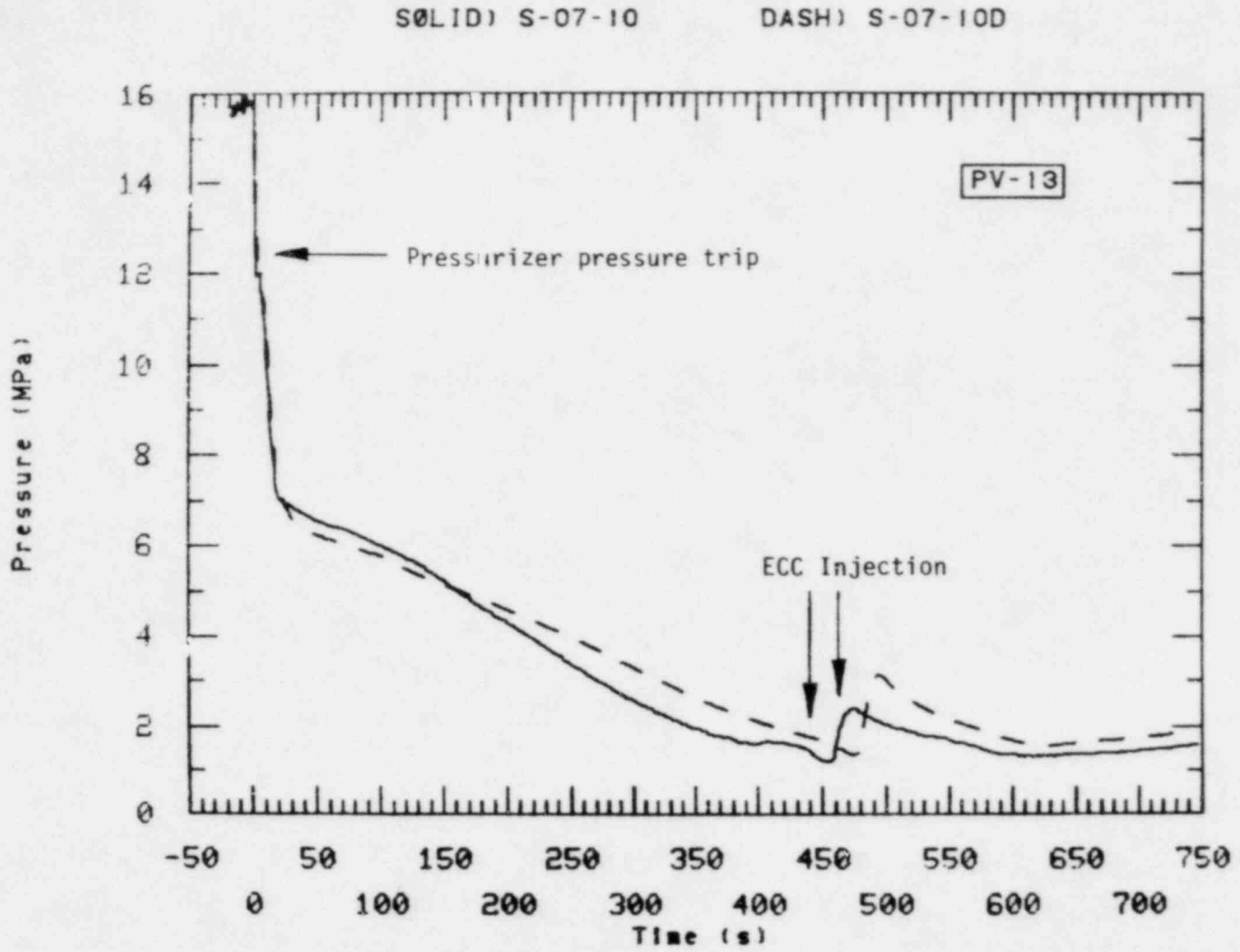

Figure 12. Comparison of system pressures from Tests S-07-10 and S-07-10D.

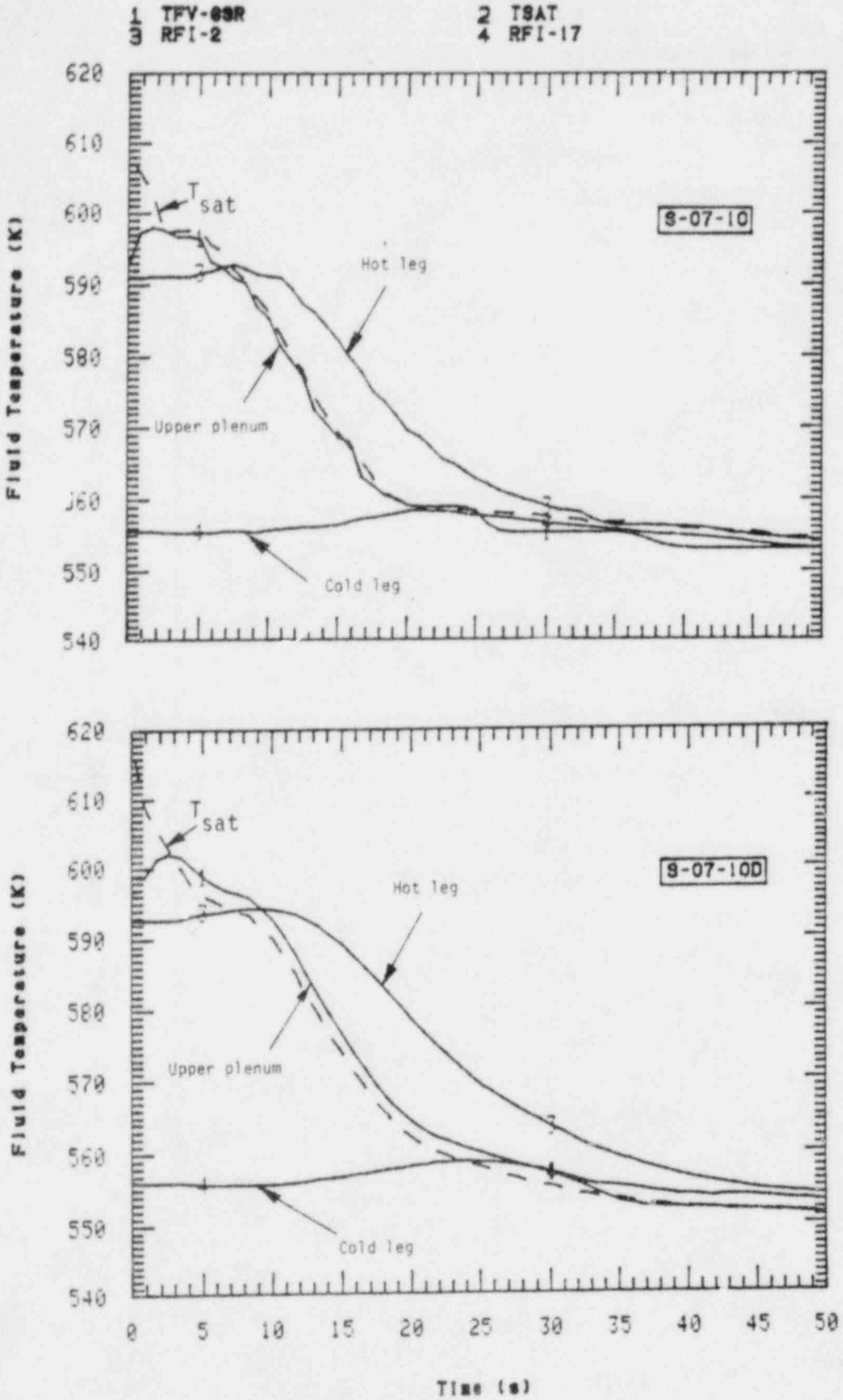

Figure 13. Selected system fluid temperatures compared to saturation temperature for Tests S-07-10 and S-07-10D.

Test S-07-10D. Figure 14 shows a short term plot of system pressure where this is more clearly seen. As indicated earlier, the steam generators (with the exception of the broken loop in S-07-10D) were isolated at approximately 17 to 21 s. At about this time the broken loop hot and cold leg temperatures in Test S-07-10 were seen to converge (Figure 15, top), while in Test S-07-10D there is evidence of sufficient continued cooling of the fluid to have resulted in the more gradual decline in the pressure out to 35 s (Figure 15, bottom). The possibilty also exists that the pressure response in the initial 40 s of the transient could have been influenced somewhat by such factors as a variance in system "soaking" time prior to rupture, and the extensive system insulation changes made between the two tests. This included installation of the downcomer honeycomb insulator. Overlays of the primary system pressure and steam generator secondary pressures are shown in Figure 16. The feedwater valves were closed at approximately 7 to 8 s on a pressure trip from the primary system pressurizer. Steam valves were closed about 10 s later except for the broken loop steam valve in Test S-07-10D. In the isolated steam generators the pressure increased slightly and then decreased slowly throughout the remainder of the test. In Test S-07-10D, the broken loop steam generator blew down below the primary system pressure initially, and then depressurized at a much slower rate than the primary system. The relative behavior of the primary and secondary pressures indicates that the two are rather decoupled during the transients due to high steam generator tube voiding and resultant poor heat transfer.

Figure 17 presents a conservatively high calculation of energy removal from the broken loop steam generator based on secondary side liquid boiloff. The calculation is considered conservatively high because the Mod-3 steam generator has an inefficient steam separator and a good deal of liquid may be removed by entrainment. It can be seen that as the primary side of the tubes voids early in the transient energy removal from the steam generator decreases sharply, denoting the decrease in heat transfer from the primary to the

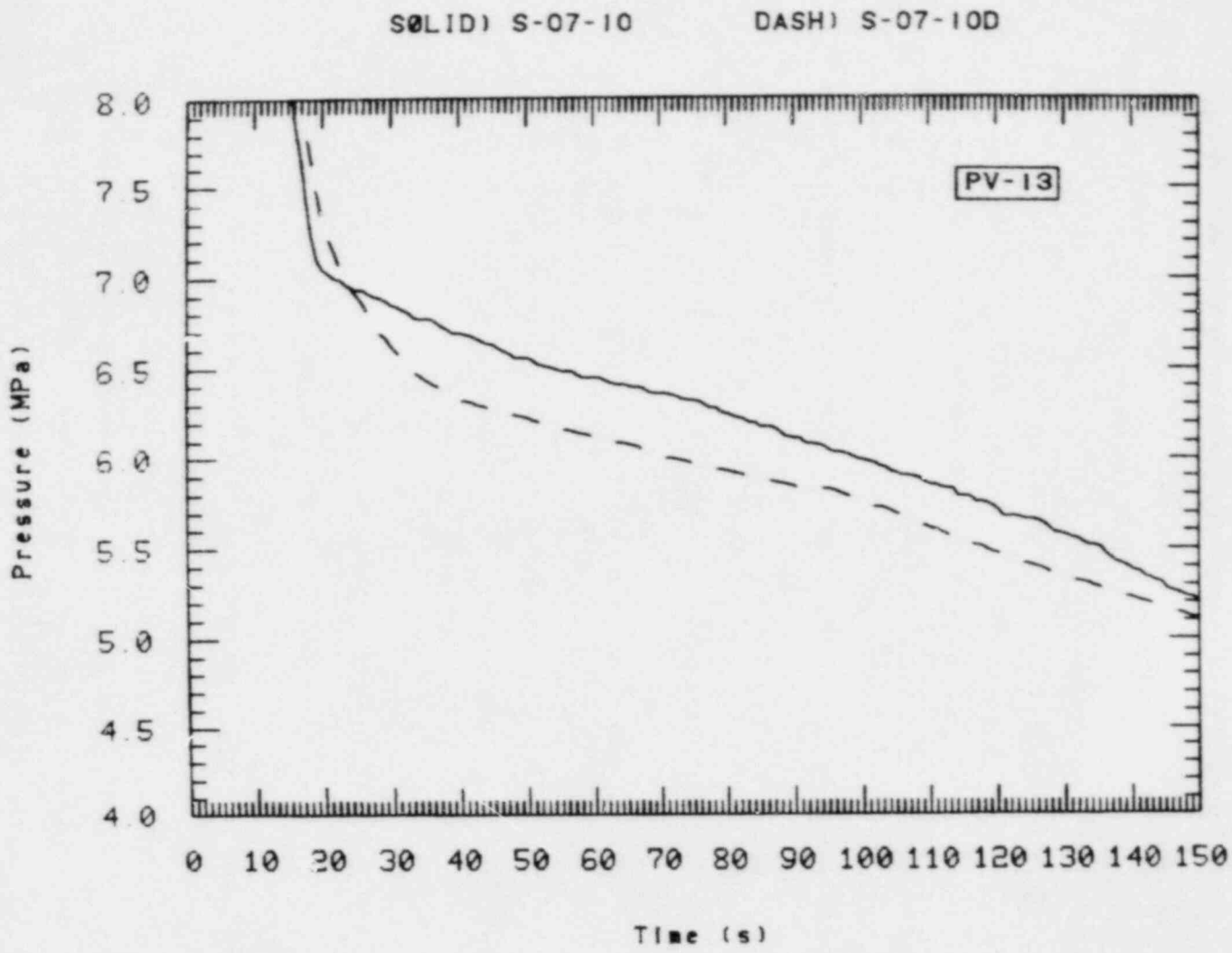

Figure 14. Short term plot of system pressures from Tests S-07-10 and S-07-10D.

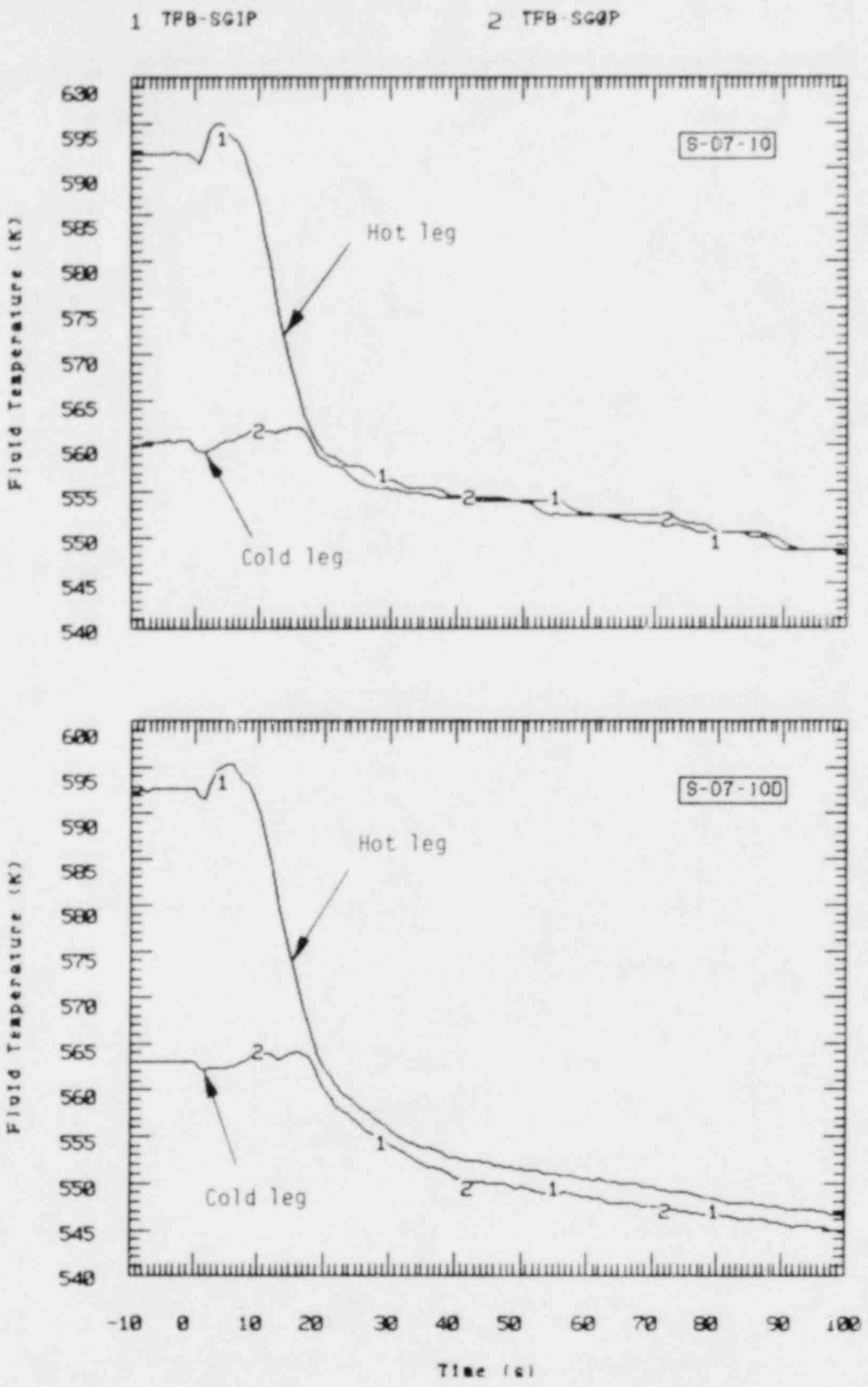

Figure 15. Comparison of broken loop steam generator primary side hot and cold leg temperatures for Tests S-07-10 and S-07-10D.

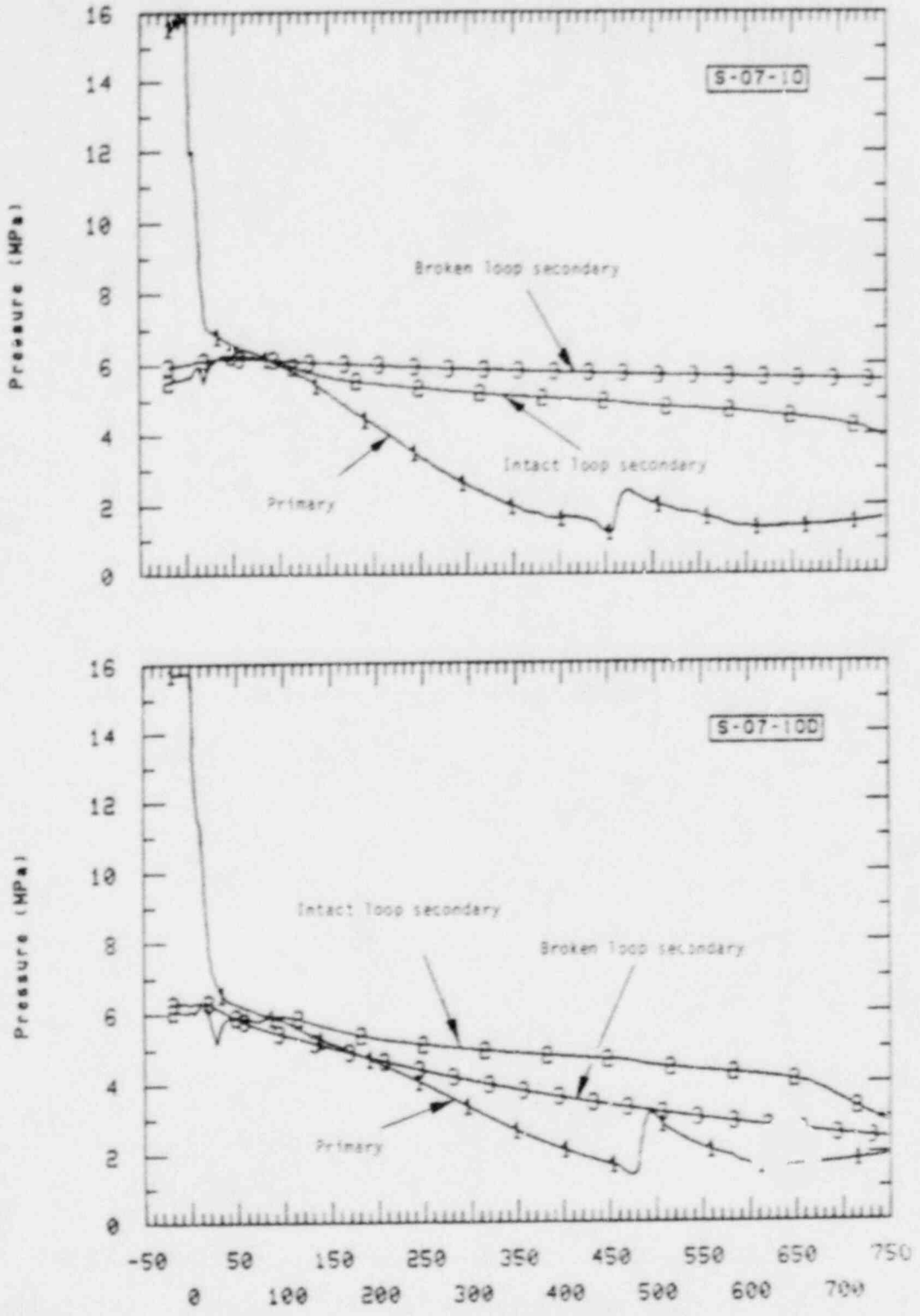

Figure 16. Comparison of primary and secondary side pressures for Tests S-07-10 and S-07-10D.

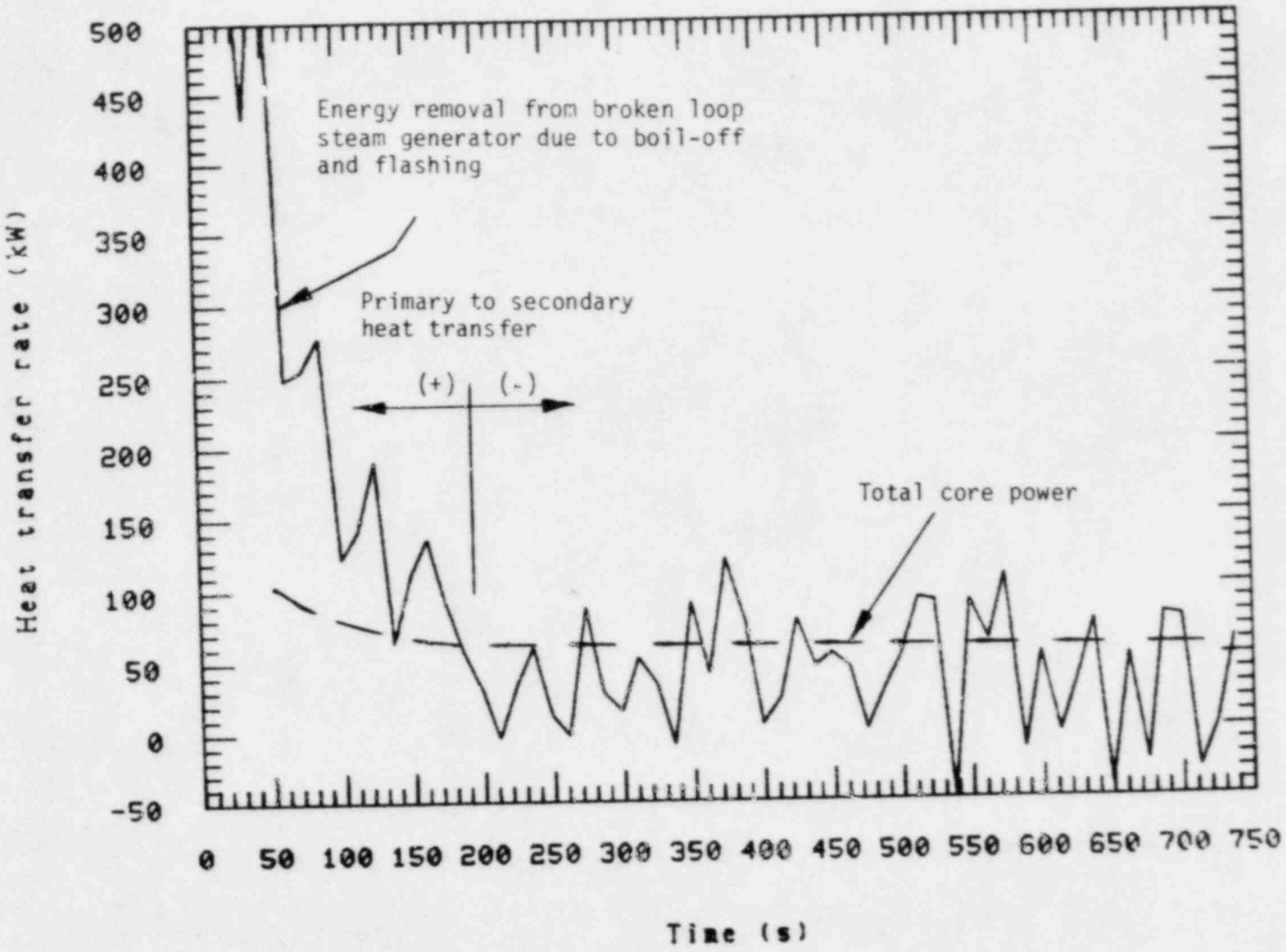

Figure 17. Calculated energy removal from the broken loop steam generator secondary for Test S-07-10D compared to total core power.

secondary. Energy removal falls to near zero as the steam generator becomes a heat source for the primary after 190 s. From then on, flashing results in an energy removal rate equivalent to about half of core power despite cooling of the secondary fluid by heat transfer to the primary.

The depressurization continued at a fairly constant rate until ECC injection began. A slight repressurization occurred as a result of steam generation in the core following penetration of ECC fluid. In each test, the system pressure rose above the accumulator pressure, as shown in Figure 18 for Test S-07-10. This caused the accumulator flow to temporarily cease and for the remainder of the tests the accumulator "floated" on the system. The initial injection spike resulted in 17.26 ℓ of liquid being injected in Test S-07-10, while 19.04 ℓ was injected in Test S-07-10D. Very low accumulator liquid outflow was calculated from differential pressure cell measurements, and liquid was still present in the accumulator at the end of the tests. In Test S-07-10, 20.45 ℓ out of the total accumulator liquid inventory of 45 ℓ was injected. For Test S-07-10D a total of 28.2 out of 45 ℓ was injected.

The system pressure in Test S-07-10D eventually crossed over that of Test S-07-10 and stayed above for the remainder of the test due to differences in break conditions as discribed below.

3.3 Break Flow

Figure 19 presents the break mass flows calculated from downstream measurements for Tests S-07-10 and S-07-10D (see Figure 7 for measurement locations.) Figures 20 and 21 compare upstream-of-break fluid densities for the two tests. Only a small difference was calculated between break mass flows between the two tests. The most notable difference occurred in the time period between 70 to 150 s when the density measurements, shown in Figures 20 and 21, indicate that the broken loop cold leg completely voided during Test S-07-10, while in Test S-07-10D a relatively lower quality fluid remained in the vicinity of the break on the pump side. The change in break conditions is most likely responsible for the slower

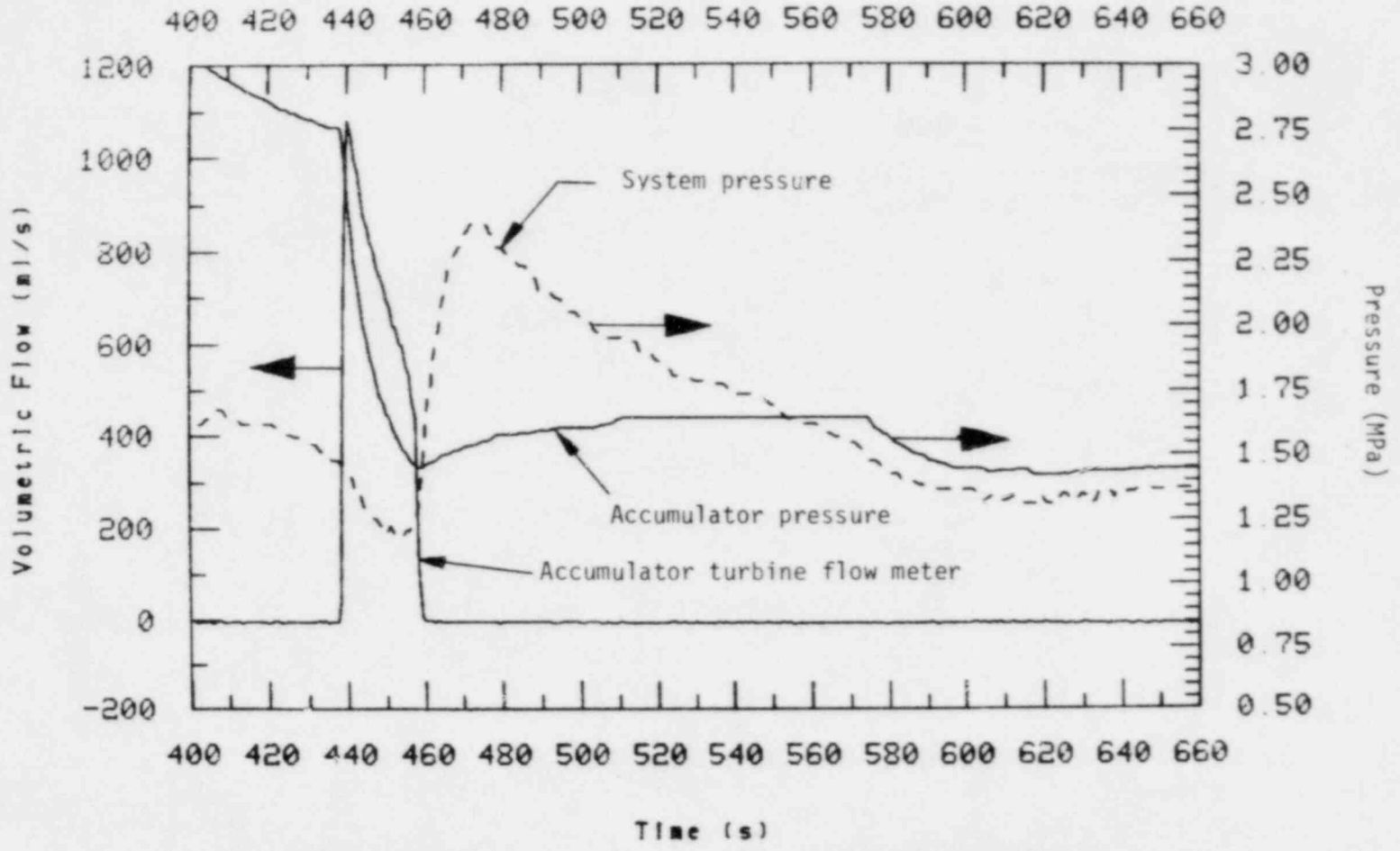

Figure 18. Accumulator response to system pressure for Test S-07-10.

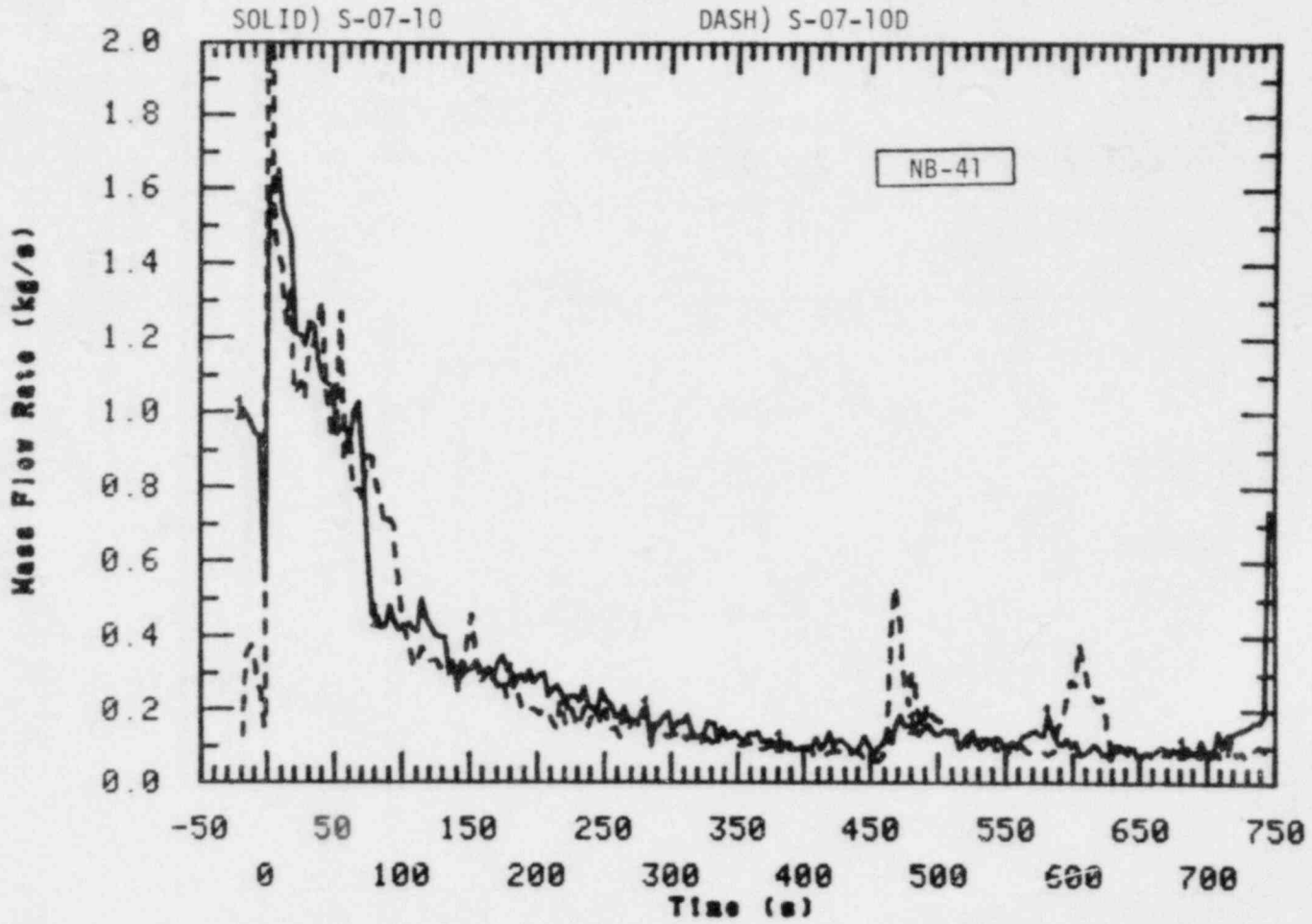

Figure 19. Comparison of break mass flow rates for Tests S-07-10 and S-07-10D as calculated from downstream measurements.

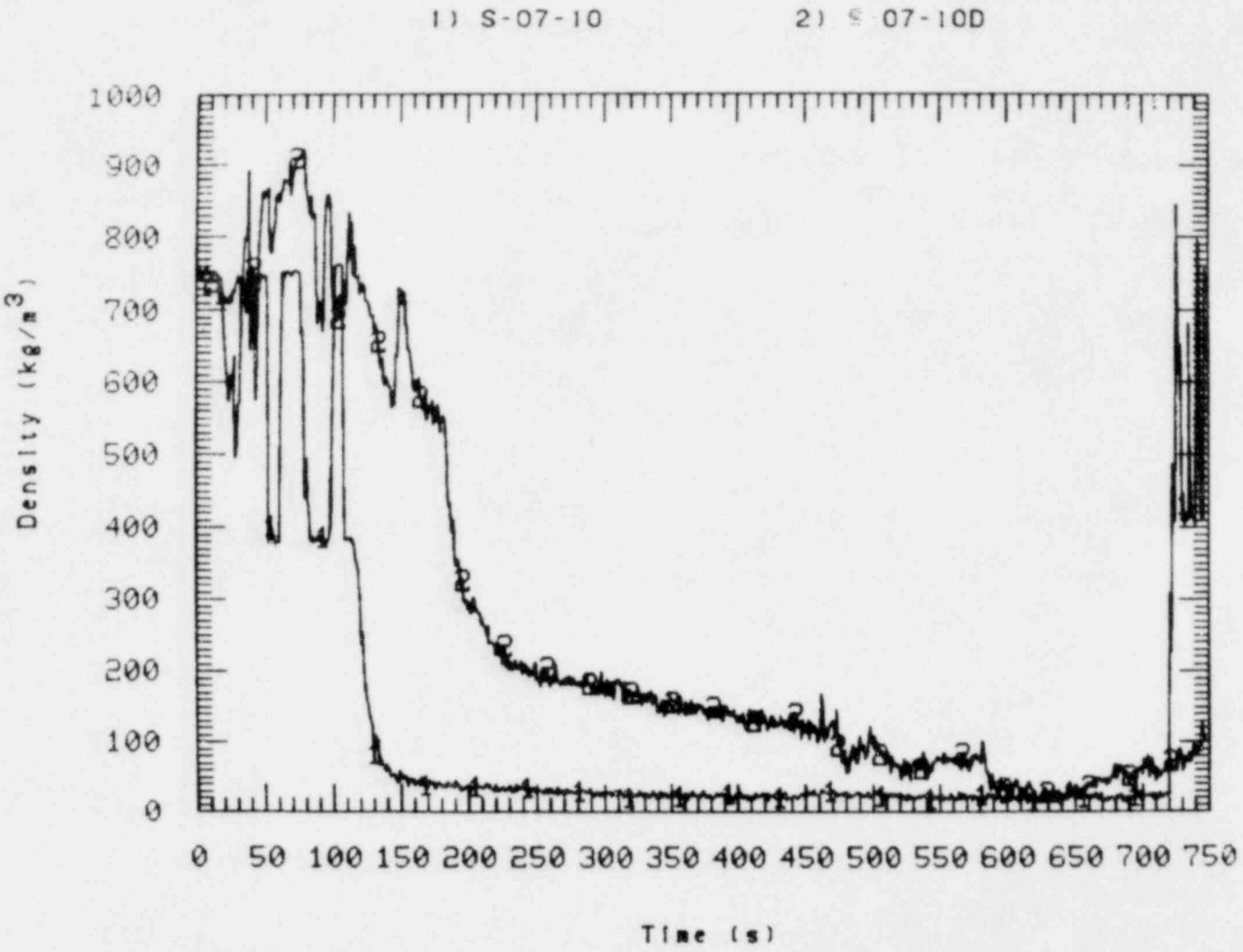

Figure 20. Comparison of fluid density measurements between the broken loop pump and break for Tests S-07-10 and S-07-10D.

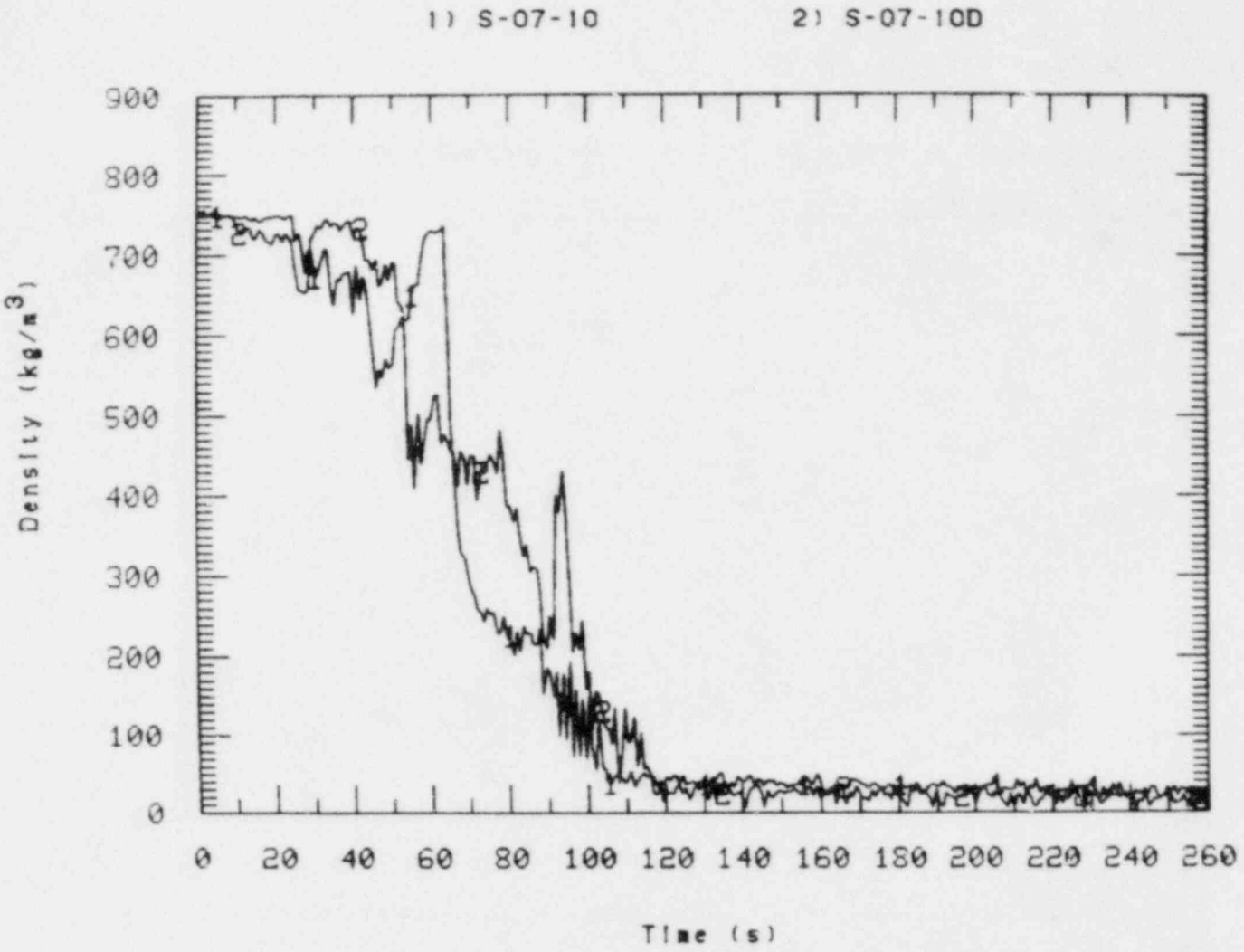

Figure 21. Comparison of fluid density measurements between the break and vessel for Tests S-07-10 and S-07-10D.

depressurization in Test S-07-10, after 50 s. This resulted in the crossover of the system pressure curves seen in Figure 12. The presence of excess liquid in the broken loop pump suction acted both as a condensation sink to enhance flow and as a probable source of liquid to the break.

3.4 Loop Response and Void Distribution

As stated previously, system behavior during the tests was characterized by voiding from the upper elevations downward. The two dominant phenomena were: gravity draining and the formation of water "seals" in the pump suctions early in the transient. Figures 22 through 25 present a pictorial view of system mass distribution at selected times during the transient. Event timing shifted from one test to the other as indicated on the figures.

After the pressurizer had voided (20 s), by dumping its fluid into the intact loop hot leg, liquid from the upper elevations began to drain down and was replaced by vapor. As seen in Figure 13, the upper plenum fluid quickly rose to saturation temperature due to the reduction in flow through the core. Figure 26 indicates that vapor was able to move along the top of the loop piping to the steam generators while liquid drained from the tubes. Once the system was predominantly voided down to the hot legs by 30 to 40 s, the liquid in the pump suctions formed a "seal" that precluded further vapor expansion through formation of a static head as illustrated in Figure 22. Once the liquid level in the intact loop had been depressed to the bottom of the pump suction, liquid was rapidly blown out the upflow side. This provided a path for pressure equalization throughout the system (Figure 23). The broken loop pump suction still had 30 to 60 cm of water in the downflow side when the intact loop blew out. The nonsymmetric behavior of the intact and broken loop is attributed to the aggregate result of different pump characteristics, loop hydraulic resistances partly influenced by different suction-to-break path lengths, and steam generator heat transfer and condensation.

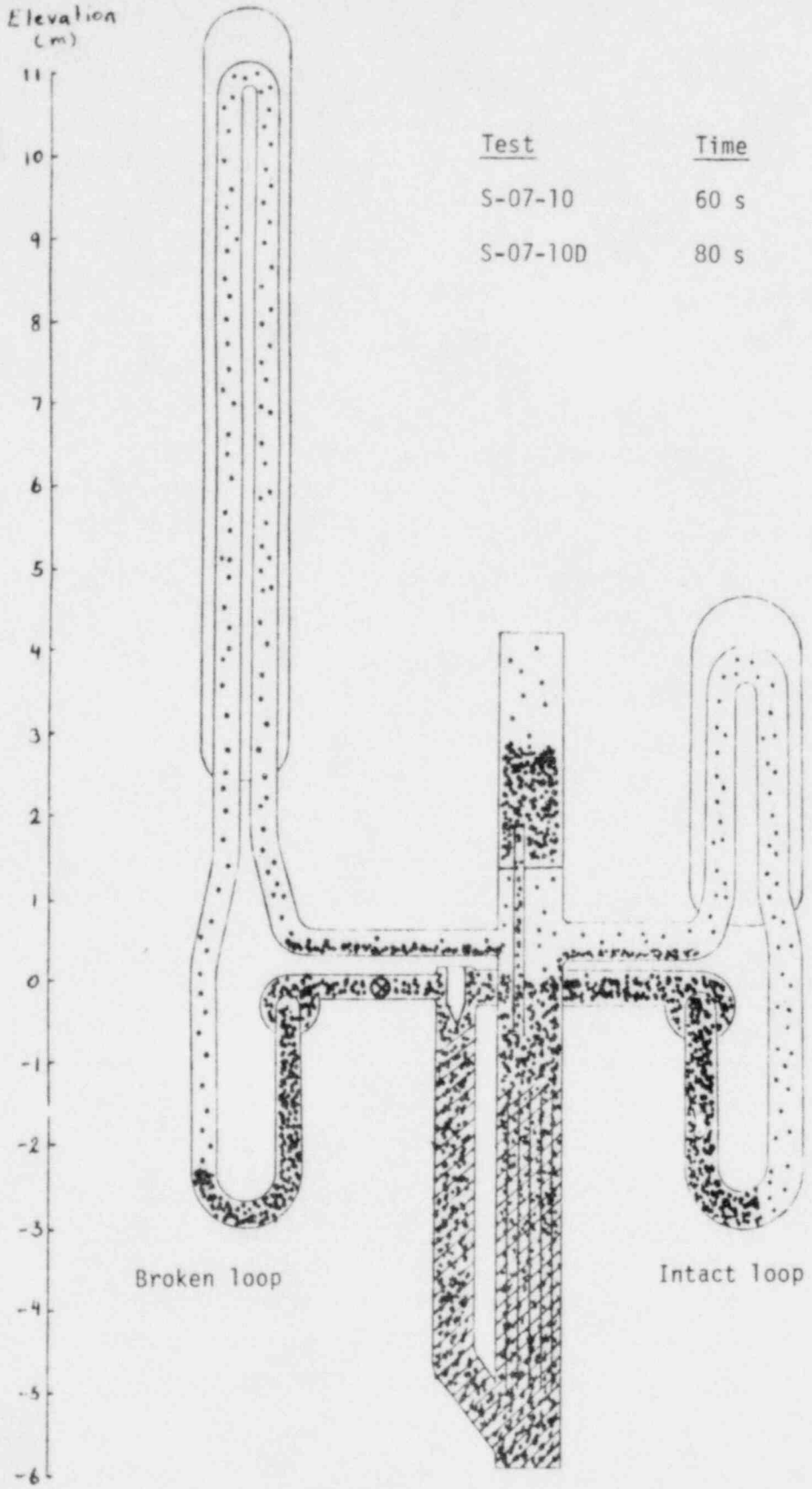

Figure 22. System mass distribution prior to intact loop pump suction blow-out.

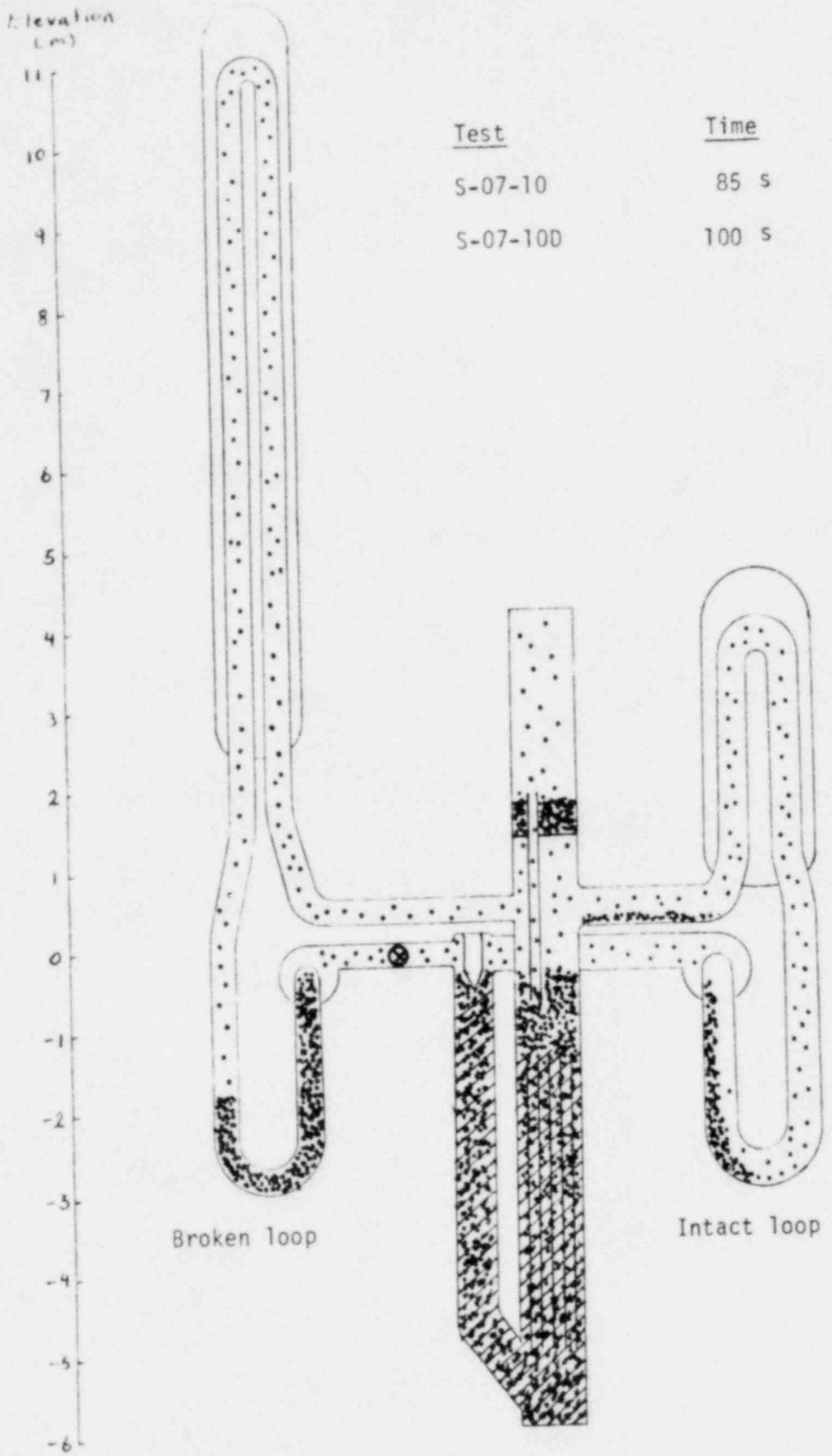

Figure 23. System mass distribution following intact loop pump suction blow-out.

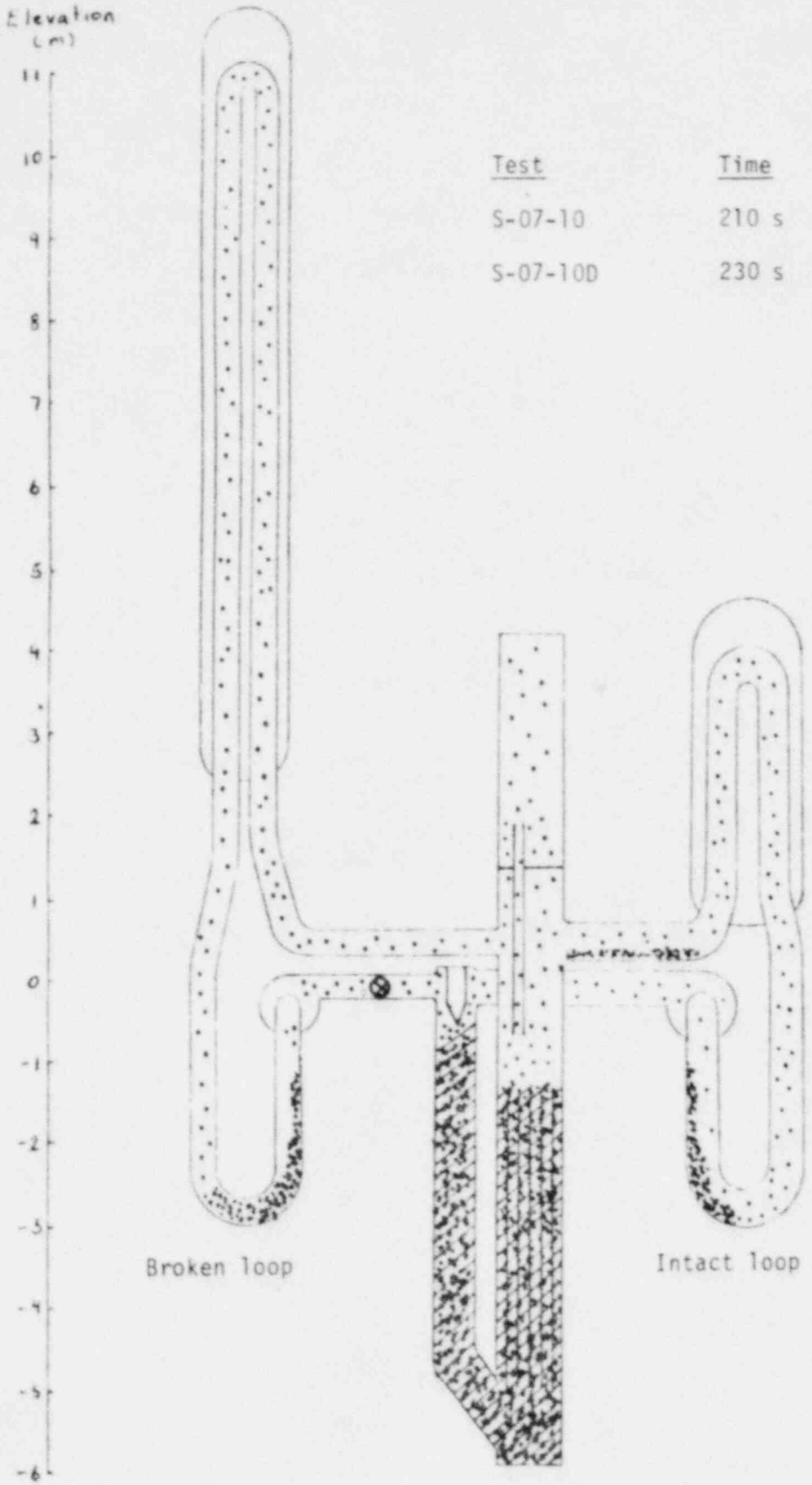

Figure 24. System mass distribution at beginning of core dry-out.

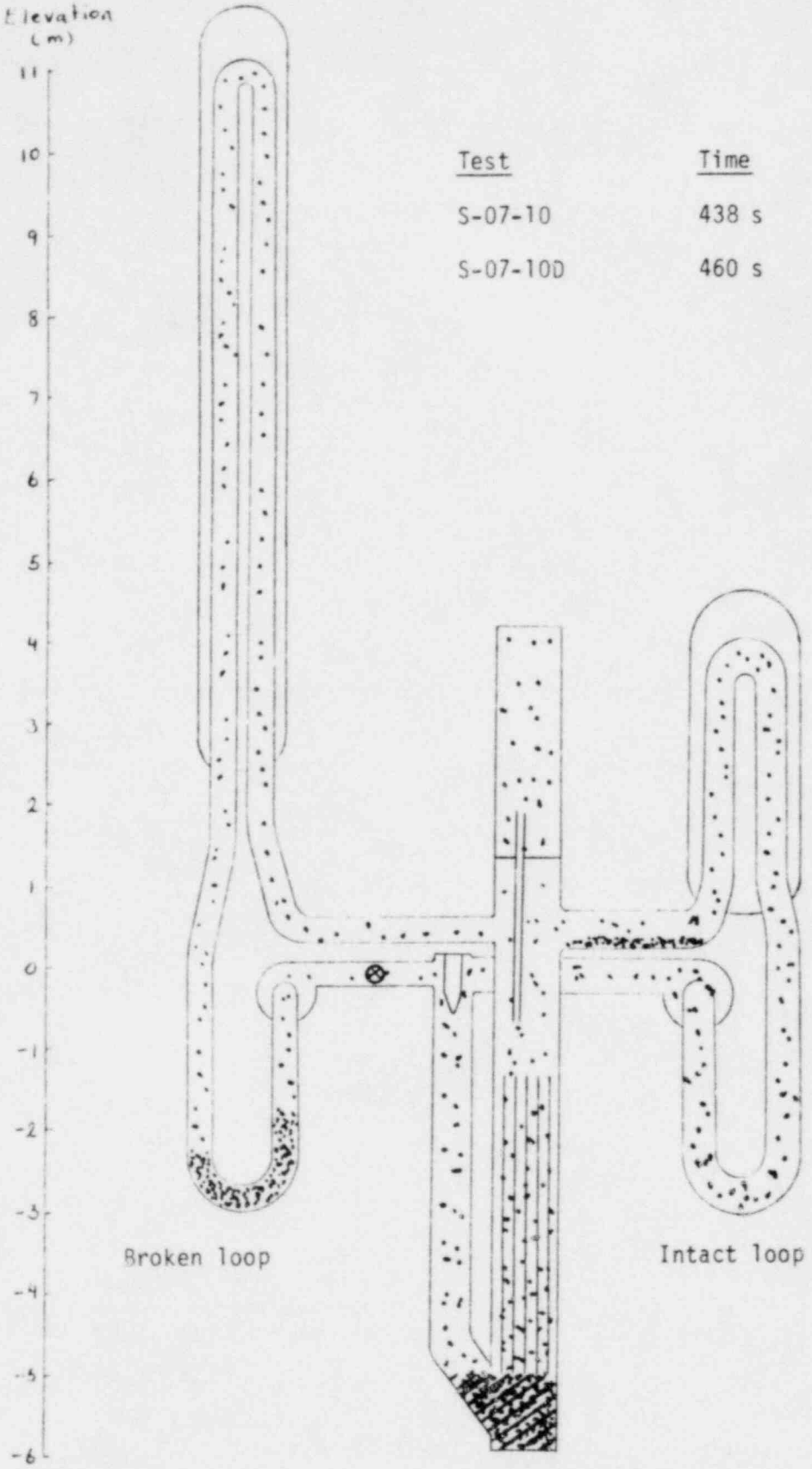

Figure 25. System mass distribution prior to emergency core coolant injection.

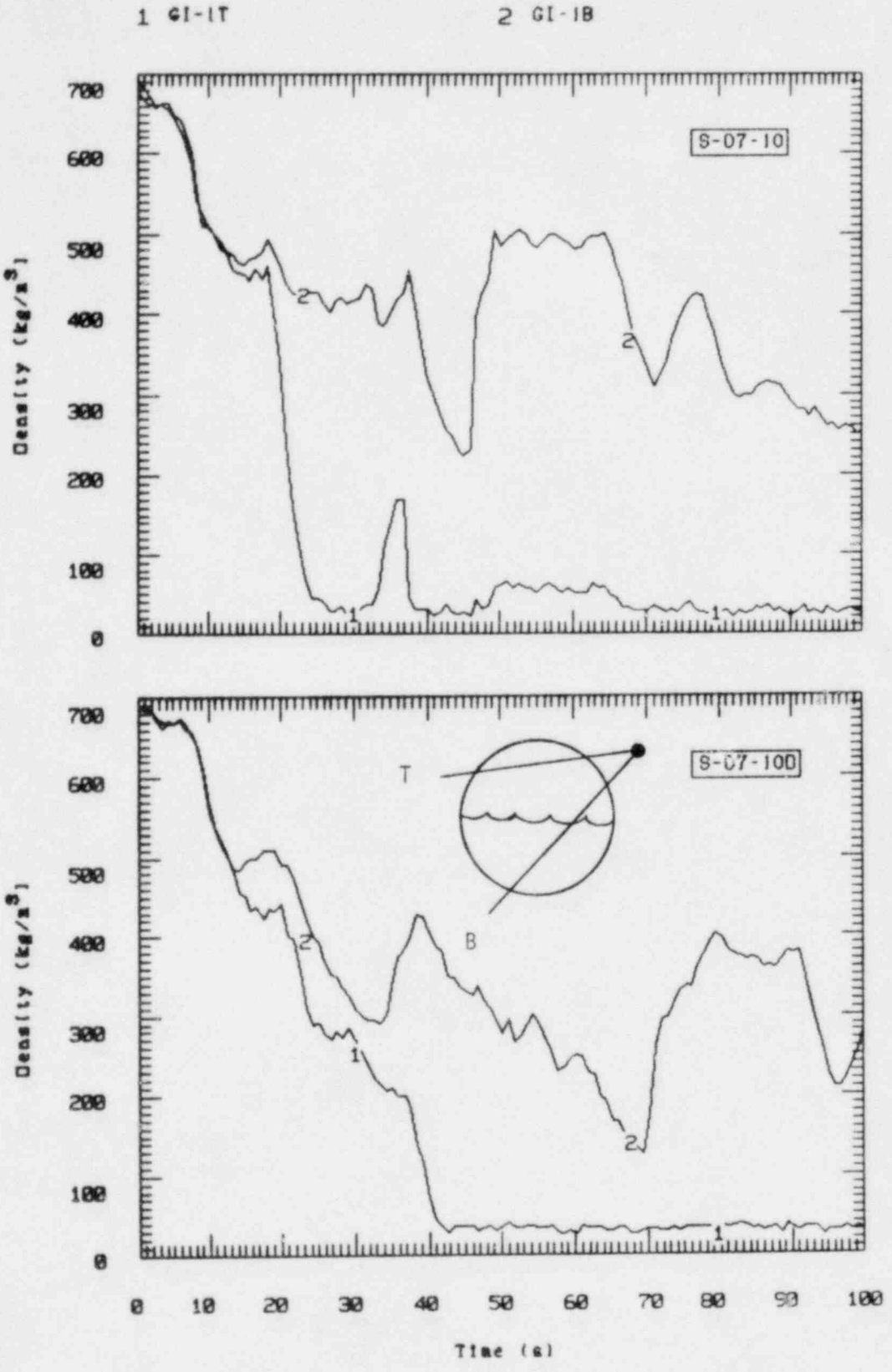

Figure 26. Comparison of intact loop hot leg densities for Tests S-07-10 and S-07-10D.

As liquid levels throughout the system equilibrated, liquid in the broken loop pump suction fell back and some liquid flowed down the downcomer to the core. This draining resulted in the transition to two-phase conditions upstream of the break plane. Figures 27 through 29 compare liquid levels for both tests in the downcomer, core and pump suctions. Comparison of measured broken loop hot leg flow rates in Figure 30 indicates that while reverse flow was observed in the broken loop in Test S-07-10 following blowout of the intact loop pump suction seal, the steam generator condensation potential in Test S-07-10D was sufficient to maintain positive loop flow.

Until the initiation of ECC injection, a continuous sweep-out process gradually removed the liquid in the pump suctions. With no ECC injection, and continuous loss of mass out the break, the loops eventually voided (except for the broken loop pump suction in Test S-07-10D) and the vessel liquid level began to deplete starting at about 210 to 230 s. After 110 s, the intact and broken loop steam generators became heat sources in Test S-07-10 and so did the intact loop steam generator secondary during Test S-07-10D. The blowdown of the broken loop steam generator secondary during Test S-07-10D delayed this event until about 190 s. Vapor from core boiloff then circulated through the loops to the break. The only anomalous occurrence observed in Test S-07-10 was the formation of a 2 cm liquid level in the 6.65 cm diameter intact loop hot leg, which slowly depleted prior to ECC injection. It is speculated that due to differential thermal expansion of the vessel and the upper plenum liner a small dam could have formed at the intact loop hot leg. No other mechanism is postulated for holding water there. Extension of horizontal flooding and entrainment analysis, presented in Reference 2, to conditions of Test S-07-10 show that there is little or no potential for either of these mechanisms to have occurred. The isolated nature of the liquid (estimated to be less than 1.2 ℓ) produced little influence on overall test results.

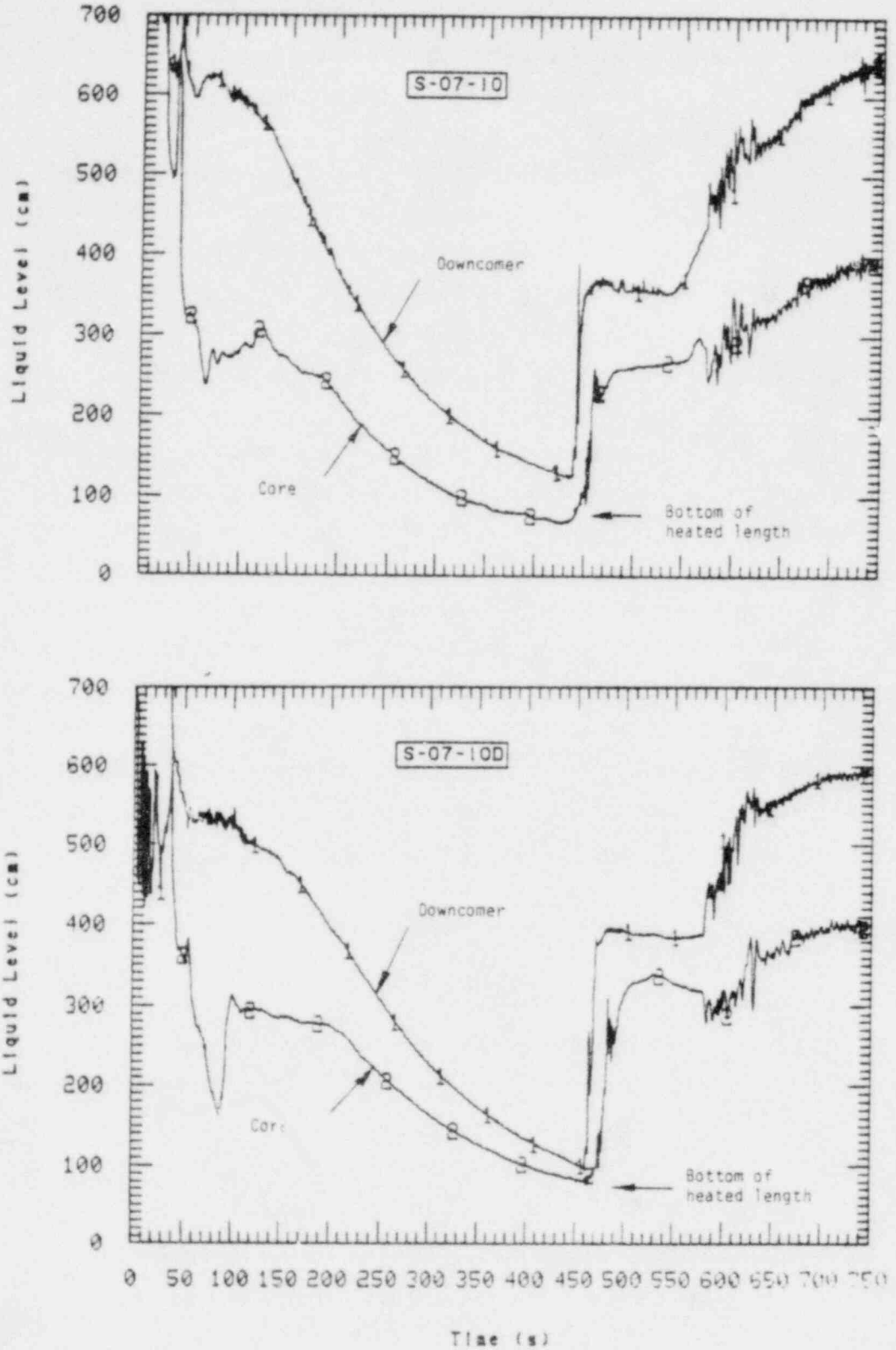

Figure 27. Calculated collapsed liquid levels in the downcomer and core for Tests S-07-10 and S-07-10D.

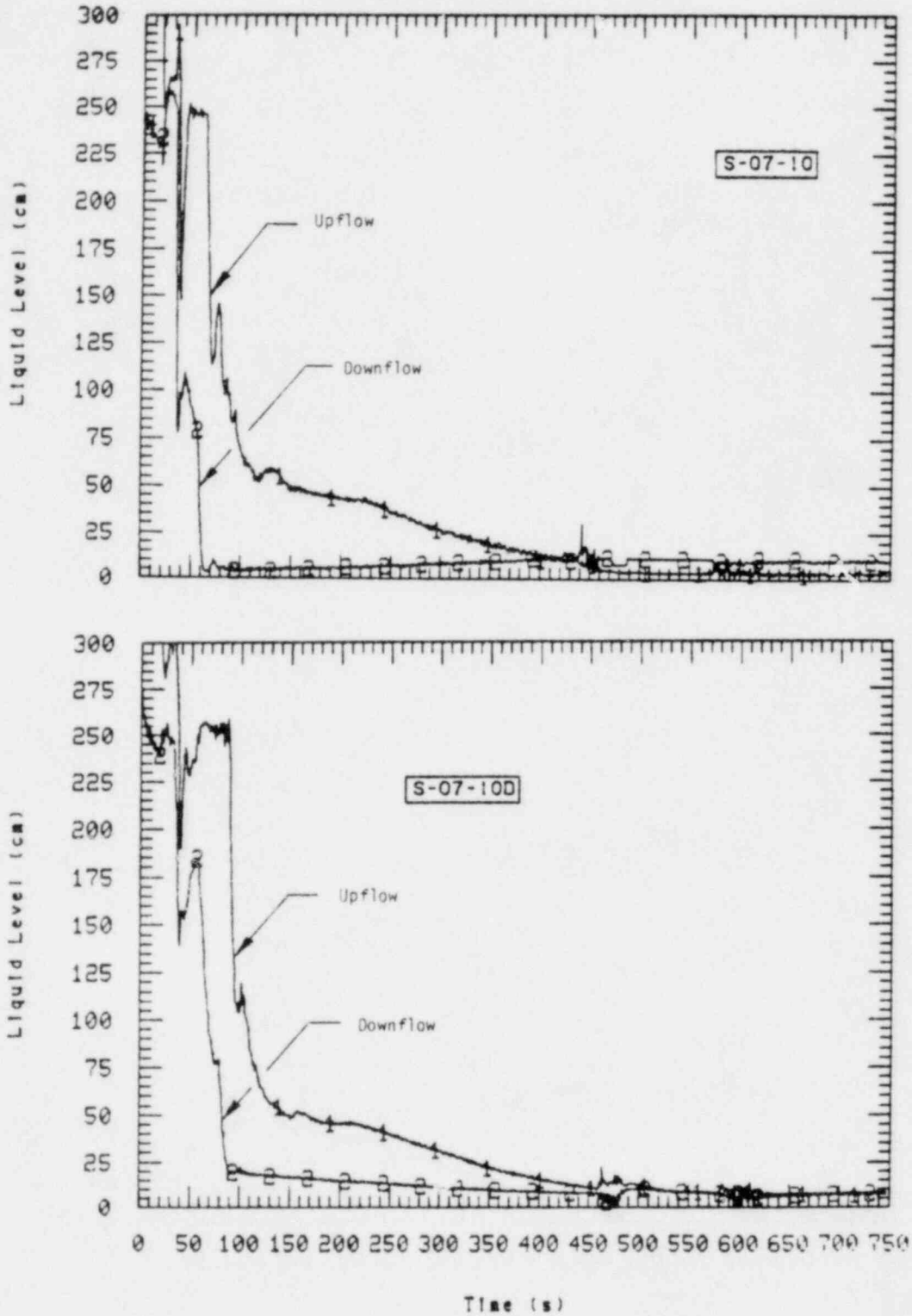

Figure 28. Calculated collapsed liquid levels in the intact loop pump suction for Tests S-07-10 and S-07-10D.

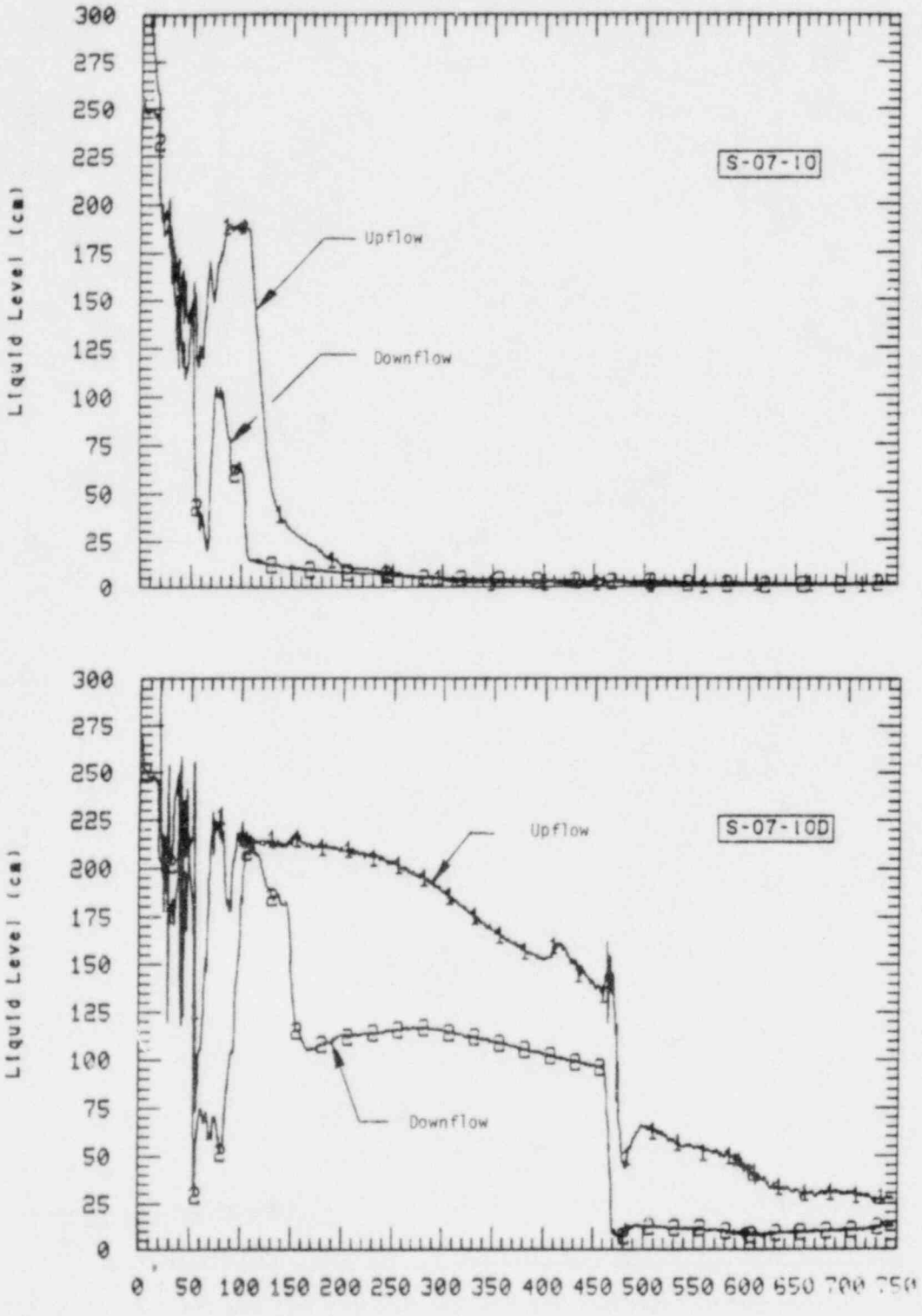

Figure 29. Calculated collapsed liquid levels in the broken loop pump suction for Tests S-07-10 and S-07-10D.

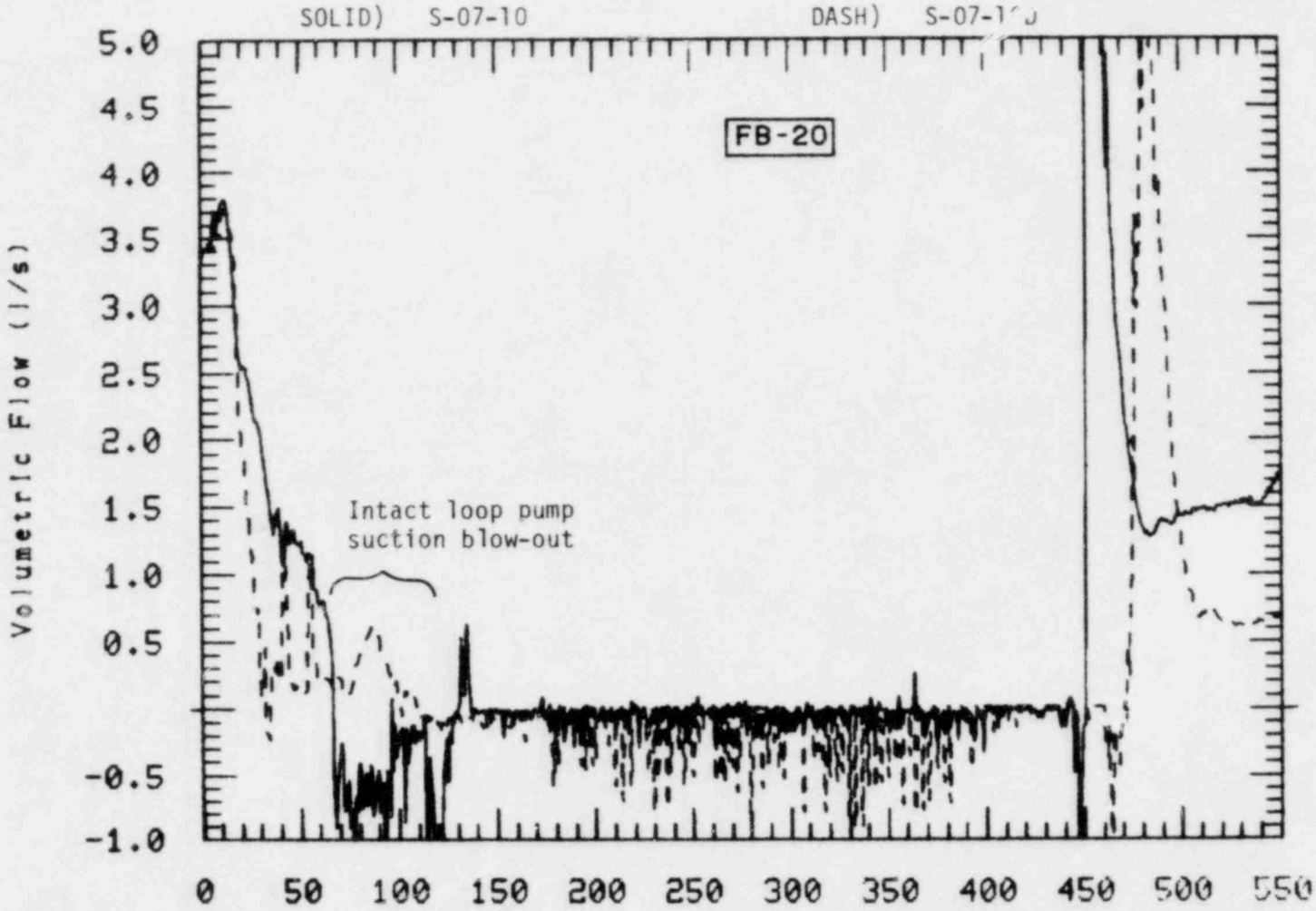

Figure 30. Comparison of broken loop hot leg flow rates for Tests S-07-10 and S-07-10D.

The differential pressures across the intact and broken loop pumps in Test S-07-10 are overlayed with pump inlet void fractions in Figure 31. A similar plot for the intact loop pump for Test S-07-10D in shown in Figure 32.[a] It can be seen that the pump heads in all cases were extremely degraded by 25 s into the tests as the void fraction apprached 20%. Very rapid degradation can be seen in the plots as soon as the void fraction begins to increase at about 16 s. Pump coastdown was not initiated until approximately 8 s into the tests. The short period of time in which pump effects would have been important supports the contention in Section 2.2 that little impact resulted from the erroneous pump speed curves.

3.5 Core Behavior

Test conditions resulted in the attainment of high heater rod temperature for both tests as the liquid in the vessel progressively boiled down. Figures 33 and 34 show plots of void fraction versus elevation in the core at selected times during the tests. Following rupture of the pressure boundary the void fraction in the core quickly rose due to level swell, as seen at times 17 and 27 s in Figure 33. Once the heater rod stored energy had been reduced (see Figures 35 and 36) the liquid collapsed back into the core as seen at 37 s. Further voiding then began, and the formation of loop seals in the pump suctions depressed the liquid level in the core, resulting in extremely high void fractions at about 60 s. Several heater rod thermocouples indicated dryout at the higher power zones of the rods during this time. These dryouts and rewets were most prominant on the high power zone rods in Test S-07-10D, as can be seen in Figure 37. Once the pump suction seals blew out, the level in the core and downcomer equilibrated and a fairly well defined liquid level appeared at 75 s (note knee in void fraction curve).

---

a. No broken loop pump inlet density measurement was available for Test S-07-10D.

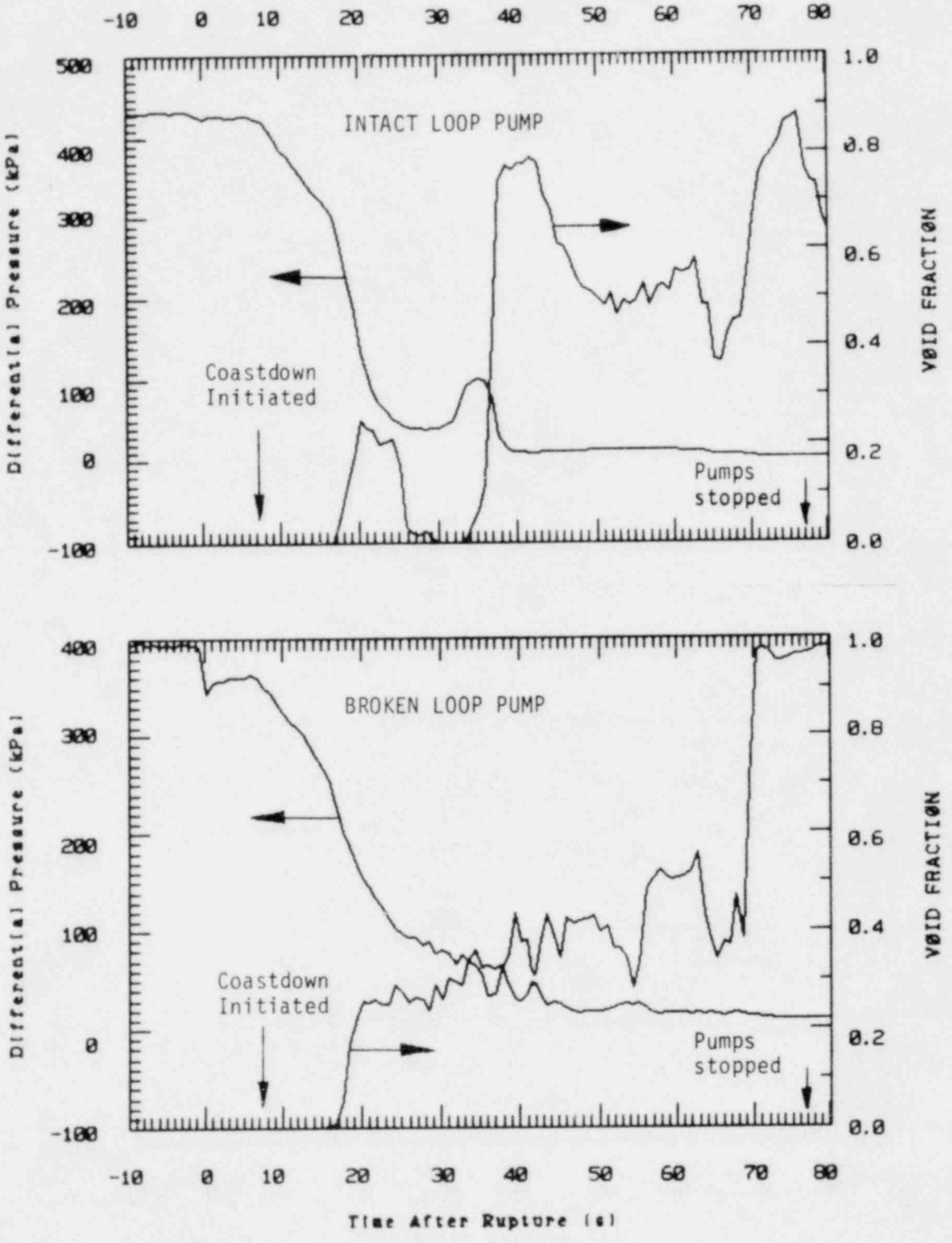

Figure 31. Comparison of pump head and inlet void fractions for Test S-07-10.

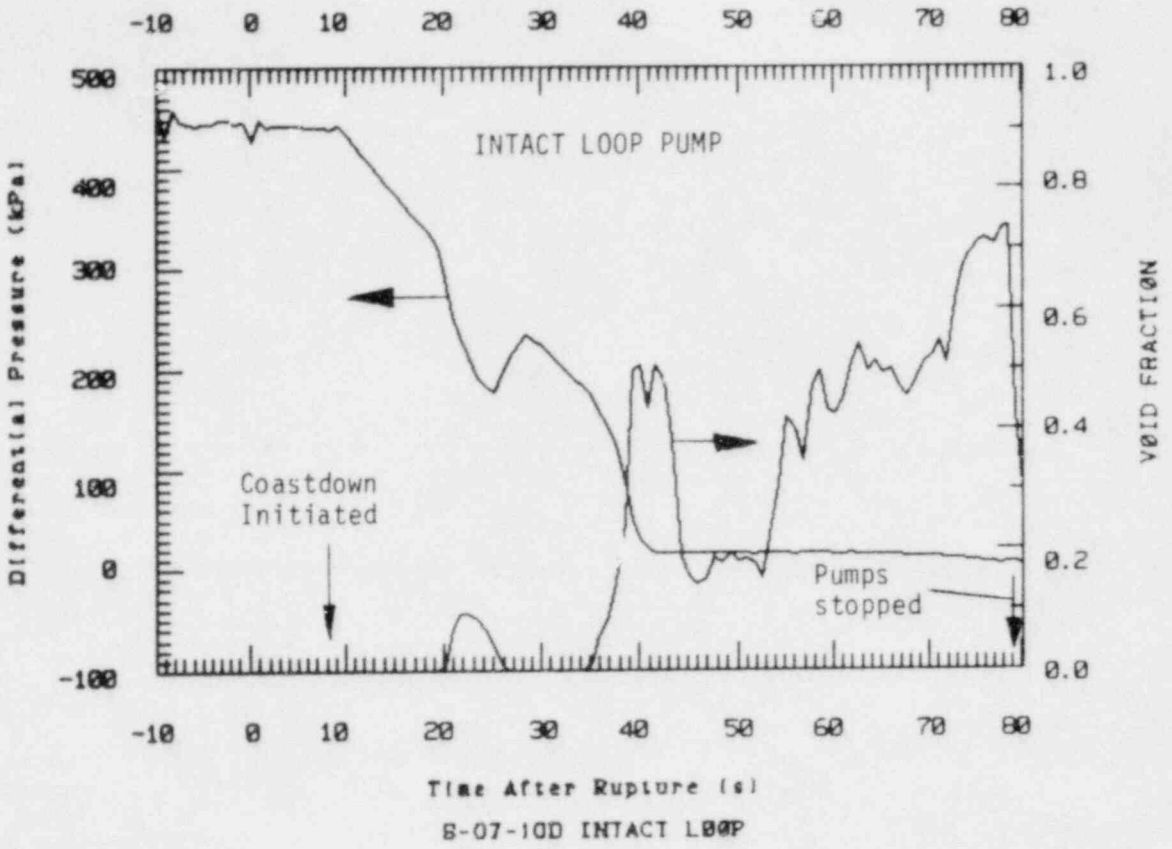

Figure 32. Comparison of pump head and inlet void fraction for intact loop pump in Test S-07-10D.

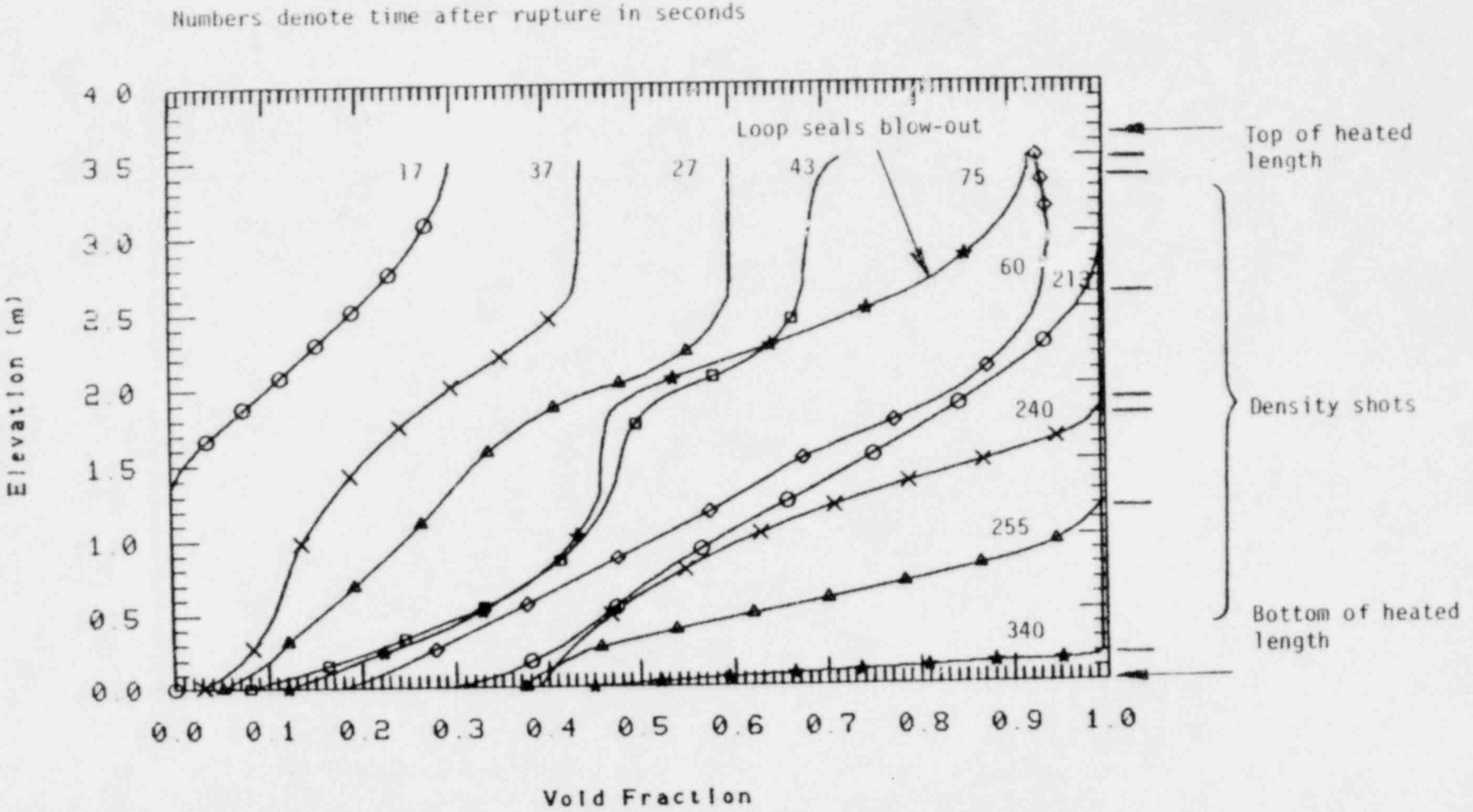

Figure 33. Homogeneous void fraction profiles in the Semiscale Mod-3 core as a function of time for Test S-07-10.

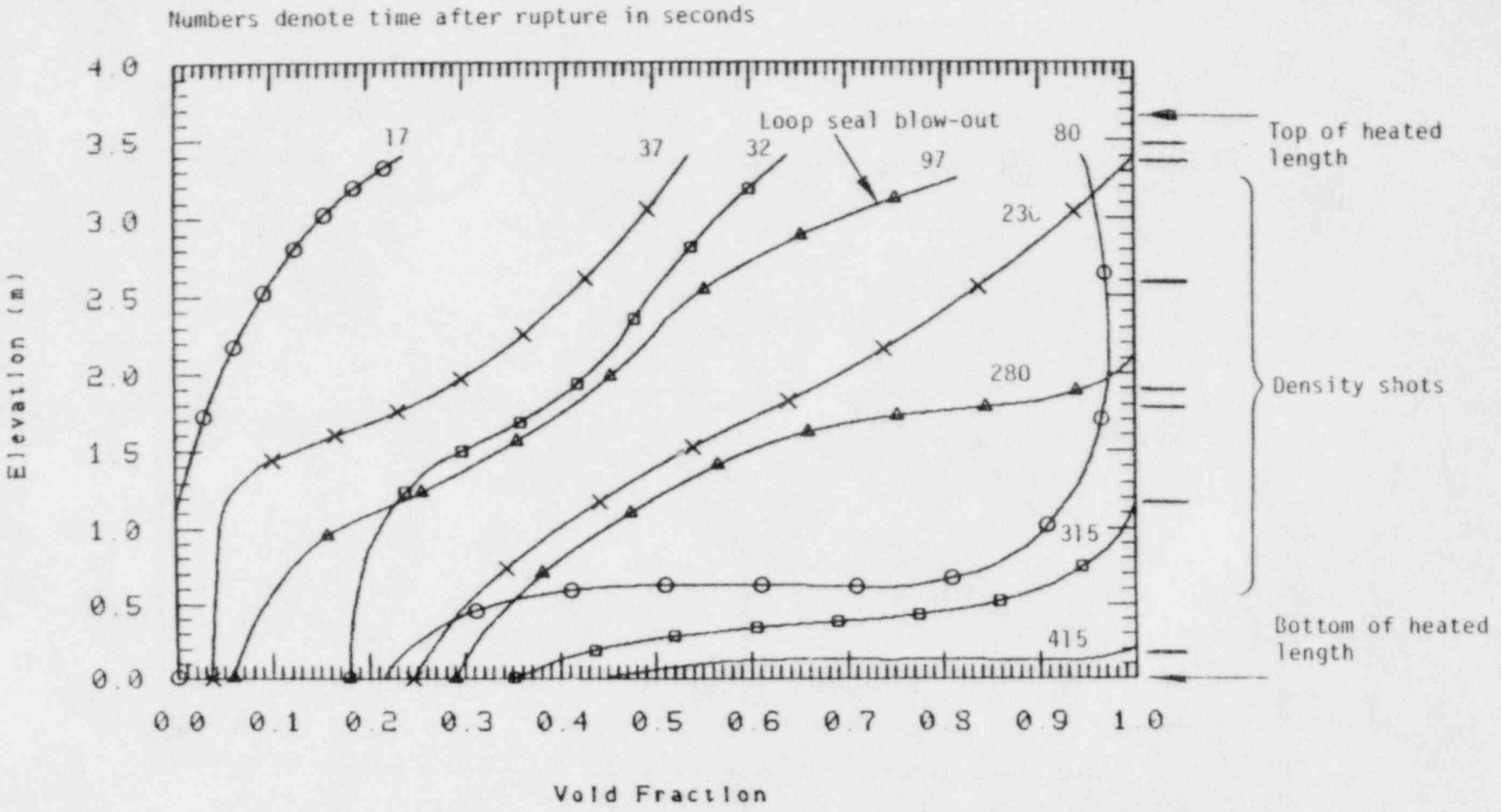

Figure 34. Homogeneous void fraction profiles in the Semiscale Mod-3 core as a function of time for Test S-07-10D.

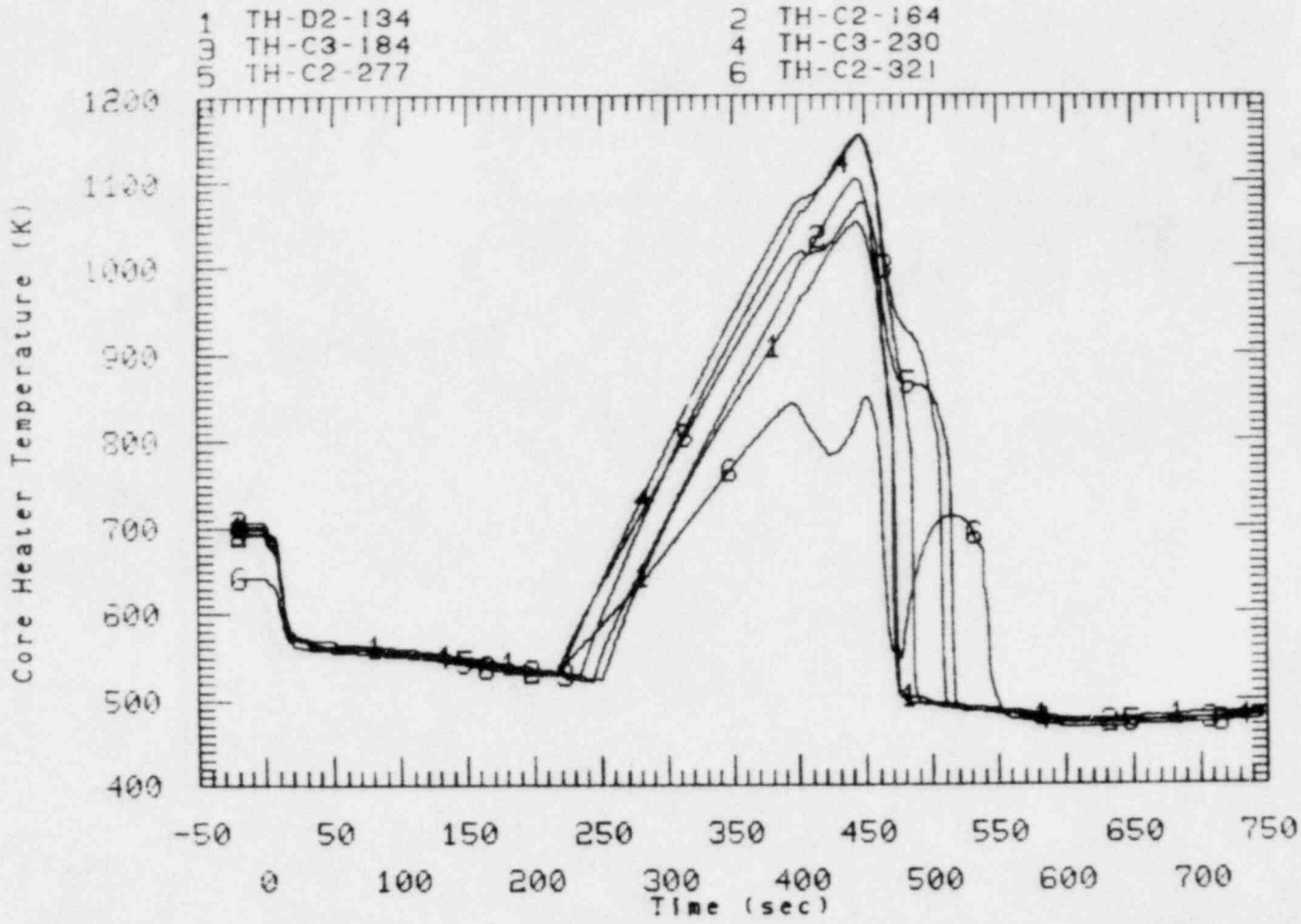

TEST S-07-10 SEMISCALE MØD-3

Figure 35. Selected high power zone heater rod thermocouples from Test S-07-10.

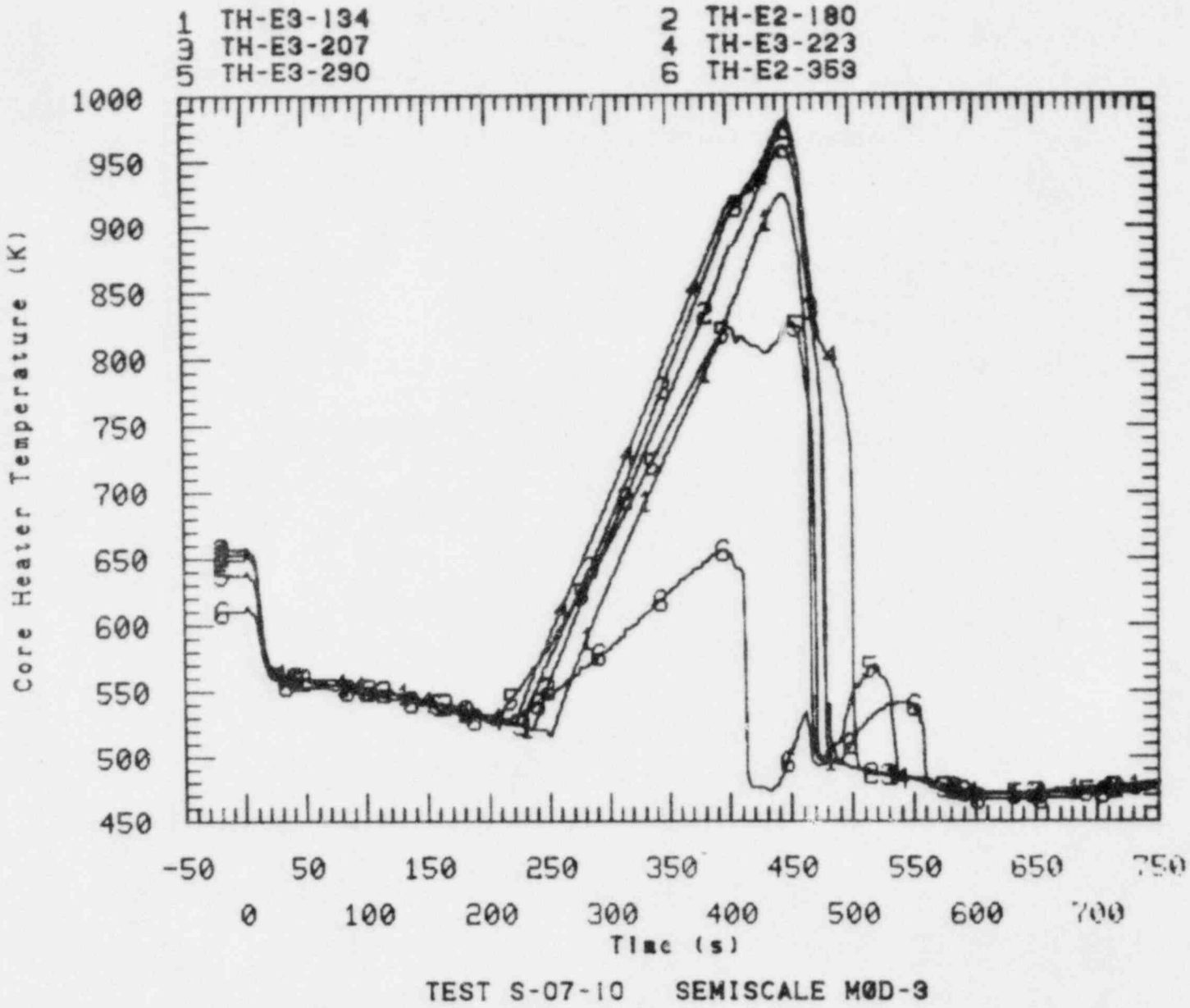

Figure 36. Selected low power zone heater rod thermocouples from Test S-07-10.

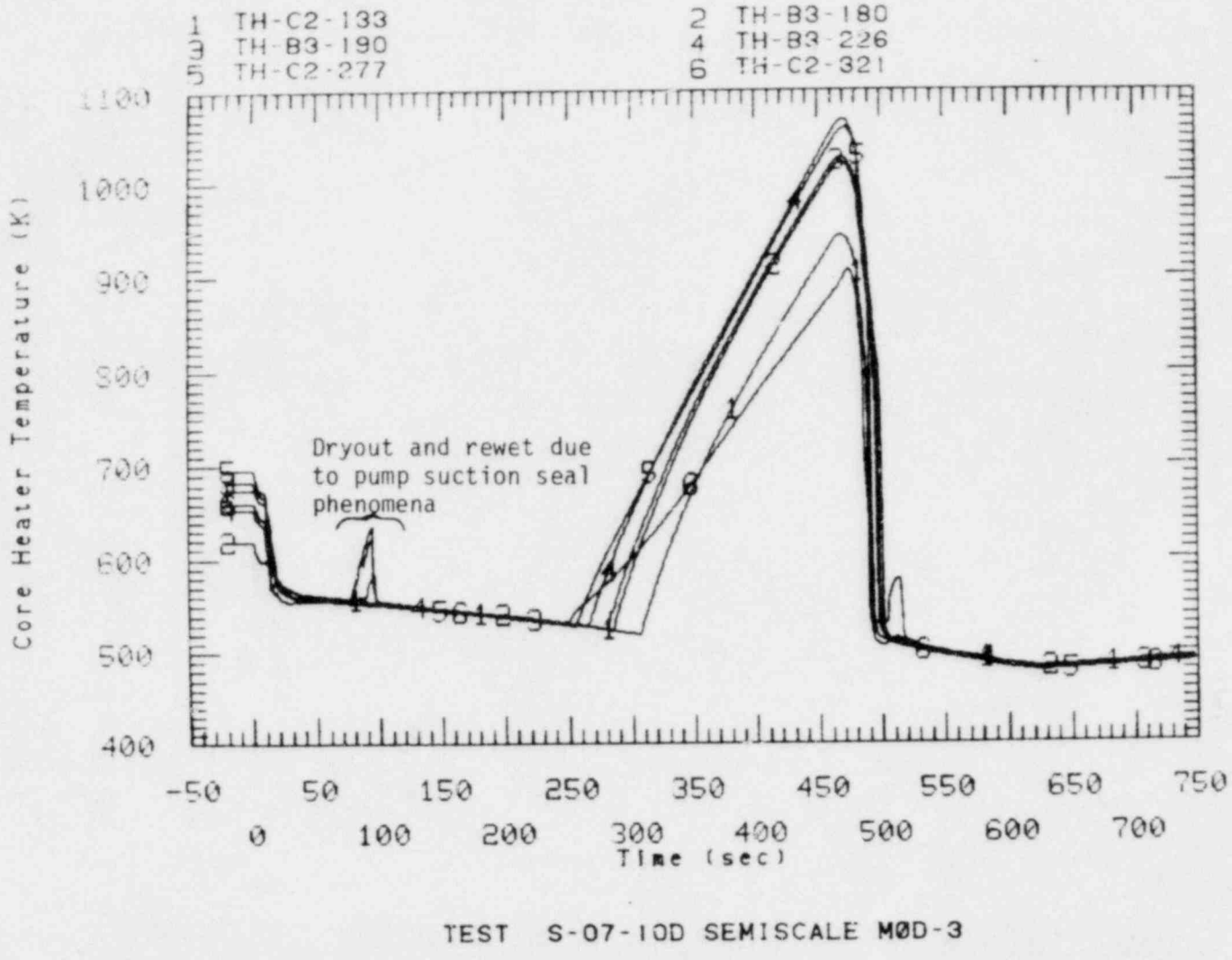

Figure 37. Selected high power zone heater rod thermocouples from Test S-07-10D.

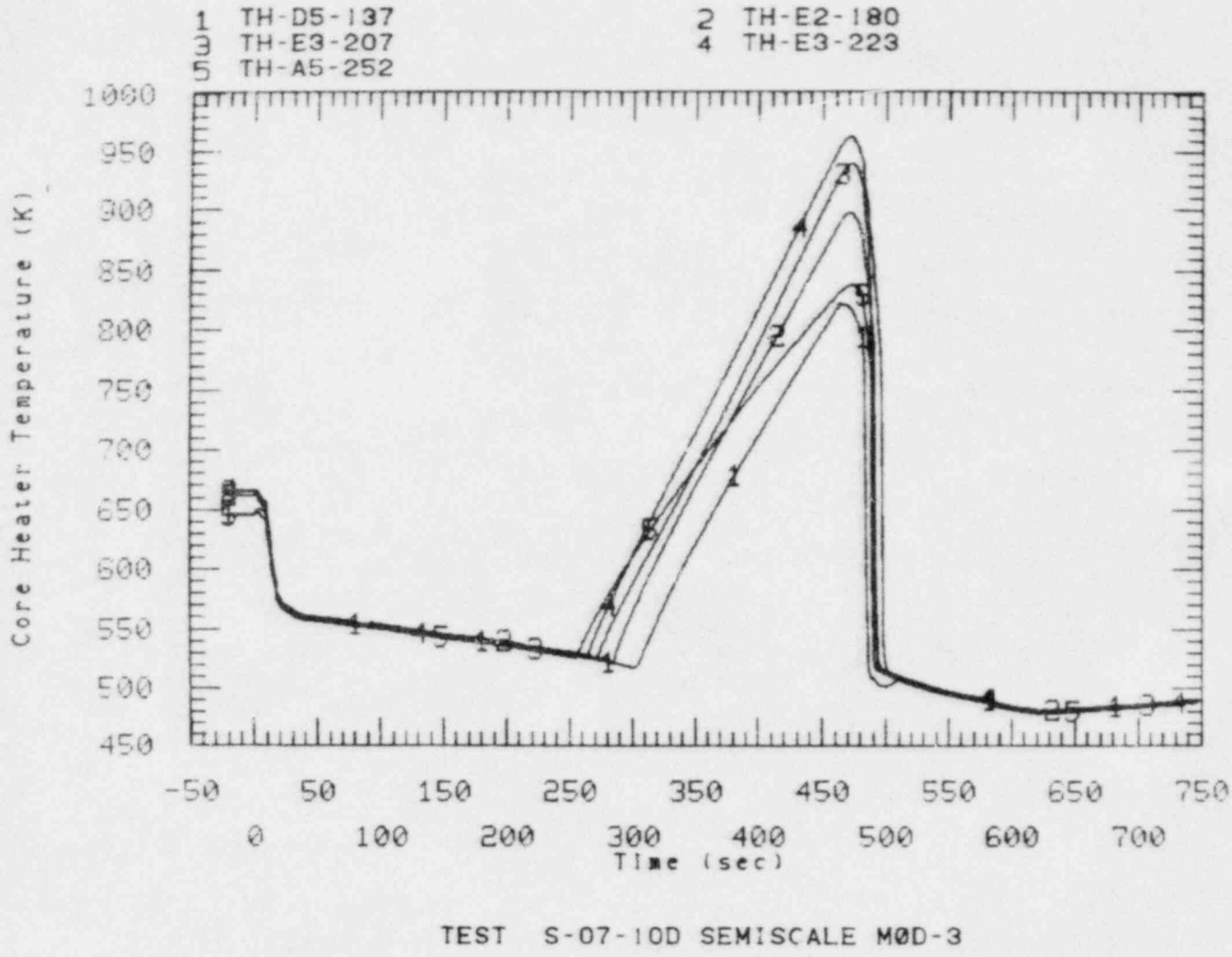

Figure 38. Selected low power zone heater rod thermocouples from Test S-07-10D.

The vessel liquid then progressively boiled off as seen at times 213, 240 and 255 s. By 340 s it is seen that the core was completely voided. Similar phenomena occurred in Test S-07-10D (Figure 34) but were shifted to later in time. It is seen that well before ECC injection the core had been completely voided. Figures 35 through 38 present overlays of selected high and low power rod thermocouples, respectively, at several axial locations. It is seen that, even with the high void fractions that existed in the upper elevations early in the test, the heater rods were adequately cooled and closely follow the saturation temperature. The first dryout was observed at 210 s and 230 s in Tests S-07-10 and S-07-10D, respectively. Referring to Figures 39 and 40, it is seen that dryouts in the upper third of the core occurred rapidly, (and somewhat sporadically in Test S-07-10), while the dryout front progressed much slower in the lower part of the core.

This phenomenon was also observed in Semiscale simulations of the Three Mile Island (TMI) transient[7] and can be explained through considerations of entrainment and fluid distribution mechanisms. While liquid remains covering a significant fraction of the rod height the boiling and resultant steam generation promotes the formation of a froth height and high entrainment to cool the rods above the collapsed liquid level. As this level falls, frothing and entrainment are suppressed and the dryout level more closely follows the collapsed liquid level. Unlike the much slower TMI transient simulation, heat losses did not become a dominating factor in Test S-07-10 due to the relatively rapid depressurization. As a result, little or no subcooling was prevalent in the lower vessel fluid (see Figure 41), and a froth level was maintained through boiling as the level fell to the bottom of the core. This is supported by Figure 42 which compares the dryout front and core collapsed liquid level for Test S-07-10D.

Cladding temperatures were monitored during the test and allowed to climb to a maximum of 1060 K before ECC injection was manually initiated. The temperature of thermocouples TH-C3-184 and TH-B1-321

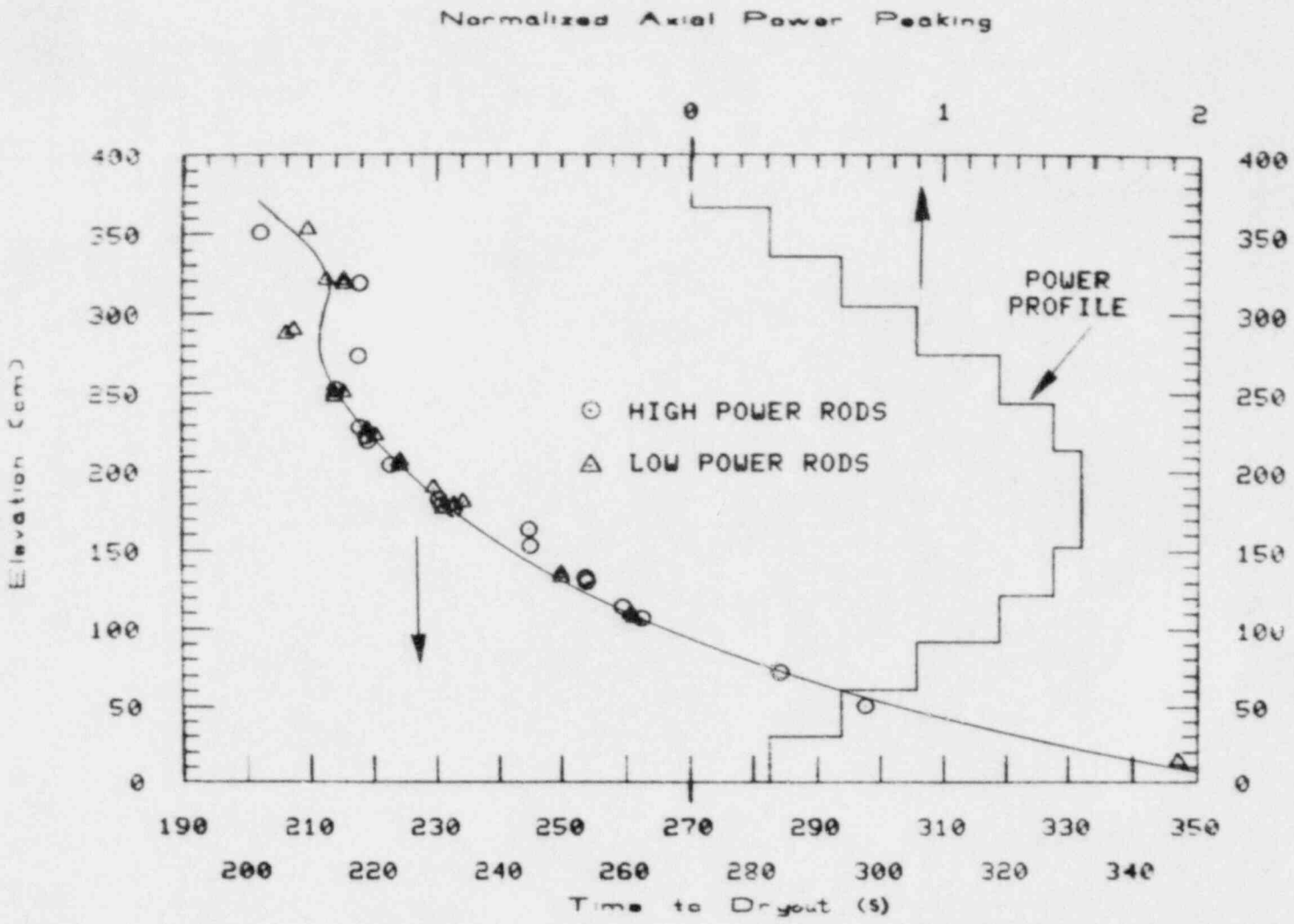

Figure 39. Dryout of core in Test S-07-10.

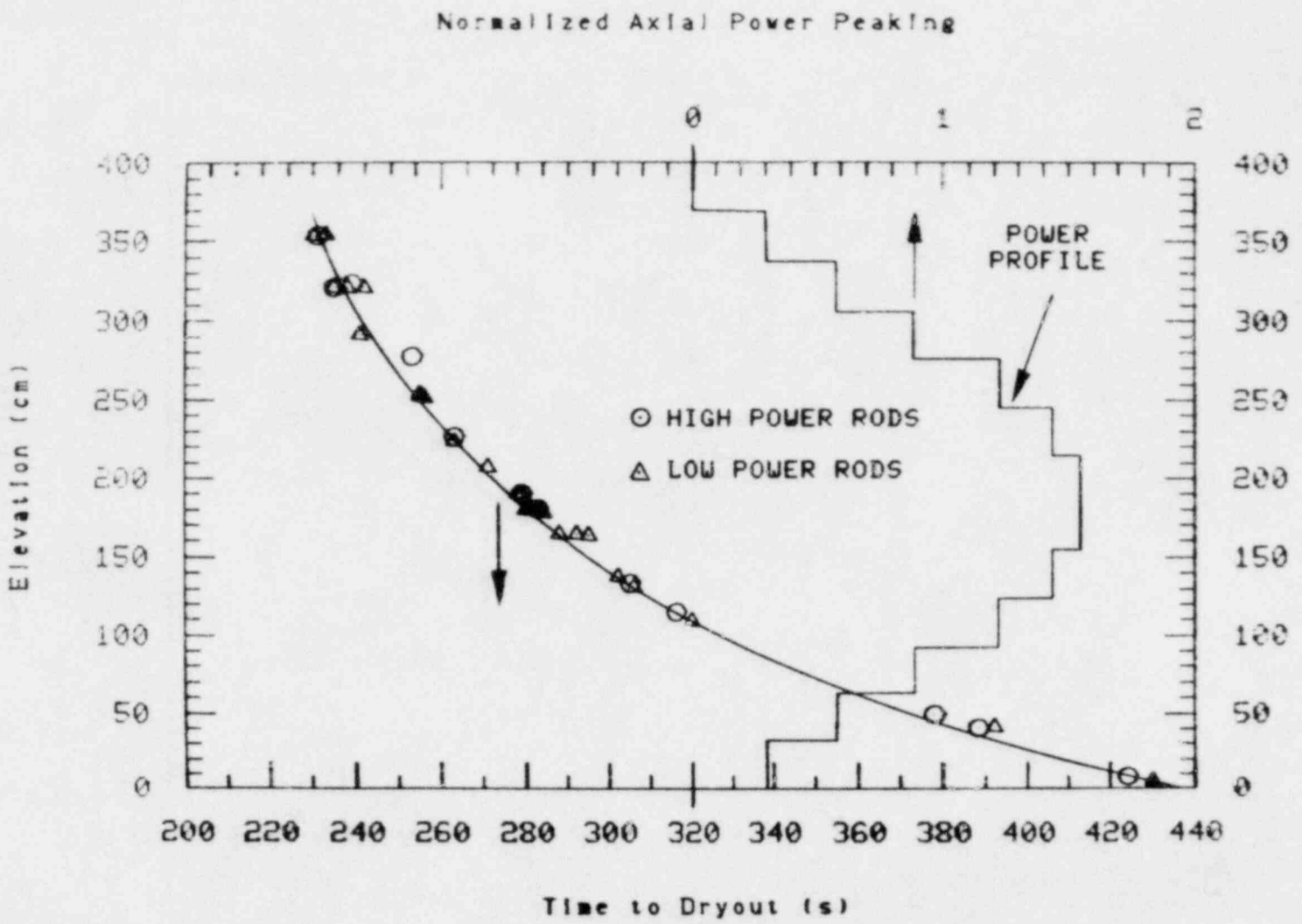

Figure 40. Dryout of core in Test S-07-10D.

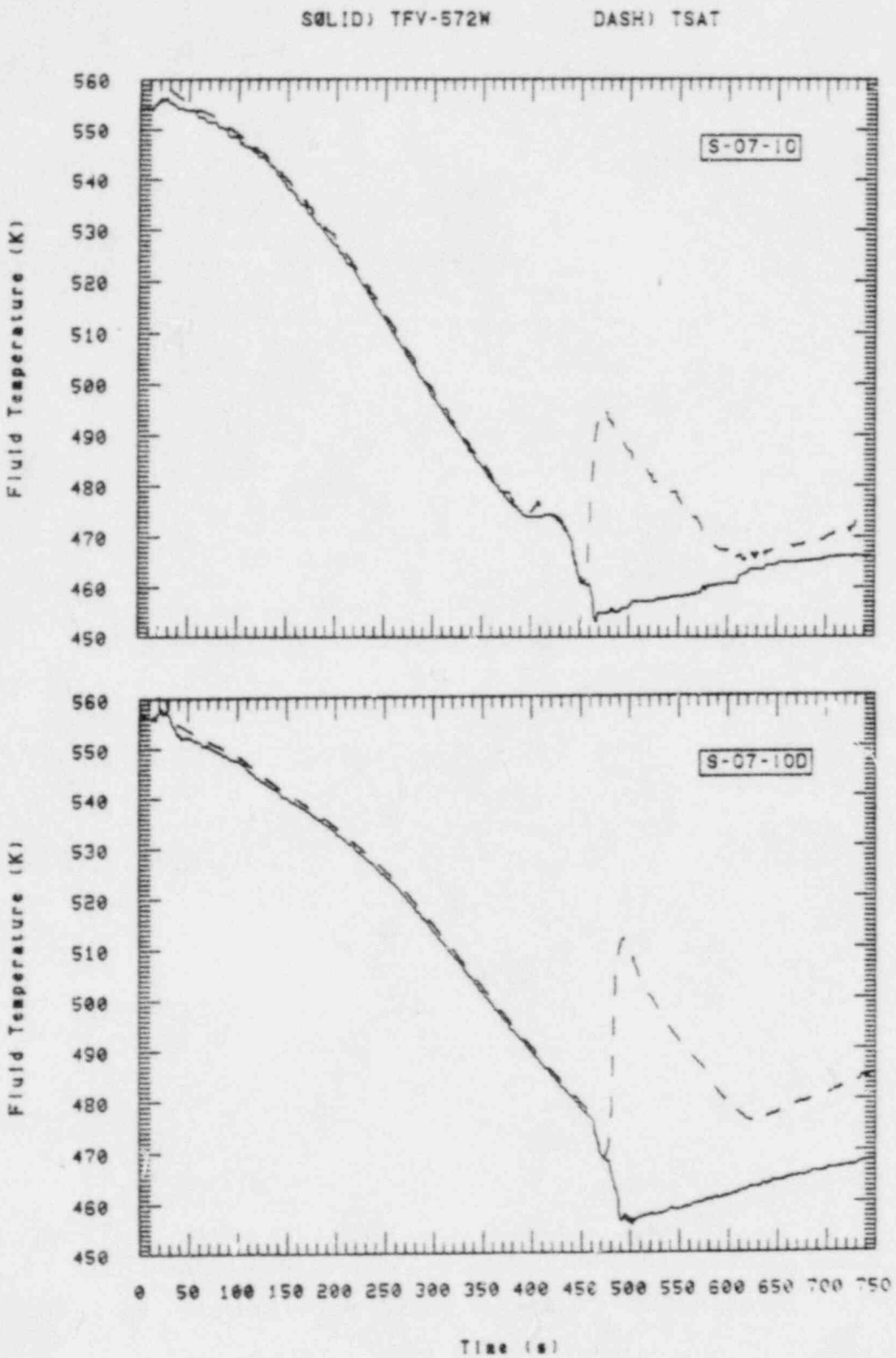

Figure 41. Comparison of fluid temperatures in vessel lower plenum to saturation temperatures for Tests S-07-10 and S-07-10D.

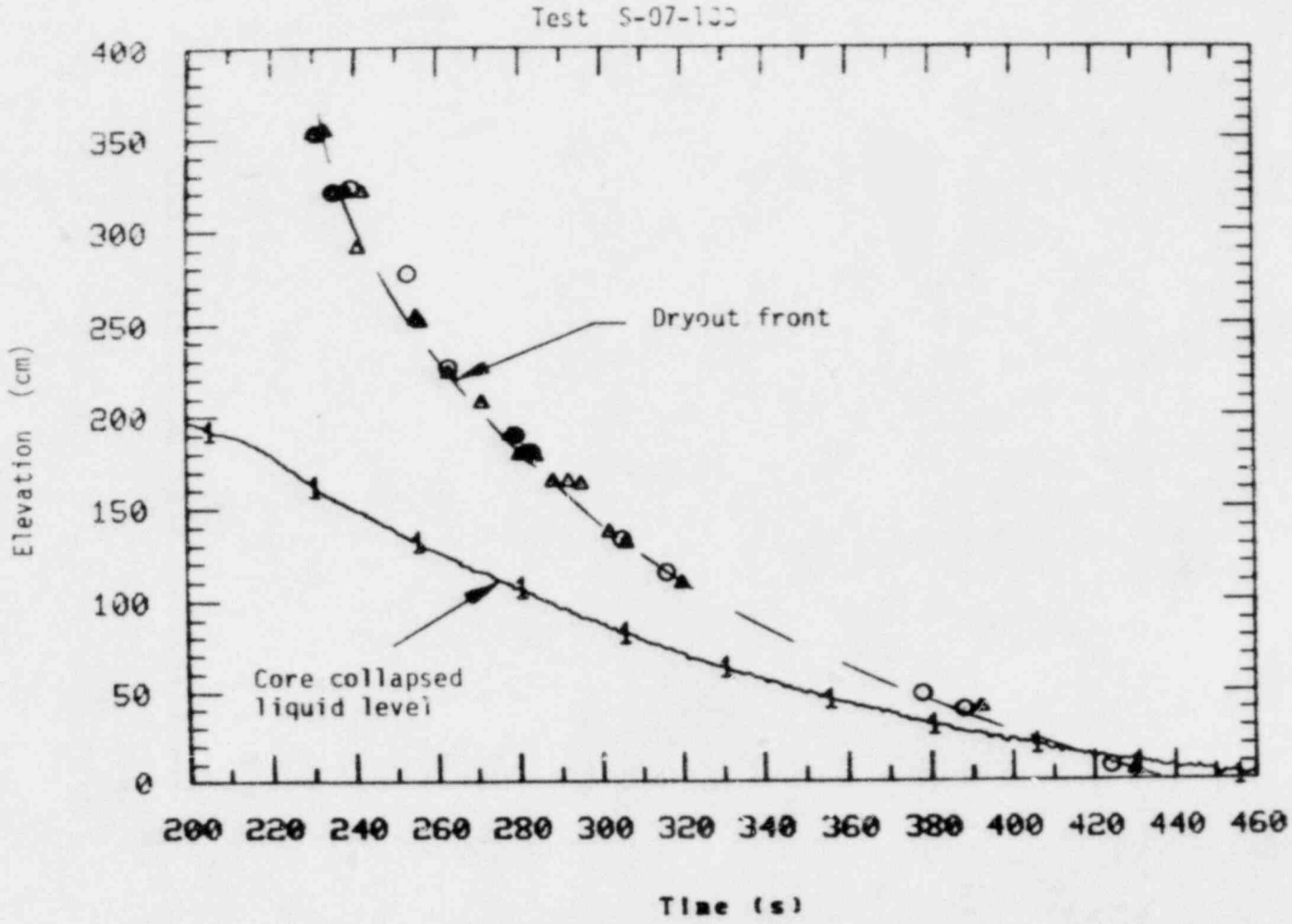

Figure 42. Comparison of core collapsed liquid level to heater rod dryout front for Test S-07-10D.

during Test S-07-10 are compared with adiabatic heatup calculations in Figures 43 and 44. It is seen that, only when the core was severely dried out did the heatup rates begin to approach adiabatic. As indicated on Figure 43, at about the time the core became completely voided (370 s), the heat transfer coefficient due to steam cooling was on the order of 0.035 to 0.07 kW/m^2K. (This range comes from selecting either saturation temperature or a grid spacer thermocouple temperature as the fluid temperature measurement.) As steam flow decreased the heatup rate began to increase, with the heat transfer coefficient dropping about a factor of two until being curtailed by some liquid fallback.

Between approximately 390 and 415 s, during Test S-07-10, several thermocouples in the upper core were observed to progressively turnover, rewet, or deflect, indicative of a small amount of water falling back into the core and being vaporized by the time it fell to about mid-core (see Figures 35 and 36). While there was liquid in the intact loop hot leg, instruments do not indicate that it drained into the vessel, and no liquid was detected falling past the upper plenum densitometer (GV-11) although entrainment from the resultant steam generation was seen. Figure 45 shows the volumetric flow at the top of the core for both tests and compares them to the calculated flow rate as necessary to maintain a flooded condition at the upper core support plate. The flooding criteria are based on the Wallis correlation:[8]

$$j_g^{*\,1/2} + m j_f^{*1/2} = C$$

where

$$j_i^* = \frac{j_i \rho_i}{gd(\rho_f - \rho_g)}$$

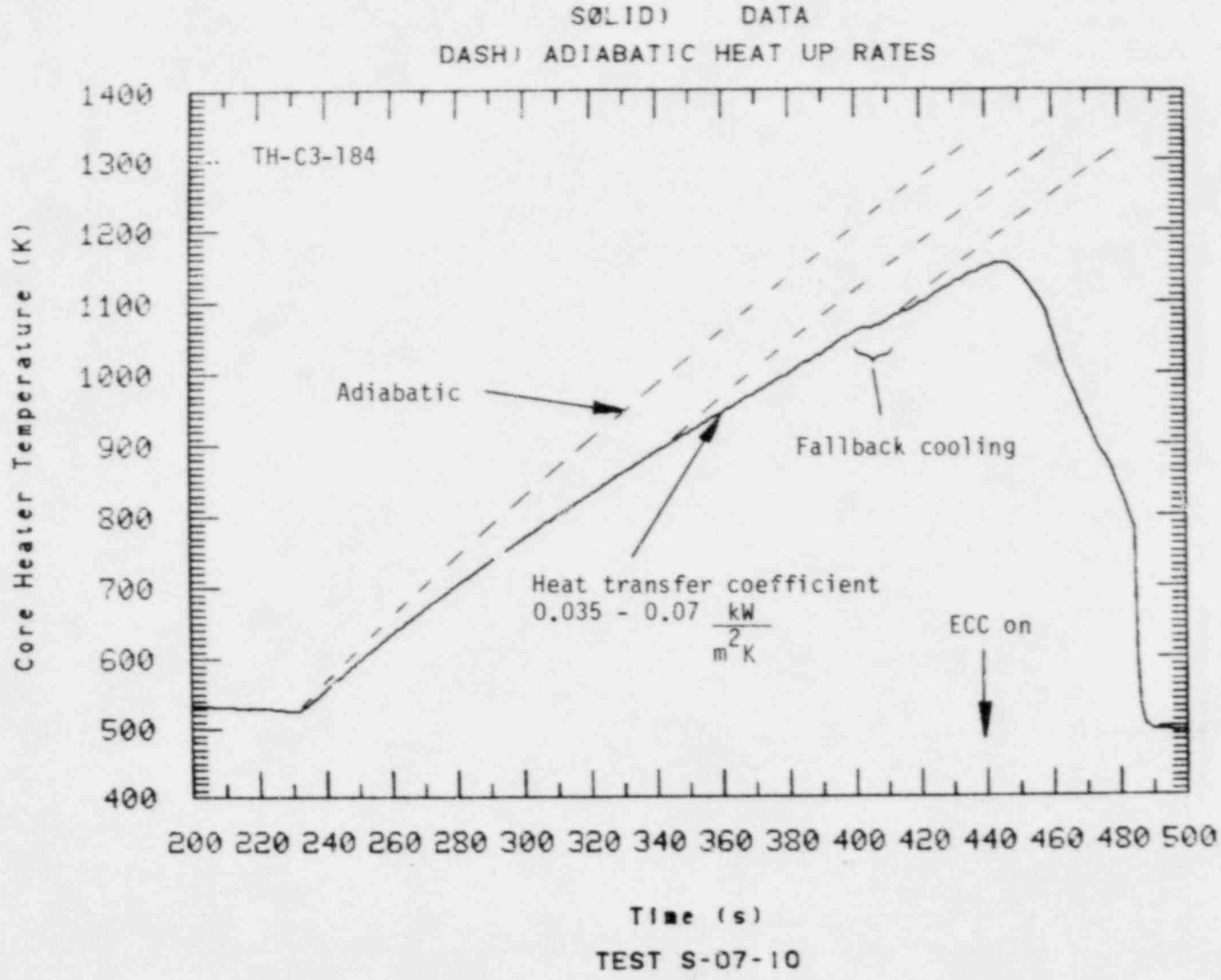

Figure 43. Comparison of heat up rate for mid-core heater rod thermocouple TH-C3-184 to adiabatic heat up rates at selected times for Test S-07-10.

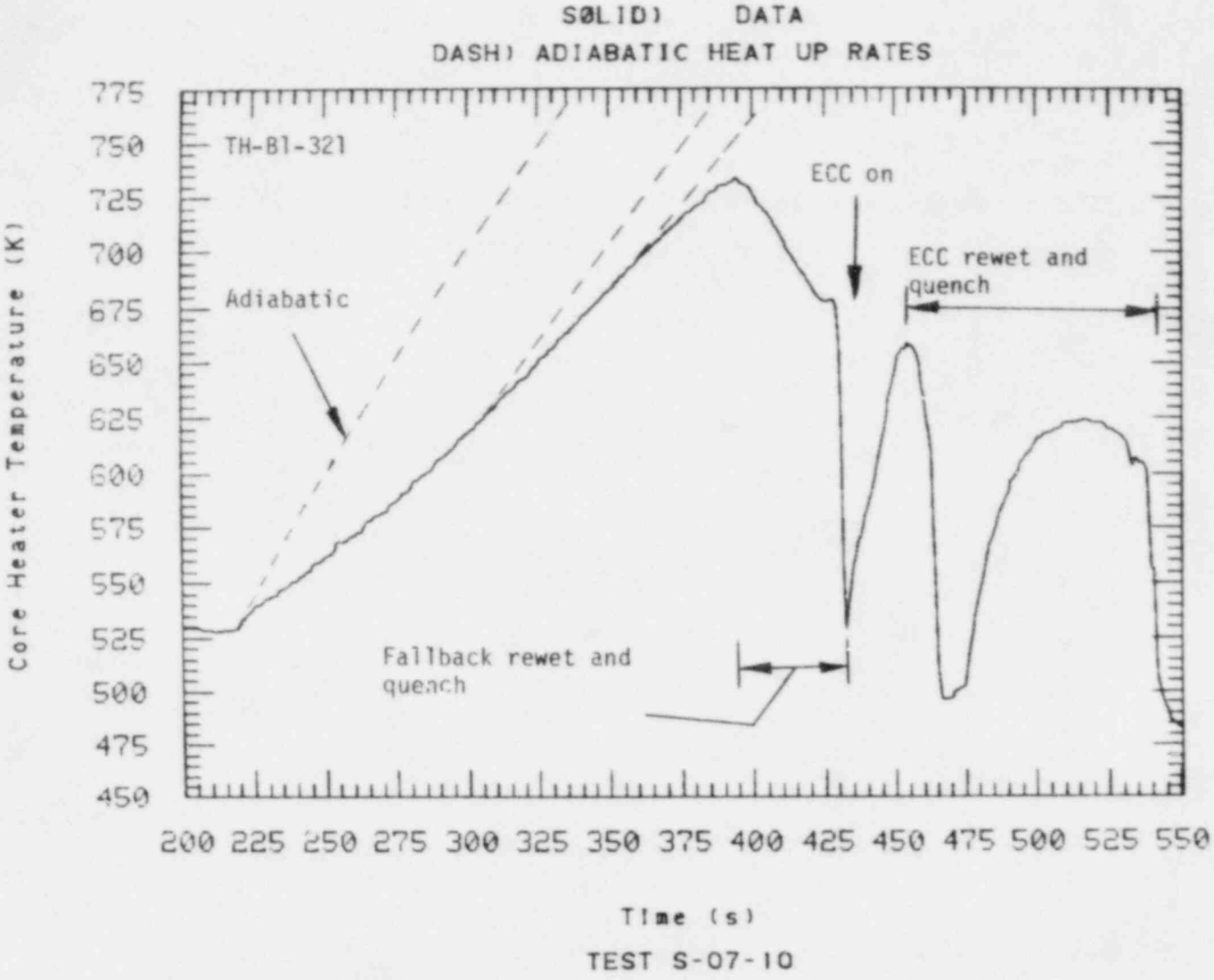

Figure 44. Comparison of heat up rate for upper core heater rod thermocouple TH-B1-321 to adiabatic heat up rates at selected times for Test S-07-10.

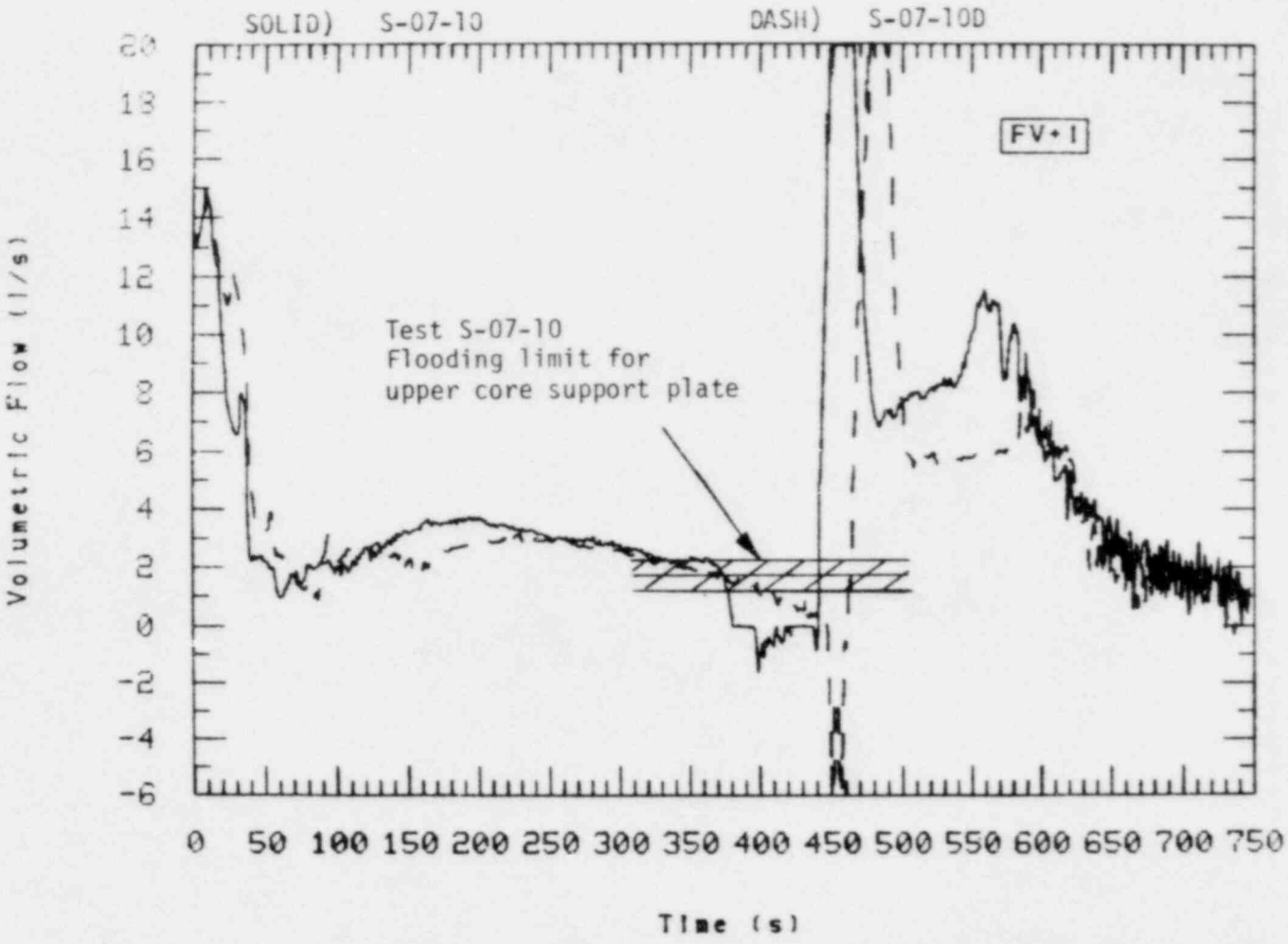

Figure 45. Comparison of core outlet flowrates for Tests S-07-10 and S-07-10D.

j_i = superficial velocity = Q/A
Q = volumeric flow rate
A = flow area
ρ_f = liquid density
ρ_g = vapor density
d = characteristic dimension
c, m = constants.

For flooding, $j_f^* = 0$, for turbulent flow m = 1, and C = 0.5 to unflood a sharp edged tube. Solving for j_g, and calculating the associated total upper plenum flow and plotting, gives the range shown on Figure 45. While the vessel metal temperature was above saturation, it is postulated that liquid films could have formed on the many other surfaces in the upper plenum area (guide tube, support tubes, etc.) and fell back once the core liquid was boiled away and steam flow stopped. The amount of liquid was apparently small as it was detected by densitometer measurement GV-154-23 while only the resultant upward entrainment was seen by densitometer GV-164-AB (see Figure 3 for orientations).

ECC injection was initiated at 438 s and 460 s in Tests S-07-10 and S-07-10D, respectively. Liquid was observed to penetrate to the core in approximately 6 s in both tests. Since the loops were highly voided there was little resistance to steam flow. Flow turbine measurements around the system were saturated (i.e., beyond upper limit) for about 20 s. This promoted rapid filling of the vessel as evidenced by the calculated collapsed liquid level rises in Figure 46. The core was observed to quench progressively from the bottom up and was completely quenched at 562 s in Test S-07-10 and 525 s in Test S-07-10D.

As can be seen from examination of Figures 47 and 48, there was a significant difference in quenching behavior observed between the two tests. This difference occurs as a result of a greater amount of liquid entering the vessel in Test S-07-10D. This liquid came from both increased accumulator injection (see Section 3.2) and the blowout of liquid from the broken loop pump suction. The combined total liquid from these two sources is calculated to be approximately 4 ℓ. This additional liquid helped to

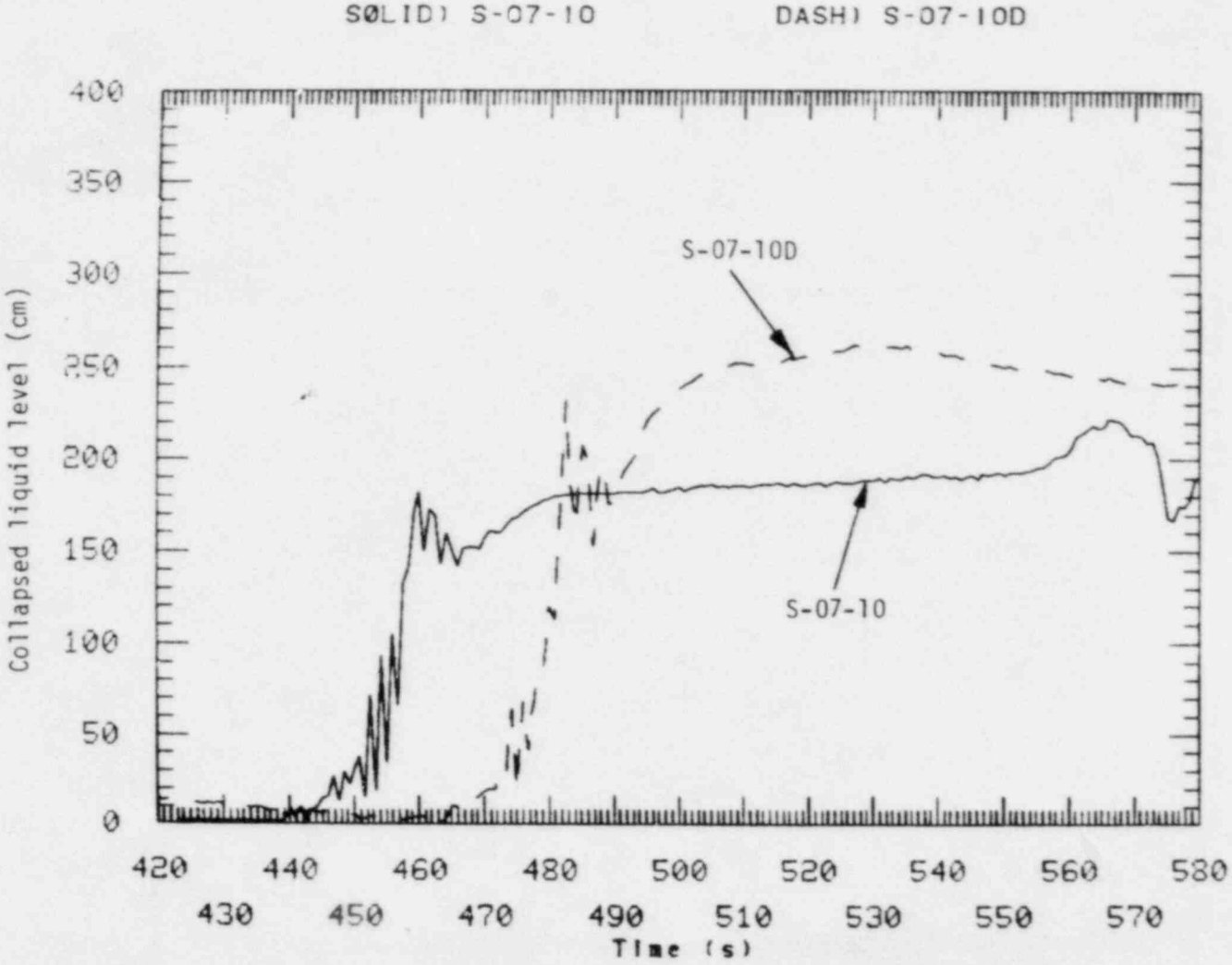

Figure 46. Comparison of collapsed liquid levels in the core during reflood for Tests S-07-10 and S-07-10D.

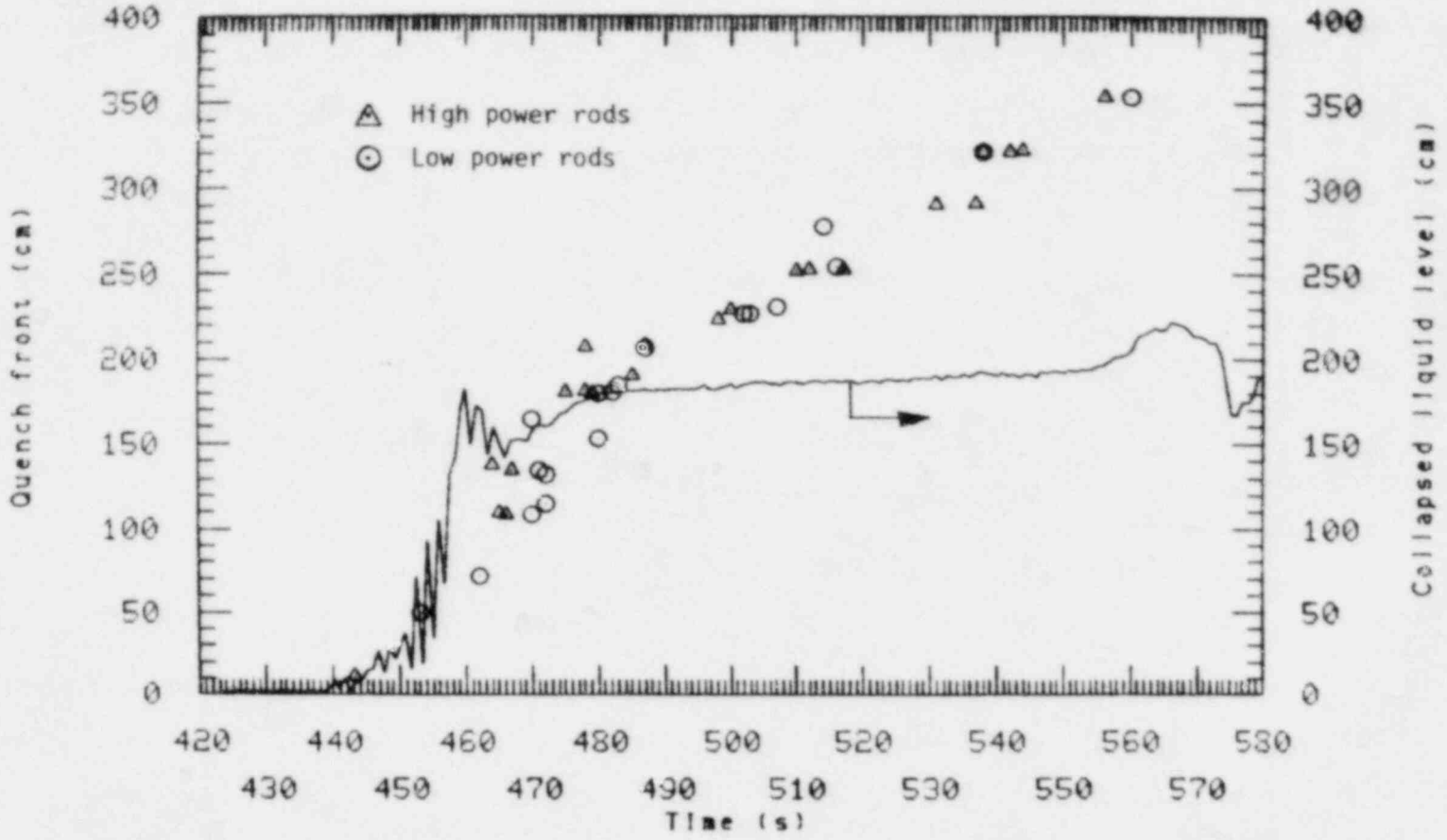

Figure 47. Comparison of quench front to the collapsed liquid level in the core for Test S-07-10.

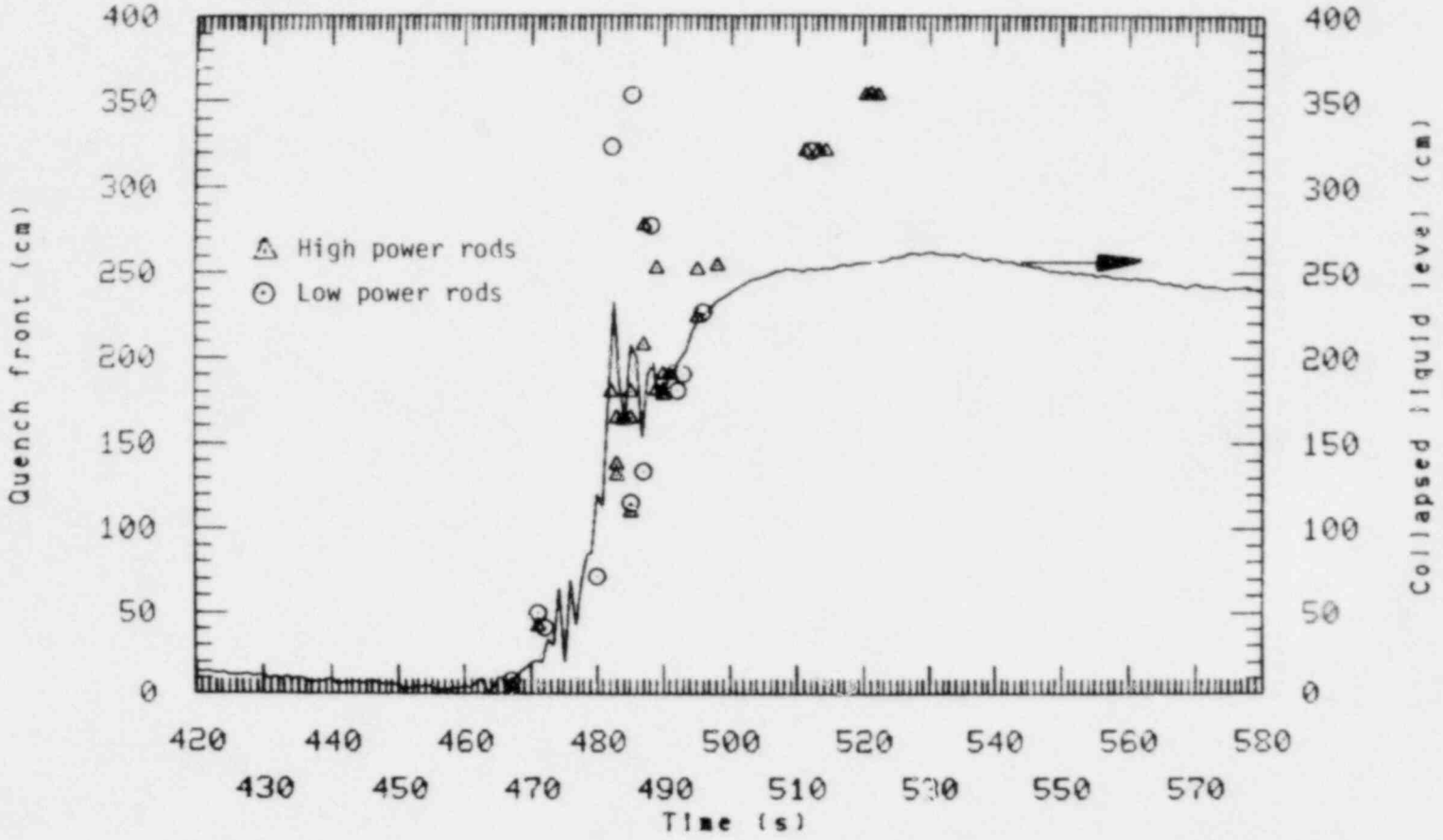

Figure 48. Comparison of quench front to the collapsed liquid level in the core for Test S-07-10D.

rapidly fill the core as seen in Figure 46. It can also be seen from examining Figure 27 that there was less time for the liquid in the lower plenum to have depleted prior to ECC injection in Test S-07-10D, relative to Test S-07-10. This reduced the amount of liquid required to refill to the bottom of the core. Approximately another 50 to 60 cm of liquid initially penetrated to the core in Test S-07-10D. This higher liquid level and the accompanying increased entrainment caused nearly the entire core to more rapidly quench in Test S-07-10D. While for Test S-07-10 (as seen in Figure 47) following the initial rapid liquid penetration, a slow, ECC driven, reflood of the core occurred. Failure to account for either the pump suction liquid inventory or the accumulator injection behavior would be expected to adversely affect code predictions of core reflood and quenching for these tests.

CONCLUSIONS

Results from Tests S-07-10 and S-07-10D have provided insight into system pressure response, fluid mass distribution, and core uncovery behavior for a small (10%) cold leg break, loss-of-coolant experiment in which no emergency core coolant is injected. Information from these tests provides a useful data base which will enable assessment of the capability of computer codes to predict important phenomena occurring during a small break transient. The following are some specific phenomena identified during the tests.

Further information has been obtained on the behavior and influence resulting from the formation of liquid seals in the pump suctions. The formation of the seals caused a brief period of high core voiding early in the transient but had little effect on overall severity of the transient. The effects were greatly enhanced in Test S-07-10D where steam generator heat transfer resulted in liquid remaining in the broken loop suction throughout the blowdown.

Useful information concerning system voiding and mass distribution throughout the transients was obtained. The system was observed to void from the upper elevations downward. Nearly complete voiding of the loops was observed prior to the beginning of core uncovery.

Blowing down the broken loop steam generator introduced asymmetries in loop behavior for Test S-07-10D. Enhanced heat transfer to the steam generator early in the transient resulted in a large liquid inventory remaining in the broken loop pump suction throughout the blowdown. This, in turn, had some affect on break fluid conditions causing a slower depressurization. This liquid also assisted in core reflood following ECC injection. Overall impact of single steam generator blowdown on the transient appeared to be small. The predominant effect was to delay the occurrence of various phenomena. Initial core uncovery was delayed 20 s and rod temperatures were high and rapidly climbing in either test by the time ECC injection was initiated.

A very clearly defined boiloff and dryout of the core was observed in both tests. In-core instrumentation has allowed determination of fluid mass inventory and distribution in the Mod-3 vessel. This may be coupled with heater rod thermal behavior to provide insight into the influence of entrainment and liquid swell on thermal-hydraulics during core uncovery and reflood.

New information concerning the behavior of the accumulator with delayed ECC injection has been obtained. Correct prediction of this behavior will be important to accurate predictions of core reflood and quenching phenomena.

REFERENCES

1. T. K. Larson, J. L. Anderson, and D. J. Shimeck, Scaling Criteria and an Assessment of Semiscale Mod-3 Scaling for Small Break Loss-of-Coolant Transients, EGG-SEMI-5121, EG&G Idaho, Inc., March 1980.

2. D. J. Olson letter to R. E. Tiller, DJO-30-79, Transmittal of Initial Conditions for Semiscale Mod-3 Test S-07-10B (Small Break Test), EG&G Idaho, Inc., February 22, 1979.

3. L. P. Leach letter to R. E. Tiller, LPL-64-80, Experimental Operating Specification for Test S-07-10C, EG&G Idaho, Inc., May 7, 1980.

4. System Design Description (SDD) for the Mod-3 Semiscale System, EG&G Idaho, Inc., July 1978.

5. D. J. Olson letter to R. E. Tiller, DJO-150-78, Experimental Operating Specification for Test S-07-10, EG&G Idaho, Inc., November 27, 1978.

6. K. E. Sackett, Experiment Data Report for Semiscale Mod-3 Small Break Test S-07-10 (Baseline Test Series), NUREG/CR-1456, EGG-2035, EG&G Idaho, Inc., May 1980.

7. T. K. Larson, G. G. Loomis, and R. W. Shumway, Semiscale Simulations of the Three Mile Island Transient - A Summary Report, SEMI-TR-010, EG&G Idaho, Inc., July 1979.

8. Graham B. Wallis, One-Dimensional Two-Phase Flow, Dartmouth College, McGraw-Hill, Inc., 1969 pp 336-339.

APPENDIX A

ORZ LENS VIDEOTAPES OF SEMISCALE MOD-3

TESTS S-07-10 AND S-07-10D

APPENDIX A

STORZ LENS VIDEOTAPES OF SEMISCALE MOD-3

TESTS S-07-10 AND S-07-10D

A Storz lens and video camera combination was used to film phenomena in the Semiscale Mod-3 system for Tests S-07-10 and S-07-10D. The following frames were selected from the videotapes to show highlights of what was observed. The intent is to provide a qualitative feel for fluid conditions which exist during a small break transient.

For Test S-07-10 the Storz lens was installed in the lower portion of the downcomer. Figure A-1 illustrates the orientation of the unit. For Test S-07-10D two lenses were installed. One was used to observe the break plane and the other to view a section of intact loop piping immediately downstream of the pump. Figure A-2 illustrates the orientations for these photos.

Photos have been selected from the videotapes in the downcomer for Test S-07-10 and at the break for Test S-07-10D. Table A-1 provides a brief interpretation of the phenomena being observed and the time frame involved for each photo.

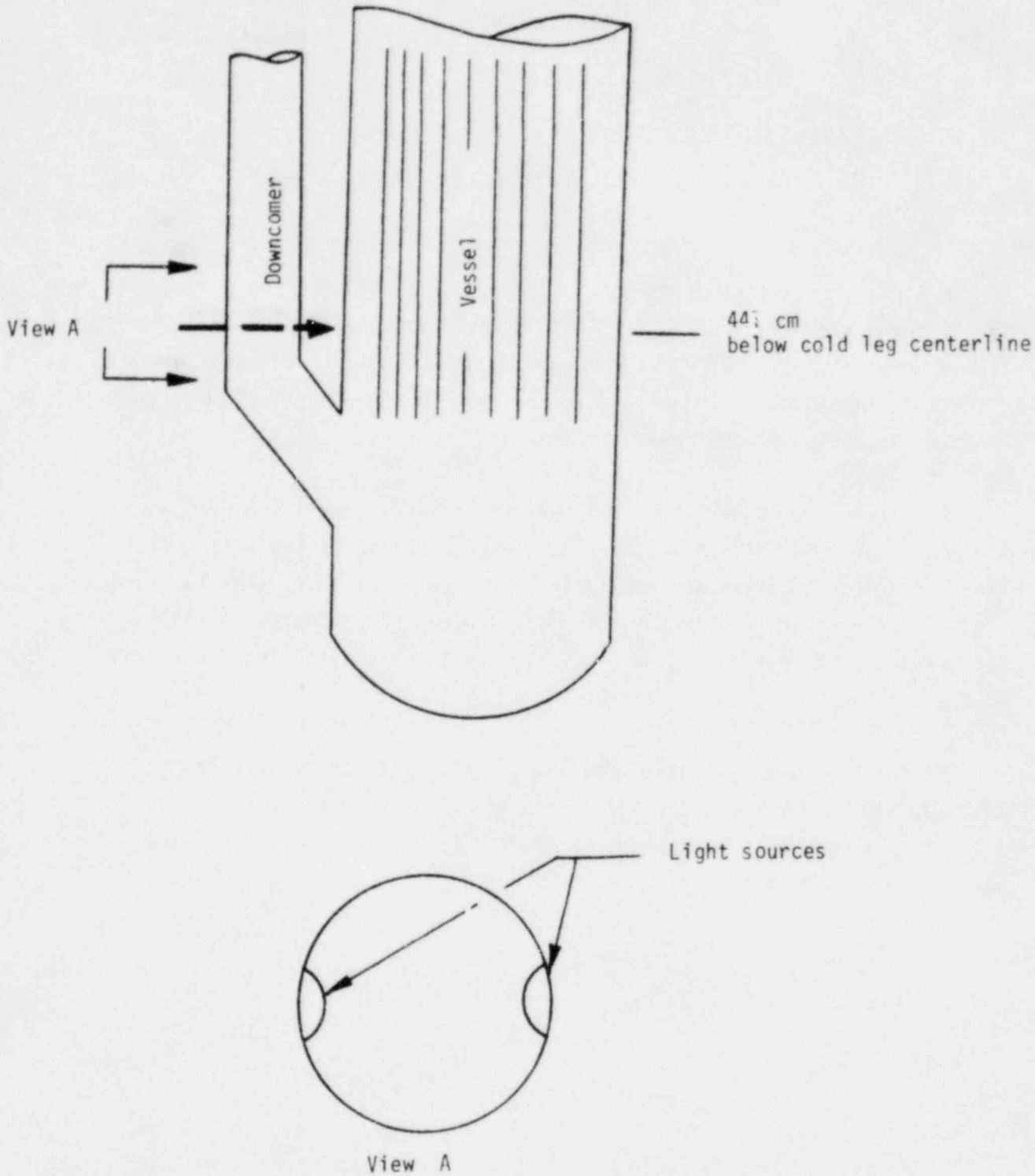

Figure A-1. Orientation of Storz lens for Test S-07-10.

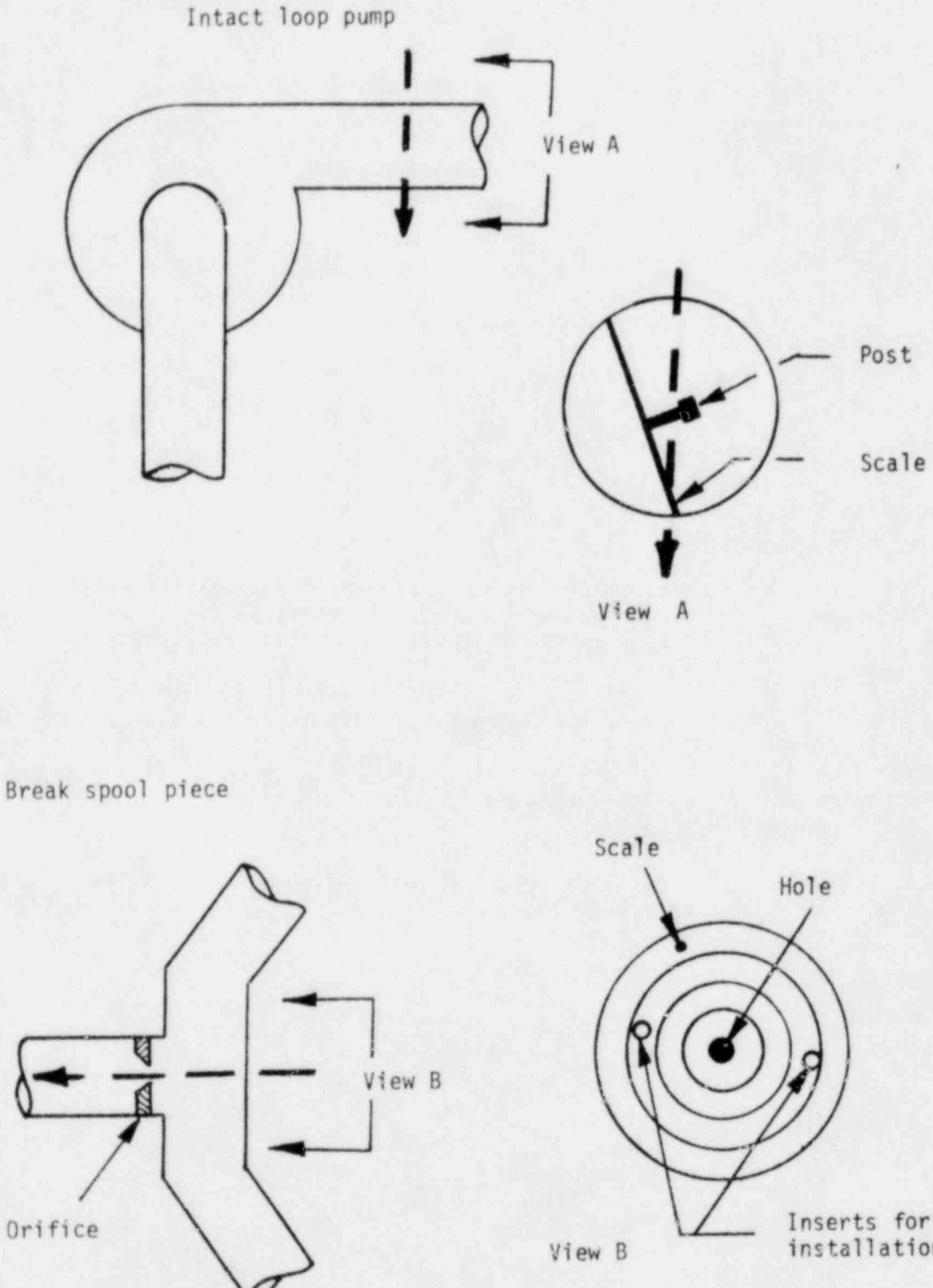

Figure A-2. Orientation of Storz lenses for Test S-07-10D.

TABLE A-1. DESCRIPTION OF STORZ LENS

Figure	Description
Test S-07-10	
A-3	Test S-07-10. Flashing of downcomer fluid and movement of vapor up the downcomer from the core as observed until about 250 s. (Two sequential frames are shown).
A-4	Test S-07-10. Entrained droplets in vapor above the downcomer liquid level just prior to ECC injection at 438 s. Light sources are visible on both sides.
Test S-07-10D	
A-5	Test S-07-10D. Break orifice immediately prior to rupture. Dark center circle is orifice hole. Scale markings of 0.27 cm radius are visible
A-6	Test S-07-10D, t = 0. Break orifice at rupture. Bright spot in orifice hole indicates flashing.
A-7	Test S-07-10D, t = 64 s. Beginning of transition to two-phase conditions upstream of the break plane.
A-8	Test S-07-10D, t = 269 s. Steam flow out the break orifice.

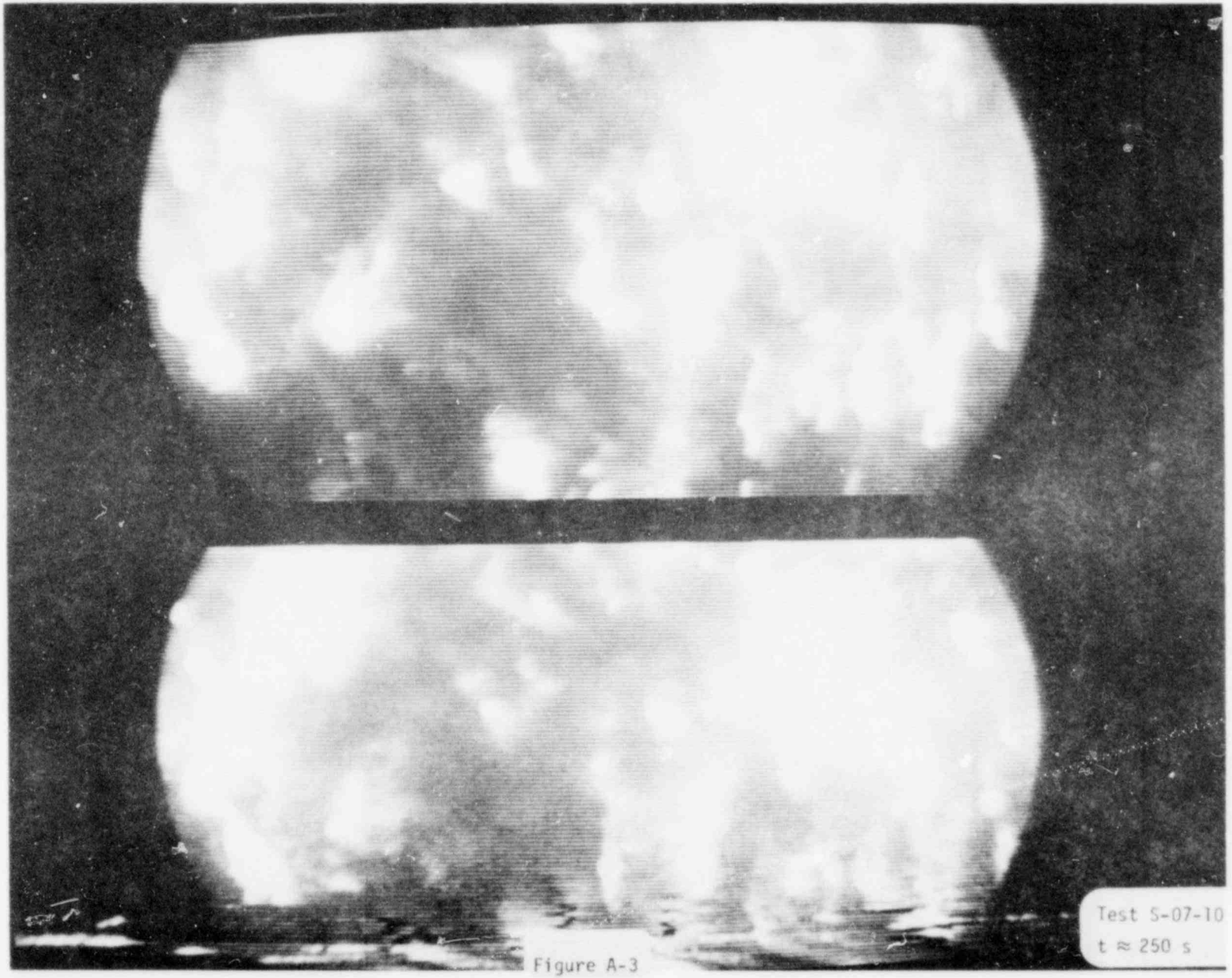

Figure A-3

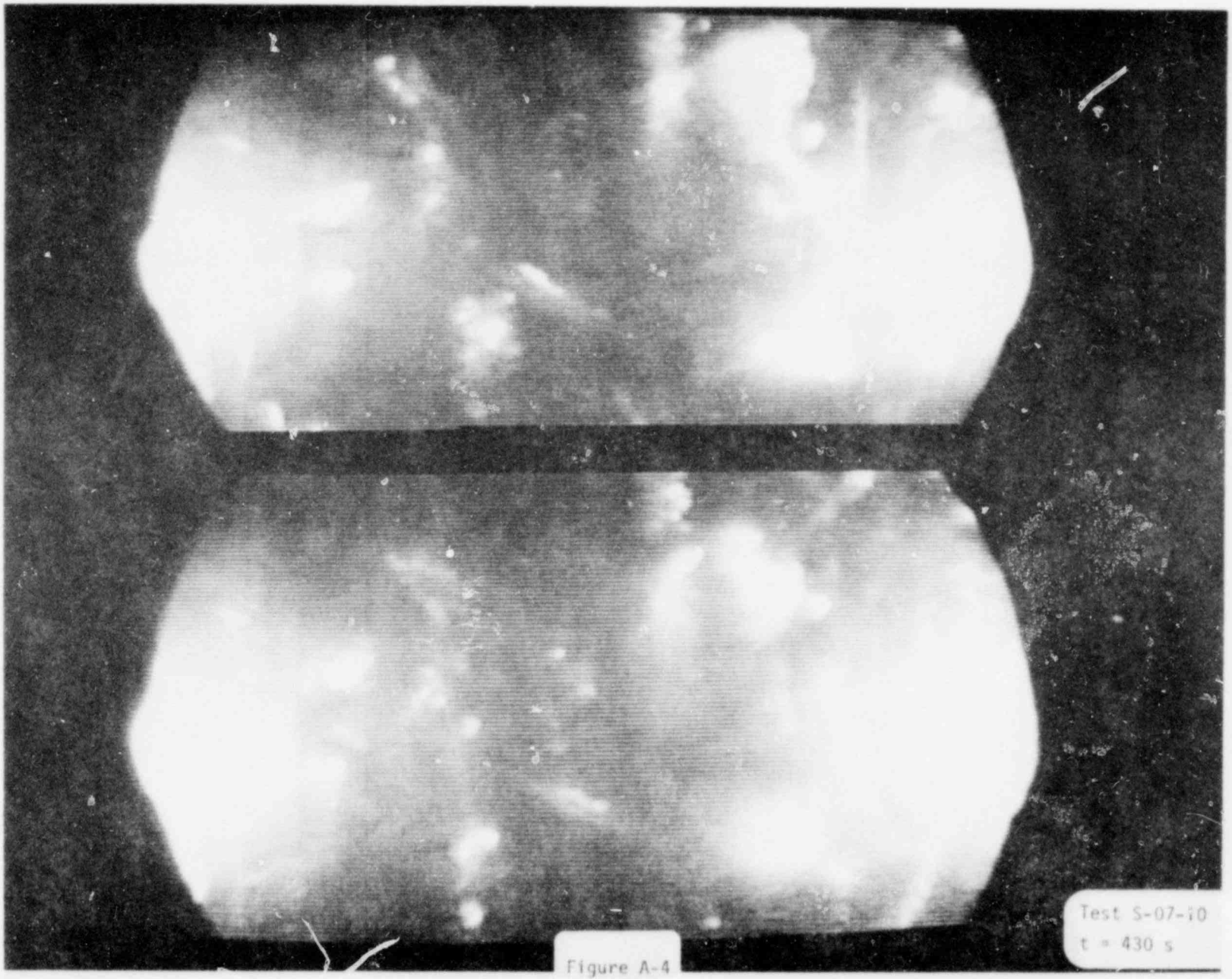

Figure A-4

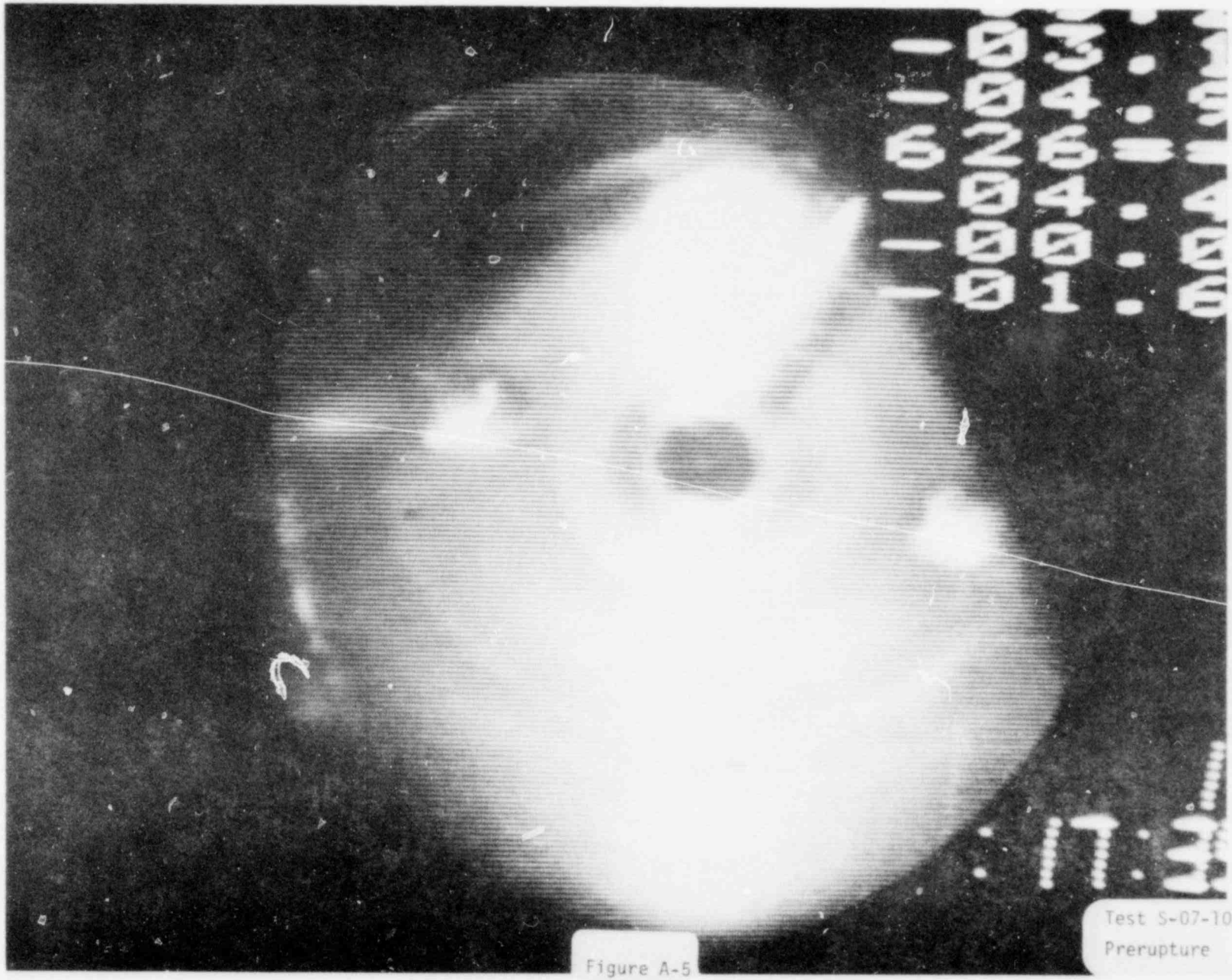

Figure A-5

Figure A-6

Figure A-7

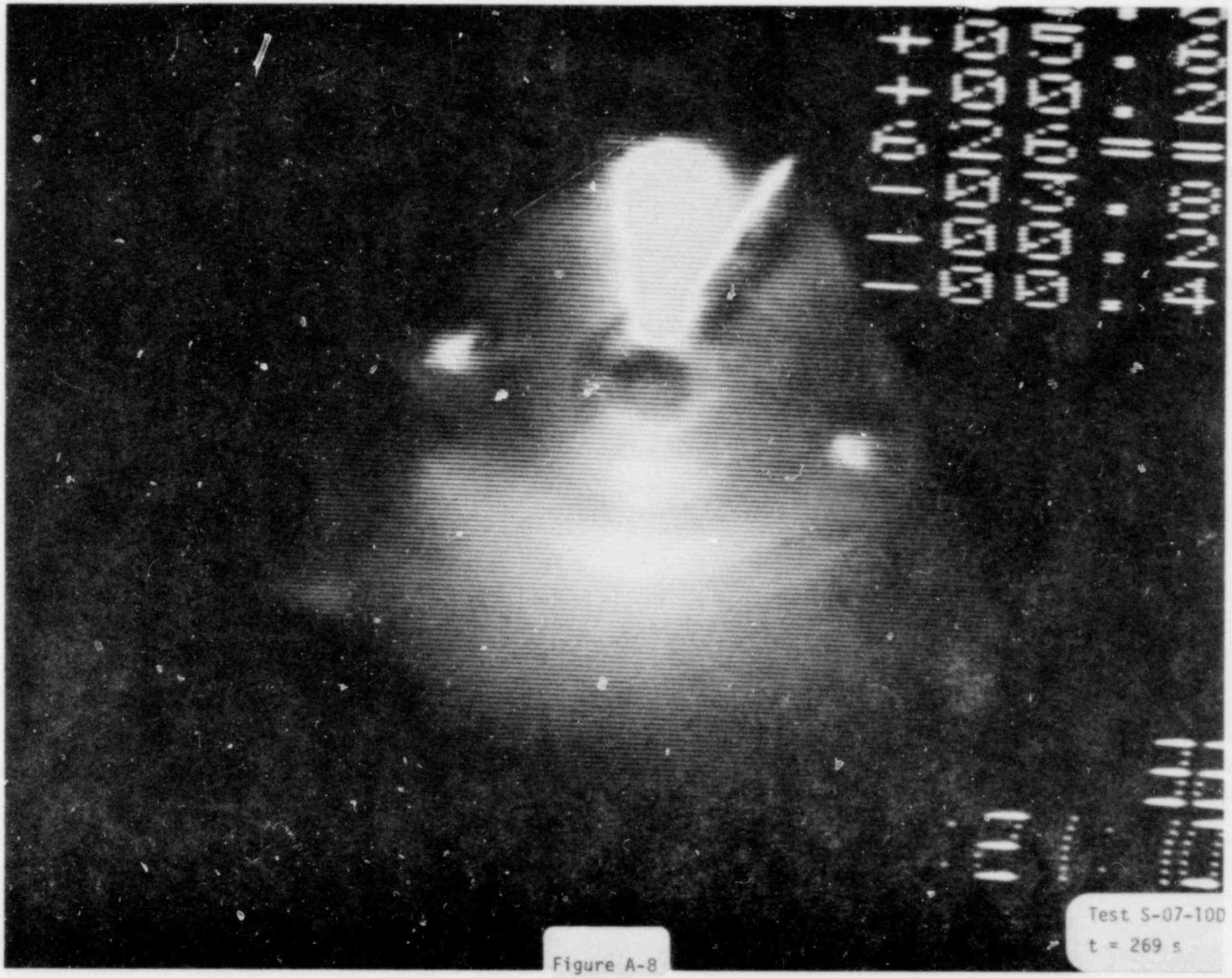

Figure A-8